A Study of Desiccant Dehumidification for a Radiantly Cooled Room

Visit Akvanich

A Thesis Submitted in Partial Fulfillment of the Requirements for the Degree of
Doctor of Philosophy in Mechanical Engineering
Prince of Songkla University
2016

A Study of Desiccant Dehumidification for a Radiantly Cooled Room

Visit Akvanich

A Thesis Submitted in Partial Fulfillment of the Requirements for the Degree of
Doctor of Philosophy in Mechanical Engineering
Prince of Songkla University
2016

Thesis Title   A Study of Desiccant Dehumidification for a Radiantly Cooled
Room

Author   Mr.Visit Akvanich

Major Program   Mechanical Engineering

Major Advisor   **Examining Committee:**

…………………………………   ………………..…….Chairperson

(Asst.Prof.Dr.Juntakan Taweekun)   (Dr.Kittinan Maliwan)

………………….……Committee

(Prof.Dr.Surapong Chirarattananon)

………………………….Committee

(Asst.Prof.Dr.Juntakan Taweekun)

The Graduate School, Prince of Songkla University, has approved this
thesis as partial fulfillment of the requirements for the Doctor of Philosophy Degree
in Mechanical Engineering

..…………………………..………

(Assoc.Prof.Dr.Teerapol Srichana)

Dean of Graduate School

This is to certify that the work here submitted is the result of the candidate's own investigations. Due acknowledgement has been made of any assistance received.

...………..…..…………. Signature

(Asst.Prof.Dr.Juntakan Taweekun)

Major Advisor

...………..…..…………. Signature

(Mr.Visit Akvanich)

Candidate

I hereby certify that this work has not been accepted in substance for any other degree, and is not being currently submitted in candidature for any degree.

...………..…..…………. Signature

(Mr.Visit Akvanich)

Candidate

ชื่อวิทยานิพนธ์　　การศึกษาการลดความชื้นด้วยสารดูดความชื้นในห้องทำความเย็น

แบบแผ่รังสี

ผู้เขียน　　　　　นายวิสิทธิ์ เอกวานิช

สาขาวิชา　　　　วิศวกรรมเครื่องกล

ปีการศึกษา　　　2558

บทคัดย่อ

　　　　　งานวิจัยฉบับนี้จัดทำขึ้นโดยมีวัตถุประสงค์ในการออกแบบและพัฒนาระบบลด
ความชื้นและระบบการทำความเย็นแบบแผ่รังสีเพื่อพัฒนาสภาวะความสบายสำหรับภูมิอากาศแบบ
ร้อนชื้น แนวทางการดำเนินการศึกษาประกอบด้วย 3 ขั้นตอนคือ การออกแบบชุดลดความชื้นและ
ระบบการทำความเย็นแบบแผ่รังสี การใช้โปรแกรมจำลองทางคณิตศาสตร์และการทดลอง โดยทำ
การทดลองในพื้นที่ที่มีสภาวะอากาศแบบร้อนชื้นตลอดทั้งปี บริเวณอาคารชั้น 2 ของบ้านประหยัด
พลังงานภายในมหาวิทยาลัยสงขลานครินทร์ วิทยาเขตหาดใหญ่ จังหวัดสงขลา ซึ่งตั้งอยู่ภาคใต้
ตอนล่างของประเทศไทย ห้องทดลองมีขนาดพื้นที่ 19.25 ตารางเมตร และความสูง 2.8 เมตร ชุดลด
ความชื้นประกอบด้วยหอดูดซับชนิดเม็ดตัวดูดซับจำนวน 2 ถัง สำหรับลดความชื้นของอากาศใน
ระบบระบายอากาศก่อนเข้าสู่ห้องปรับอากาศ การทดสอบสมรรถนะของชุดลดความชื้น
ประกอบด้วยชุดลดความชื้นแบบการไหลในแนวตั้ง (Vertical flow bed) และการไหลในแนวรัศมี
(Radial flow bed) ขนาดเส้นผ่านศูนย์กลางภายในและภายนอกเท่ากับ 0.15 และ 0.30 เมตร
ตามลำดับ ความสูง 0.465 เมตร แต่ละหอดูดซับภายในบรรจุสารดูดซับจำนวน 10 กิโลกรัม สารดูด
ซับที่ใช้คือสารดูดซับชนิดซิลิกาเจลที่มีขนาดเม็ดประมาณ 3 มิลลิเมตร ความพรุนของชั้นเม็ดตัวดูด
ซับเท่ากับ 0.4 (อัตราส่วนปริมาตรช่องว่างระหว่างเม็ดตัวดูดซับกับปริมาตรของชั้นเม็ดตัวดูดซับที่
บรรจุในหน่วยดูดซับนั้น) และความหนาแน่นชั้นเม็ดตัวดูดซับ 670 กิโลกรัมต่อลูกบาศก์เมตร
นอกจากนี้ระบบการทำความเย็นแบบแผ่รังสีทำงานโดยการสูบน้ำเย็นปริมาณ 26.28 ลิตรต่อนาที ที่
ผลิตจากหอผึ่งเย็นผ่านท่อทองแดงที่ติดตั้งกับแผงทำความเย็นภายในห้องทดลองทั้งบริเวณฝ้าและ
ผนังของห้องปรับอากาศ พื้นที่ผิวเฉลี่ยของแผงทำความเย็นมีค่า 16.83 และ 16.32 ตารางเมตร
ตามลำดับ

จากผลการศึกษาโดยพลศาสตร์ของไหลเชิงคำนวณ (Computational Fluid Dynamics, CFD) และการออกแบบการทดลองด้วยวิธีพื้นผิวตอบสนอง (Response Surface Methodology, RSM) พบว่าชุดลดความชื้นแบบการไหลในแนวรัศมีเหมาะสมกับระบบลดความชื้น โดยที่ความดันลดภายในชุดลดความชื้นแบบการไหลในแนวตั้งจะมีค่าสูงกว่าที่ภาวะเดียวกัน ส่วน อัตราการลดความชื้นของอากาศมีค่าใกล้เคียงกันโดยเฉพาะช่วงแรกของการทำงาน แต่อัตราการลด ความชื้นเฉลี่ยของชุดลดความชื้นแบบการไหลในแนวรัศมีจะมีค่าสูงกว่า จากการศึกษาที่ระดับ ความชื้นในอากาศ 18 กรัมต่อกิโลกรัมอากาศและอัตราการระบายอากาศ 26 กิโลกรัมต่อชั่วโมง พบว่า ขนาดชุดลดความชื้นแบบการไหลในแนวรัศมีที่เหมาะสมมีขนาดเส้นผ่านศูนย์กลางภายใน และภายนอกขนาด 0.15 และ 0.30 เมตร ตามลำดับ และมีสมรรถนะในการลดความชื้นในอากาศ 0.46 กิโลกรัมต่อชั่วโมง โดยที่มีความดันลดภายในชุดลดความชื้น 23.34 พาสคาล นอกจากนี้ที่ สภาวะอากาศ 25-40 องศาเซลเซียส อัตราส่วนความชื้นในอากาศ 10-20 กรัมต่อกิโลกรัมอากาศ และอัตราการไหลของอากาศ 60-120 กิโลกรัมต่อชั่วโมง อัตราการลดความชื้นในอากาศและความ ดันลดภายในชุดลดความชื้นเฉลี่ยของชุดลดความชื้นแบบการไหลในแนวตั้งและการไหลในแนว รัศมีมีค่า 0.52 กิโลกรัมต่อชั่วโมง ที่ความดันลด 107.14 พาสคาล และ0.66 กิโลกรัมต่อชั่วโมง ที่ ความดันลด 63.23 พาสคาล ตามลำดับ

ระบบทำความเย็นโดยสารดูดความชื้นประกอบด้วยระบบลดความชื้นโดยใช้สาร ดูดซับและระบบทำความเย็นได้แก่ระบบปรับอากาศแบบทั่วไปหรือระบบการทำความเย็นแบบแผ่ รังสี งานวิจัยฉบับนี้ได้ทำการทดลองในพื้นที่ที่มีสภาวะอากาศแบบร้อนชื้น ส่งผลให้ชุดลด ความชื้นแบบหอดูดซับชนิดเม็ดตัวดูดซับสามารถลดภาระการทำความเย็นแฝงเนื่องจากความชื้นใน อากาศได้มากและพัฒนาสภาวะความสบายของผู้อยู่อาศัยได้เป็นอย่างดี จากผลการจำลองทาง คณิตศาสตร์โดยใช้โปรแกรม TRNSYS และการทดลองระบบปรับอากาศแบบแยกส่วนร่วมกับ ระบบระบบลดความชื้นโดยใช้สารดูดซับพบว่า ความชื้นในห้องปรับอากาศและภาระการทำความ เย็นแฝงของระบบปรับอากาศลดลง 2 กรัมต่อกิโลกรัมอากาศหรือคิดเป็น 14 เปอร์เซ็นต์ และ 0.71 กิโลวัตต์ความร้อนหรือคิดเป็น 19 เปอร์เซ็นต์ ตามลำดับ เมื่อสภาวะอากาศภายนอกห้องปรับอากาศ 25.5-32.7 องศาเซลเซียส ความชื้นสัมพัทธ์ในอากาศ 55.5-95.6 เปอร์เซ็นต์ และสภาวะอากาศ ภายในห้องปรับอากาศเฉลี่ย 25.3 องศาเซลเซียส ความชื้นสัมพัทธ์ในอากาศ 52.3 เปอร์เซ็นต์ ส่งผล ให้ค่าสภาวะความสบาย (Predicted Mean Vote, PMV) ดีขึ้นจาก 0.3-0.6 (ค่าเฉลี่ย 0.5) เป็น 0.1-0.4 (ค่าเฉลี่ย 0.3) หรือทำให้สัดส่วนผลโหวตความไม่สบายตัว (Predicted Percentage Dissatisfied, PPD) ลดลงจาก 6.77-12.85 เปอร์เซ็นต์ (ค่าเฉลี่ย 10.12 เปอร์เซ็นต์) เหลือ 5.17-8.81 เปอร์เซ็นต์ (ค่าเฉลี่ย 7.04 เปอร์เซ็นต์) นอกจากนี้ จากผลการจำลองทางคณิตศาสตร์โดยใช้โปรแกรม TRNSYS

ระบบการทำความเย็นแบบแผ่รังสีร่วมกับระบบลดความชื้นโดยใช้สารดูดซับพบว่า ค่าสภาวะความ
สบายตลอดทั้งปีโดยเฉลี่ยดีขึ้นจาก 1.46 เป็น 1.21 เมื่อเปรียบเทียบระหว่างระบบการทำความเย็น
แบบแผ่รังสีที่มีและไม่มีระบบลดความชื้น ซึ่งสอดคล้องกับผลการทดลองโดยพบว่า ค่าช่วงสภาวะ
ความสบายของห้องทดลองที่ไม่มีแผงทำความเย็นเท่ากับ 1.48 ในกรณีมีแผงทำความเย็นเท่ากับ
0.89 กรณีมีระบบลดความชื้นร่วมกับแผงทำความเย็นมีค่า 0.62 และพบว่าความชื้นในห้องปรับ
อากาศลดลงจาก 19.81 กรัมต่อกิโลกรัมอากาศคงเหลือ 10.28 กรัมต่อกิโลกรัมอากาศ นอกจากนี้
การกระจายตัวของอุณหภูมิ ความชื้น และค่าสภาวะความสบายภายในห้องทดลองสามารถแสดงได้
จากการจำลองทางคณิตศาสตร์โดยใช้โปรแกรม ANSYS และพบว่ากรณีที่ห้องทดลองมีพัดลม
หมุนเวียนภายในร่วมกับระบบการทำความเย็นแบบแผ่รังสีร่วมและระบบลดความชื้นโดยใช้สาร
ดูดซับ จะส่งผลให้ค่าช่วงสภาวะความสบาย ดีขึ้นที่ -0.24 หรือทำให้สัดส่วนผลโหวตความไม่สบาย
ลดลงเหลือ 6.24 เปอร์เซ็นต์

Thesis Title   A Study of Desiccant Dehumidification for a Radiantly Cooled Room

Author   Mr.Visit Akvanich

Major Program   Mechanical Engineering

Academic Year   2015

ABSTRACT

This dissertation aims to design and develop a solid desiccant dehumidification and radiant cooling system which are suitable for tropical climate to achieve thermal comfort. This study consists of three steps of research works such as design, simulation, or experimentation. The experiment systems are set up at the 2nd floor of the low energy house in Prince of Songkla University (PSU), Hatyai Campus, Songkhla Province located in the Southern part of Thailand, where is hot and humid climate throughout the year. The total floor area of the experiment room is 19.25 m^2 and height 2.8 m. The dehumidification system is used by the solid desiccant dehumidifiers in two columns to remove water vapour from the ventilation air before passing into the experimental room. The experimental dehumidifiers consist of two desiccant beds configuration, a vertical flow bed and a radial flow bed or hollow cylindrical packed bed, with an inner and outer diameter of 0.15 m and 0.30 m, respectively. A length of the packed bed is 0.465 m containing 10 kg of adsorbent material in each column. The spherical particles of silica-gel are used as the working desiccant in the dehumidifiers. The physical properties of silica-gel are: average diameter: 3 mm, porosity: 0.4 (the open volume fraction of the medium) and bulk density: 670 kg/m^3. Furthermore, the radiant cooling system is operated by using cool water supplied from cooling tower passing through the radiant cooling panel which made from copper tube bond with aluminium sheet. The total area of the ceiling and wall radiant cooling panels are 16.83 m^2 and 16.32 m^2 with 26.28 litre/min of supplied water by the cooling tower for radiant cooling system.

The results of simulation on a computational fluid dynamics (CFD) and experiment by response surface methodology (RSM) indicate that the radial flow bed, hollow cylindrical bed are the feasible and practical dehumidifier for dehumidification

system. Pressure drop of the vertical flow bed is too high comparing with the radial flow bed under the same conditions. An adsorption rate is especially a similar capacity during the starting period at a time intervals, but the average capacity of the radial flow bed is usually the greater adsorbed rate. For moisture air with inlet humidity ratio of 18 g_w/kg and ventilation air of 26 kg/h, the practical optimum configurations of the inner diameter and the outer diameter are equal 0.15 and 0.30 m, respectively; as a result, the feasible and optimum performance values are 23.34 Pa and 0.46 kg_w/h. Moreover, the average operating parameters of the air temperature, the humidity ratio and the mass flow rate are range of 25-40°C, 10-20 g_w/kg_{da}, and 60-120 kg/h, respectively. For the vertical bed flow dehumidifier, the pressure drop and the adsorption rate are 107.14 Pa and 0.52 kg_w/h, respectively. In other hand, for the radial bed flow dehumidifier, the pressure drop and the adsorption rate are 63.23 Pa and 0.66 kg_w/h.

The desiccant cooling systems consist of the dehumidification and air-conditioning system or the radiant cooling system. From this research work under the humid tropical region condition which being hot and high humidity, the desiccant dehumidification has an extreme effect to decrease the energy consumption from latent heat load, and to develop thermal comfort conditions. The results of TRNSYS simulation and experiment for using a dehumidifier in air-conditioning system indicate that the humidity ratio of conditioning space and cooling load of split type air conditioner are decreased by 0.002 kg_w/kg_{da} (14%) and 0.71 kW_{th} (19.26%) respectively, when the temperature and the relative humidity of the outdoor air are in the ranges of 25.5-32.7^{o}C and 55.5-95.6%, and the average temperature and relative humidity of the indoor air are found to be around 25.3^{o}C and 52.3%. Consequently, the predicted mean vote (PMV) is improved from 0.3-0.6 (0.5 averages value) to 0.1-0.4 (0.3 averages value) or the predicted percentage dissatisfied (PPD) is reduced from 6.77-12.85% (10.12% averages value) to 5.17-8.81% (7.04% averages value). Furthermore, the results of TRNSYS simulations for using a dehumidifier in the radiant cooling system indicate that the PMV values can be improving from 1.46 to 1.21 throughout the year with the uses of cooling panel in comparison with the case of without cooling panel. The experimental studies with the desiccant humidifier coupled to the radiant cooling system confirmed the accuracy of simulations. The

values of predicted mean vote for the cases of without cooling panel, with cooling panel, and cooling panel with dehumidifier are 1.48, 0.89 and 0.62, respectively. Moreover, the average moisture content of the interior air is reduced from 19.81 g_w/kg_{da} to 10.28 g_w/kg_{da}. Furthermore, the air temperature, the relative humidity, and the predicted mean volte distribution in the experimental room are explained by the results of the ANSYS contour plots. In the case of the ventilation fan installation in the radiant cooling system, the value of predicted mean vote improves to -0.24 and the predicted percentage dissatisfied is 6.24%.

ACKNOWLEDGEMENT

Visit Akvanich

CONTENTS

CONTENTS (Continued)

LIST OF TABLES

LIST OF TABLES (Continued)

LIST OF TABLES (Continued)

LIST OF FIGURES

LIST OF FIGURES (Continued)

LIST OF FIGURES (Continued)

LIST OF ABBREVIATIONS AND SYMBOLS

$\lvert v \rvert$	=	Magnitude of the velocity
μ	=	Dynamic viscosity (N.s/m^2)
b	=	Langmuir constant (m^3/kg)
C	=	Inertial resistance factor
C^*	=	Concentration of adsorbate in the steady state equilibrium (kg/m^3)
C_b	=	Concentration of adsorbate (kg/m^3)
C_e	=	Concentration of adsorbate in the steady state equilibrium
C_f	=	Concentration of adsorbent in the outlet side
C_o	=	Concentration of adsorbent in the inlet side
D	=	Diameter of the column (m)
D_e	=	Effective diffusivity
D_p	=	Mean particle diameter (m)
D_{ri}	=	Inner diameter of the radial flow bed (m)
D_{ro}	=	Outer diameter of the radial flow bed (m)
f_{cl}	=	Clothing area factor
H	=	Height of the column (m)
h_c	=	Convective heat transfer coefficient (W/m^2.K)
H_{sr}	=	Height of silica-gel for radial bed (m)
H_{sv}	=	Height of silica-gel for vertical bed (m)
I_{cl}	=	Thermal resistance (clo)
K	=	Henry constant (m$^3_{gas}$/m^3)
k_p	=	Particle-phase mass transfer coefficient (s^{-1})
L	=	Thermal load on the body (W/m^2).
L	=	Bed depth (m)
M	=	Rate of metabolic heat production (W/m^2)
M	=	Mass flow rate (kg/h)
M_{act}	=	Activity level (met)
PMV	=	Predicted Mean Vote

LIST OF ABBREVIATIONS AND SYMBOLS (Continued)

PPD	=	Predicted Percentage Dissatisfied
P_v	=	Partial pressure of water vapor in moist air (kPa)
q^*	=	Concentration of adsorbent in the steady state equilibrium (kg/m^3)
$\bar{q}$	=	Average concentration of adsorbent (kg/m^3)
R_{adsorp}	=	Adsorption rate (kg_w/h)
R_{cl}	=	Thermal resistance, ($m^2.K/W$)
R_p	=	Radius of desiccant particle (m)
S_i	=	Source term for the momentum equation ($kg/m^2.s^2$)
t	=	Time (s)
T	=	Temperature (^oC)
T_a	=	Air temperature (°C)
T_{cl}	=	Clothing temperature (°C)
T_r	=	Mean radiant temperature (°C)
u	=	Interstitial velocity inside desiccant bed (m/s)
V	=	Quantity of adsorbate (kg/m^3)
V	=	Air velocity (m/s)
V	=	Diameter of the column (m)
V_m	=	Quantity V of adsorbate adsorbed in a single monolayer (kg/m^3)
W	=	External work accomplished (W/m^2)
W	=	Humidity ratio (kg_w/kg_{da})
z	=	Distance of desiccant bed (m)
α	=	Permeability
ΔP	=	Pressure drop (Pa)
ΔW	=	Adsorption rate (kg_w/h)
ε	=	Porosity
ε_b	=	Porosity of desiccant bed
ρ	=	Density of fluid properties (kg/m^3)

Chapter 1

Introduction

1.1 Background

Energy statistics of Thailand reported that the electrical consumption increased approximately 3.79% per annum from 2005 to 2014, whereas it decreased 0.25% and 0.30%, especially in 2009 and 2011, respectively, as seen in Fig. 1.1. The breakdown of electrical consumption can be classified into eight sectors namely, industrial, residential, commercial or business, small general services, government and non-profit, agriculture, free of charge, and others.
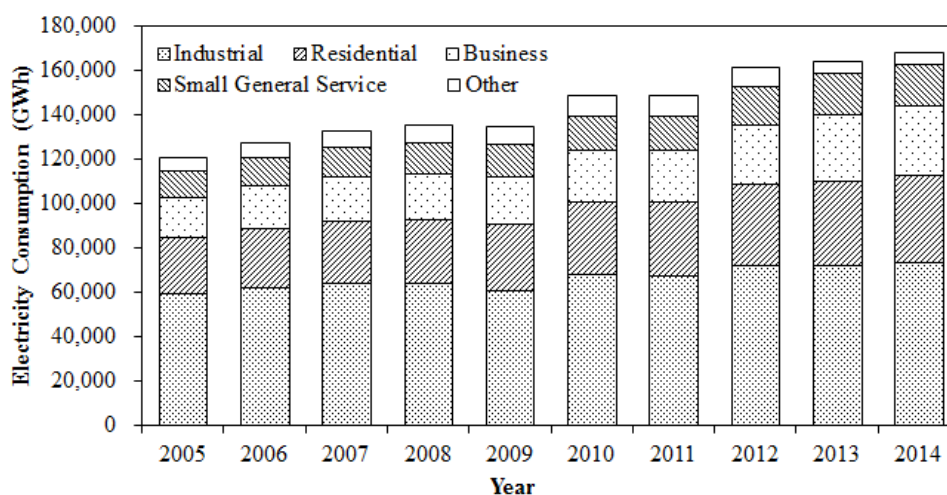
Fig. 1.1 Electrical consumption in Thailand
(Source: EPPO, 2015)

In Thailand, 2014, the electrical consumption of the industrial clusters such as food, iron and steel, electronics, textile, or automotive is 73,782 GWh (44%). For residential building and commercial cluster such as department store, hotel, apartment and guest house, retail trade, and real estate service are 38,993 GWh (23%) and 31,362 GWh (19%), respectively. Moreover, in small general service, it is 18,807 GWh (23%), and the other sector including government and non-profit, agriculture, free of charge, and other, it is about 5,676 GWh (3%), as shown in Fig. 1.2.
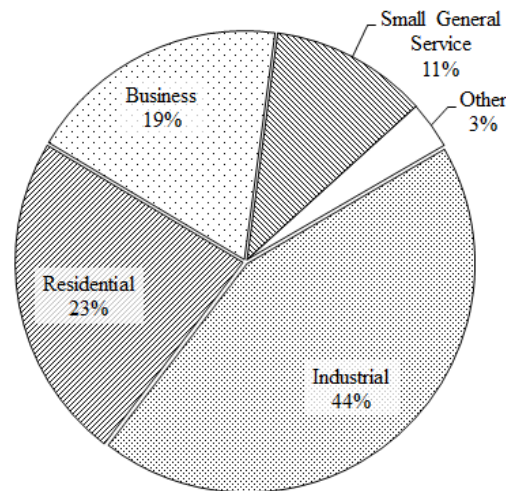
Fig. 1.2 Breakdown of electrical consumption in Thailand, 2014
(Source: EPPO, 2015)

For residential and business buildings, the air-conditioning systems are widely used to provide thermal comfort conditions for humans. The electrical consumption is approximately 60-70%. So that, it is important to use the alternative of air-conditioning system for improving the thermal comfort with the lower electrical consumption.

1.2 Rationale

The thermally comfortable environment can be achieved by using heating and cooling panels. In cooling system, sensible heat load is reduced by the cooling panels with mainly from thermal radiation and some heat convection. Principle advantages of radiant cooling system are more comfort levels and lower energy consumption comparing with a conventional air-conditioning system. However, it can satisfy only sensible heating. In the area of high humidity, moisture presents the major problem for the human comfort and the air-conditioning systems. Unitary dehumidifiers should be used. Both mechanical refrigeration systems and desiccant dehumidification can remove the moisture from a supply air, whereas desiccant dehumidifier is advantageous in dealing with latent load and improving indoor air quality with adsorbing moisture directly.

1.3 Objective of the Study

The aim of this study is to design and develop the solid desiccant dehumidification with the use of the radiant cooling system which is suitable for tropical climate to achieve thermal comfort.

1.4 Scope of the Study

The experiment systems are set up at the 2nd floor of the low energy house in Prince of Songkla University (PSU), Hatyai Campus, Songkhla Province located in the Southern part of Thailand. The dehumidification system used solid desiccant dehumidifiers with silica-gel bed in column to remove water vapour from the ventilation air before passing into the experimental room. The radiant cooling system is designed using cool water supplied from cooling tower passing through the cooling panels which made of copper tube bond with aluminium sheet.

1.5 Organization of the Report

Chapter 2 focuses on literature reviews, such as the dehumidification with solid desiccant dehumidifiers, heating ventilation and air-conditioning by the radiant cooling system, an assessment of thermal comfort, modeling and simulation on commercial software tools, and experimental design with response surface methodology. The design of dehumidification, radiant cooling, control system, methodology of simulation and experimental setup, and record parameters including instruments are described in Chapter 3. Chapter 4 presents design of the dehumidifiers and applying the solid desiccant dehumidifier for the air-conditioning system and the radiant cooling system. The simulation results for using of ANSYS and TRNSYS software are also examined in this chapter. Moreover, the experimental results are described in Chapter 5. Conclusion and recommendation are presented in Chapter 6.

Chapter 2
Literature Reviews

2.1 Solid Desiccant Dehumidification

Dehumidification processes are important operation in various applications for the removal of water vapor from air, gases, or other fluids. Drying gases under pressure are normally used, such as eliminating condensation and subsequent corrosion, maintaining a dry atmosphere in a closed space or container, controlling humidity in warehouses and caves for storage, and drying process and industrial gases. In common practice, the dehumidification usually refers to equipment operating at essentially atmospheric pressures, and built to standards similar to other types of air-handling equipment. The solid desiccant dehumidifiers usually employ stationary beds or rotary wheel beds for packing desiccant media, namely desiccant column and desiccant wheel, respectively. In the former case, two or more desiccant columns are constructed with controlled valves to work alternatively in adsorption and regeneration process. Secondly dehumidifier, a moist air is dried through one side of the wheel, while a heated air stream dries the wet desiccant on the other side of wheel at the same time.

The desiccant media is natural or synthetic substances capable of absorbing or adsorbing water vapour due to the difference of water vapour pressure between the surrounding air and the desiccant surface. Many desiccant materials are available, such as silica-gel, activated alumina, synthetic zeolites (molecular sieve), or alumina gel (Thomas, W.J. and Crittenden, B., 1998). All desiccants behave in a similar way to attract the moisture until reaching equilibrium state in adsorption process, and the moisture is usually removed from the desiccant by heating with temperatures between 50 and $260^{\circ}C$ in desorption process to attract moisture once again. Adsorption process always generates the sensible heat equal to the latent heat of the water vapor taken up by the desiccant plus an additional heat of the sorption that varies between 5 and 25% of the latent heat of water vapor (ASHRAE, 2005).

Silica-gel is a partially dehydrated polymeric form of colloidal silicic acid with the formula $SiO_2.nH_2O$. This amorphous material comprises spherical

particles 2-10 nm in size which aggregate to form the adsorbent with pore sizes in the range 6-25 nm. Surface areas are in the range 100-850 m^2/g. The surface comprises mainly S_iOH and S_iOS_i groups being polar can be used to adsorb water, alcohols, phenols, amines, etc. by hydrogen bonding mechanisms. A capacity of silica-gel for water is high, especially at the low temperature with moderate water vapor pressure. Moreover, the heat of adsorption of water vapour is about 45 kJ/mol, and the regenerated temperature is 150^oC. Typical properties of adsorbent grade silica-gel are summarized in Table 2.1 (Keller et al., 1987).

Table 2.1 Typical properties of adsorbent-grade silica-gel

		Physical Properties
1	Surface area (m^2/g)	830
2	Density (kg/m^3)	720
3	Reactivation temperature (^{o}C)	130-280
4	Pore volume (% of total)	50-55
5	Pore size (nm)	1-40
6	Pore volume (cm^3/g)	0.42
	Adsorption properties	Percent by weight
7	H_2O capacity at 4.6 mm Hg, 25^oC	11
8	H_2O capacity at 17.5 mm Hg, 25^oC	35
9	O_2 capacity at 100 mm Hg, 183^oC	22
10	CO_2 capacity at 250 mm Hg, 25^oC	3
11	n-C_4 capacity at 250 mm Hg, 25^oC	17

(Source: Keller et al., 1987)

In theories of adsorption equilibrium, a variety of different isotherm equations have been proposed, such as Henry law (linear isotherm), Langmuir (non-linear isotherm), BET, DR, Freundlich, Sips, Toth, Jovanovich, or Tempkin equation, which have a theoretical foundation or more empirical nature. The Langmuir isotherm is used in this study to design a dehumidifier. The Langmuir equation, of which one from is explained in Eq. 2.1. (Langmuir, 1918)

$$\frac{V}{V_m} = \frac{bC_e}{1+bC_e}$$

Eq. 2.1

Where V is a quantity of adsorbate (gas or vapour) adsorbed by an adsorbent (porous solid desiccant) (kg/m^3); V_m is the quantity V of adsorbate adsorbed in a single monolayer (kg/m^3); b is Langmuir constant (m^3/kg), and C_e is a concentration of adsorbate in the steady state equilibrium.

In dynamics of fixed-bed adsorption, many analytical solutions for breakthrough curves are available. The Klinkenberg equation is used in this study to calculate breakthrough and equilibrium time. For ideal plug flow model, linear isotherm, isothermal, and low concentration, the governing equation is shown in Eq. 2.2. The solution is calculated in Eq. 2.3 for full solution and in Eq.2.4 for approximate solution. (Klinkenberg, 1954)

$$\frac{\partial \overline{q}}{\partial t} = k_p(q^* - \overline{q}) = k_p K(C_b - C^*) \qquad \text{Eq. 2.2}$$

$$\frac{C_b}{C_o} = e^{-\xi}\int_0^{\tau} e^{-v}I_0(2\sqrt{\zeta v})dv + e^{-(\tau+\xi)}I_0(2\sqrt{\tau\xi}) \qquad \text{Eq. 2.3}$$

$$\frac{C_b}{C_o} = \frac{1}{2}\left[1 - erf\left(\sqrt{\xi} - \sqrt{\tau}\right)\right] \qquad \text{Eq. 2.4}$$

Where

$$k_p = \frac{15D_e}{R_p^2} \qquad \text{Eq. 2.5}$$

$$K = bV_m \qquad \text{Eq. 2.6}$$

$$I_0 = \sum_n^{\alpha} \frac{(x/2)^{2n}}{n!\,n!} = \text{modified Bessel function} \qquad \text{Eq. 2.7}$$

$$\tau = k_p\left[t - \frac{z}{u}\right] \qquad \text{Eq. 2.8}$$

$$\xi = \frac{k_p K z}{u}\left(\frac{1-\varepsilon_b}{\varepsilon_b}\right) \qquad \text{Eq. 2.9}$$

Where $\overline{q}$ is an average concentration of adsorbent (kg/m^3); q^* is a concentration of adsorbent in the steady state equilibrium (kg/m^3); C_b is a concentration of adsorbate (kg/m^3); C^* is a concentration of adsorbate in the steady state equilibrium (kg/m^3); C_o and C_f are concentration of adsorbent in the inlet and outlet side, respectively (kg/m^3); k_p is a particle-phase mass transfer coefficient (s^{-1}); D_e is an effective diffusivity; R_p is a radius of desiccant particle; K is a Henry constant (m$^3_{gas}$/m^3); u is an interstitial velocity inside desiccant bed (m/s); z is a distance of desiccant bed (m); t is a time (s), and ε_b is a porosity of desiccant bed.

In a tropical humid climate, Techajunta et al. (1999) presented the performance of a desiccant dehumidification system. The silica-gel is used in an integrated desiccant collector with light bulbs to simulate solar radiation, and forced flow of air through bed dehumidifier. Experimental results indicated that the solid desiccant can be possible to operate for the air dehumidification (adsorption process) in the night, and the regeneration (desorption process) in the day time. The desiccant column is also widely used in the process of dehumidification. The design analysis of a two-tower, silica-gel dehydration unit in drying process of natural gas was presented by Gandhidasan et al. (2001)., and the effects of various operating parameters on the dehumidification are discussed. The operating pressure of the dehumidification system increases, the silica-gel mass required decreases. The higher the regeneration temperature, the smaller are the required quantities of the hot gas. Moreover, the theoretical and experimental study of a solid desiccant packed bed dehumidifier on the transient adsorption characteristics was described by Hamed (2002). The adsorption rate is a high value at a first period of time, and decreases continually until the saturated equilibrium condition reached. There are several desiccant column configurations including solid packed bed, multiple vertical beds, radial bed, and inclined bed which have been used. Kabeel (2009) investigated on the performance of a multilayer (eight-layer) packed bed dehumidifier with the effect of design and operating parameters by theoretically and experimentally studied. The effect of inlet air humidity and velocity on the adsorption process for each bed layer is studied. Moreover, the effect of inlet temperature on desorption process is also examined. Increasing a bed length decreases humidity of the exit air, but increases the pressure drop (more power consumption). The adsorption model can be used to predict the optimum bed length. Furthermore, the radial flow bed of the solid desiccant dehumidifier was reported by Awad et al. (2008). The bed under investigation is radial flow with cylindrical shape. Five experimental test units of hollow cylindrical bed with different values of diameter ratio (outside/inside) are used. Results show that the pressure drop in radial bed is too small compared with the vertical bed. Moreover, the increase in diameter ratio increases the pressure drop within the bed, and rises the adsorption capacity for short operation periods.

The evaluation and optimization of the desiccant wheel performance was reported by Ahmed et al. (2005). A numerical model is developed to study the effect of the design parameters, such as wheel thickness, wheel speed, regeneration to adsorption area ratio, or wheel porosity, and the operating parameters, such as air flow rate, inlet humidity ratio of the air, or regeneration air temperature. Moreover, Nia et al. (2006) presented the modeling of a desiccant wheel using for dehumidifying the ventilation air of an air-conditioning system. The simulation of the combined heat and mass transfer processes is calculated by MATLAB Simulink to predict the temperature and humidity of outlet air, and optimize speed of the wheel dehumidifier. The temperature, humidity ratio, and flow rate of the air are the significant effect parameters on the performance of the desiccant dehumidification processes.

Hamed et al. (2010) studied experimentally the transient adsorption-desorption characteristics of silica-gel particles in fluidized bed. A simplified analytical model with isothermal adsorption assumption is developed. Transient values of the mass of adsorbed water in the bed, rate of adsorption, and water content in silica-gel particles are evaluated from the experimental measurements. The maximum decrease in air humidity occurs at the beginning of operating time, and the adsorption rate increases with the increase in the inlet air humidity. In addition, Ge et al. (2010) used desiccant dehumidifier as desiccant-coated heat exchangers, which are actually fin-tube heat exchanging devices coated with silica-gel and polymer materials. An experimental setup is designed and built to test the performance unit. Result shown that this desiccant-coated units well overcome the side effect of adsorption heat which occurs in the dehumidification process, and achieves good dehumidification performance under given conditions. Moreover, the silica-gel coated heat exchanger behaves better than the polymer materials.

2.2 Radiant Cooling System

A principal purpose of heating ventilation and air-conditioning (HVAC) system is to improve the human thermal comfort, which is the condition of mind that expresses satisfaction with the thermal environment. An air-conditioner must counterbalance the cooling load including the sensible and latent heat to

maintain the desired indoor conditions. The alternative technology which being more economic for providing thermal comfort to the occupants is always interested and proved to be very energy intensive.

The radiant cooling system is an alternative to convective air-conditioning system by using cool surfaces on the walls and ceiling for controlled indoor temperature. The comfort level is usually better than other space-conditioning systems because the thermal loads are satisfied directly, and an air motion in the space corresponds is required only ventilation (ASHRAE, 2008). Stetiu and Feustel (1994) studied on the radiant cooling system, and found that this system is suitable for the dry climates. The theoretical models are also evaluated to calculate the performances, such as cooling loads, heat extraction rates, room air temperature and room surface temperature distributions, or the thermal comfort. Moreover, the radiant cooling system can reduce the amount of air transported through the building because supply air is usually required ventilation only (Feustel and Stetiu, 1995). In hydronic panel system, the energy consumption to transport a given amount of thermal energy is less energy approximately 5% of fan energy; therefore the energy consumption and peak demand requirement of the air-conditioning system are reduced. The peak demand requirement of the radiant cooling system also compared to conventional all air systems, as seen in Fig.2.1.
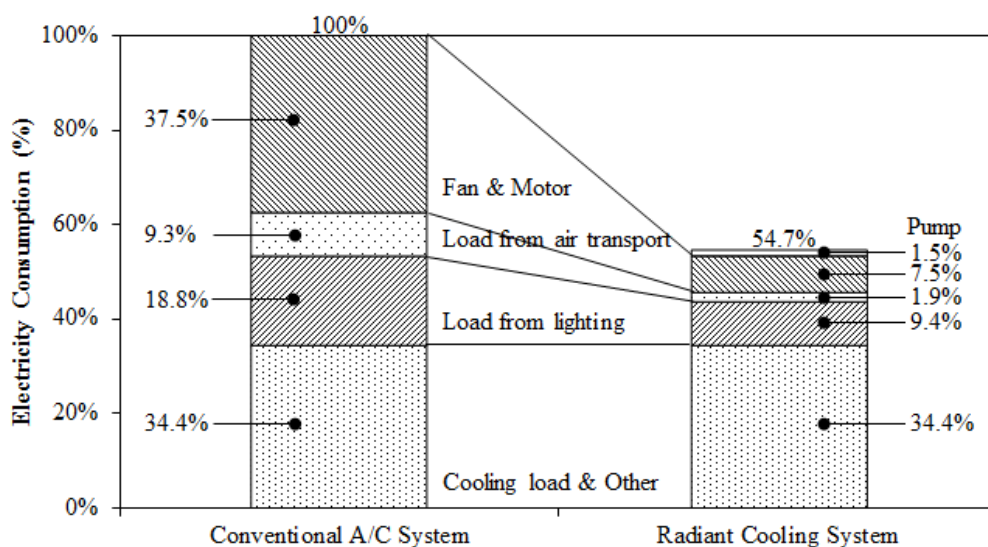
Fig. 2.1 Comparison of electrical consumption for air-conditioning system

(Source: Feustel and Stetiu, 1995)

In Europe, the radiant cooling with the ceiling panel has been refined and used successfully for more than 20 years (Mumma, 2001). The cooling panels are installed on the ceiling, or in some cases hung from a high ceiling. Cooling water is supplied to the cooling panels at the panel surface temperature above a dew-point temperature to avoid condensation of moisture. Under conditions of hot and humid climate in Thailand, Prapapong and Surapong (2006) reported an experimental and simulation study on application of radiant cooling and ventilation air. The temperature of water supplied is maintained 24°C to avoid moisture condensation on the panel. The experiments are investigated on the cool period of December, the hot and dry period of March and the humid period of May. The total area of cooling panel is 7.5 m^2 for night time application only. The TRNSYS program is simulated to compare between radiant cooling and conventional air-conditioning system. The results indicated that the radiant cooling can improve the thermal comfort conditions, and the energy consumption is less than the general conventional air-conditioning system. Moreover, the cooling panel with using cool water supplied from cooling tower in building under the southern climate of Thailand was investigated by Ar-U-Wat and Juntakan (2006). The predicted mean vote values are in the ranges of ±0.5, which are in the comfortable ranges for all selected days of the night time and early morning (until 10:00). Energy savings can be obtained approximately 40% by the use of radiant cooling system instead of the conventional air conditioner.

Furthermore, the radiant cooling systems can satisfy only the sensible heating condition. In the area of high humidity, the ambient air brings in a lot of the contents of moisture. The moisture presents the major problem for the human comfort and the condensation on cooling panel surface, so unitary dehumidifiers should be used (Mazzei et al., 2005). The desiccant dehumidification based on the air-conditioning systems offer a promising alternative to the conventional air-conditioning systems using vapour compression refrigeration, especially under conditions involving high latent loads to achieve high performance over a wide range of operating conditions. The latent load and indoor air quality are improved by the use of the desiccant dehumidifiers with adsorbing moisture directly and capturing the contamination simultaneously (Daou, et al., 2006). The detailed studies of the desiccant-based hybrid air-conditioning systems were presented by Dhar and Singh

(2001) that the hybrid systems use lower energy consumption as compared to conventional vapour compression refrigeration based air-conditioning systems. Moreover, the applications of solid desiccant dehumidification for air-conditioning system in residential buildings were investigated by Visit and Juntakan (2009). The using of solid desiccant dehumidifiers to remove water vapour from the ventilation air before passing into the air-conditioning room can be improving thermal comfort conditions, and also reducing the energy consumption of latent heat load in a tropical humid climate. A combined system of chilled ceiling, displacement ventilation and desiccant dehumidification were investigated by Nui et al (2002) and Hao et al. (2007). The desiccant dehumidifier is required to maintain the interior air humidity in comfort zone, and protect the water condensation on cooling panels. Mathematical models are used to estimate the thermal comfort levels and the energy saving potential of the combined system. The conclusions of comparison with a conventional all-air system, the combined system were to save about 8.2% of total primary energy consumption, and achieve better the levels of acceptable indoor air quality and thermal comfort.

2.3 Thermal Comfort

In general, the human thermal comfort condition occurs when body temperatures are held within narrow ranges, skin moisture is low, and the physiological effort of regulation is minimized. Temperature, air speed, humidity, their variations, and personal parameters of metabolism and clothing insulation are primary factors that directly affect energy flow and the thermal comfort. Moreover, secondary factors, such as age adaptation, sex, and seasonal and circadian rhythms are only slight differences in preferred of thermal comfort conditions. In hot and humid climate, air movement and air moisture will be an important factor in determining the thermal comfort.

As reference by ANSI/ASHRAE Standard 55 (1992), the acceptable ranges of operative temperature and relative humidity are 20-26°C and 30-60%, respectively. In the tropical region, such as Thailand climatic zones, the thermal comfort survey using 1,520 Thai volunteers from different climatic regions of

Thailand with considered parameters, such as air dry-bulb temperature, relative humidity, air velocity, the acclimatization to the use of air conditioner, or education level was investigated (Yamtraipat et al., 2005). The air temperature and relative humidity conditions at 26°C and 50%-60% are considered as the human comfortable environment. A ventilation comfort chart for the effect of air velocity on thermal comfort in non-conditioned spaces using Thai volunteers 183 male and 105 female college age under Bangkok ambient condition was presented by Khedari et al. (2000). The commercial electric fans were used to control the air velocity in the range of 0.2 to 3 m/s. Thermal sensation vote was recorded by a questionnaire. The interior air temperature and relative humidity in the comfort room varied between 26°C- 36°C and 50-80%RH, respectively. In the case of air-conditioned building, Nicol (2004) suggested that the air-conditioning area with the interior air ventilation system can improve the thermal comfort levels equivalent to be raising the comfort temperature in the range of 0 to 3.4°C for increasing velocity 0.1 to 1 m/s.

In this study, the thermal comfort (Predicted Mean Vote, PMV, and Predicted Percentage Dissatisfied, PPD) were calculated using the equations proposed by Fanger (1970). The PMV is an index that predicts the mean value of people ratings on a seven-point thermal-sensation scale as follows: +3 = hot, +2 = warm, +1 = slightly warm, 0 = neutral, -1 = slightly cool, -2 = cool, and -3 = cold. The PPD is an index that predicts the percentage of people likely to feel thermally uncomfortable as anybody not voting slightly cool, slightly warm, or neutral. For example, the PPD of 10% corresponds to the PMV range of ±0.5, and even with PMV = 0, about 5% of the people are dissatisfied. Ranges of PMV for thermal comfort conditions are shown in Table 2.2. The functional relationships between PMV and PPD are given by Eq. 2.10 and Eq. 2.11.

Table 2.2 Ranges of PMV for thermal comfort conditions

Item	Details	Value
1	Comfortable	-0.5 to 0.5
2	Warm	0.5 to 1.0
3	Cool	-1.0 to -0.5
4	Unacceptably warm	Over 1.0
5	Unacceptably cool	Under -1.0

(Source: From ASHRAE Standard 55, 1992)

$$PMV = [0.303\exp(-0.036M) + 0.028]L \qquad \text{Eq. 2.10}$$

$$PPD = 100 - 95\exp[-(0.0335PMV^4 + 0.2179PMV^2] \qquad \text{Eq. 2.11}$$

Where PMV is predict mean vote. M is rate of metabolic heat production (W/m²) and L is the thermal load on the body (W/m²).

For a neutral condition of the thermal comfort zone, there is no heat storage either in the core or in the skin compartment. The metabolic rate and work must match heat dissipation as a requiment for thermal neutrality to be reached. Fanger (1970) combined heat transfer equations to obtain the following equation for evaluation of the neutral condition.

$$L = M - W - 3.96 \times 10^{-8} f_{cl}[(T_{cl} + 273)^4 - (T_r + 273)^4]$$
$$- f_{cl}h_c(T_{cl} - T_a) - 3.05[5.73 - 0.007(M - W) - P_v]$$
$$- 0.42[(M - W) - 58.15] - 0.0173M(5.87 - P_v)$$
$$- 0.0014M(34 - T_a) \qquad \text{Eq. 2.12}$$

Where W is external work accomplished (W/m²); f_{cl} is clothing area factor; T_{cl} is clothing temperature (°C); T_r is mean radiant temperature (°C); T_a is air temperature (°C); h_c is convective heat transfer coefficient (W/m².K), and P_v is partial pressure of water vapor in moist air (kPa).

As part of this calculation, clothing temperature is found by iteration as

$$T_{cl} = 35.7 - 0.028(M - W) - R_{cl}\{39.6 \times 10^{-9} f_{cl}[(T_{cl} + 273)^4$$
$$- (T_r + 273)^4] + f_{cl}h_c(T_{cl} - T_a)\} \qquad \text{Eq. 2.13}$$

Where

$$W = 5.5 - 15(M_{act} - 0.8) \qquad \text{Eq. 2.14}$$

$$R_{cl} = 0.155 I_{cl} \qquad \text{Eq. 2.15}$$

$$h_c = \begin{cases} 2.38(T_{cl} - T_a)^{0.25} & 2.38(T_{cl} - T_a)^{0.25} > 12.1\sqrt{V} \\ 12.1\sqrt{V} & 2.38(T_{cl} - T_a)^{0.25} < 12.1\sqrt{V} \end{cases} \qquad \text{Eq. 2.16}$$

$$f_{cl} = \begin{cases} 1.0 + 0.2I_{cl} & I_{cl} < 0.5\,\text{clo} \\ 1.05 + 0.1I_{cl} & I_{cl} > 0.5\,\text{clo} \end{cases} \qquad \text{Eq. 2.17}$$

Where M_{act} is activity level (met); R_{cl} is thermal resistance, (m².K/W); V is air velocity (m/s); f_{cl} is clothing area factor, and I_{cl} is thermal resistance (clo).

2.4 Modeling and Simulation

The simulation tools under investigation consisted of ANSYS version 13.0 and TRNSYS version 16.0 software. The ANSYS software is a computational fluid dynamics (CFD) program, which is often used to solve the governing equation of the fluid dynamic, heat transfer problem and associated phenomena, such as the Navier-Stokes, energy equations or chemical reactions by numerical method. TRNSYS software is a transient simulation program, which consists of the mathematical models with the ordinary differential or algebraic equations for subsystem components.

The CFD with finite volume method technique is very powerful and using a wide range of many applications area (Tomas Norton and Da-Wen Sun, 2006). Hassan and Noam (2008) investigated an effect of duct with different cross-sectional geometries such as square, circular, or triangular on the performance of a solid desiccant (silica-gel) by using a finite control-volume method and validated relative to available experimental data. The circular duct is the best cross-sectional geometries with a low pressure drop and a high adsorption rate. Moreover, Masoud and Mohsen (2008) reported an effect of two different sizes of absorbent in a packed bed column on the dehumidifier performance by CFD modeling and experimental study. The replacing of the big silica-gel absorbents with the small size, as a result the water adsorption rate and pressure drop increase. The designed simulation system using TRNSYS and CFX programs with a desiccant silica-gel bed (DB) and a photovoltaic air collector (PVAC) was investigated by Punlek et al. (2009). The DB system is used to dehumidify air before passing through the drying chamber. The dehumidifying unit has three beds of silica-gel in a DB case, such as V-shape, C-shape, or P-shape. The CFX results indicated that the PVAC with fins and V-shape DB were suitable to improve performance of the drying.

In the subtropical region of Pakistan, A field assessment of thermal comfort was conducted by Memon et al. (2008). The people of the area were feeling thermally comfortable at effective temperature of $29.85^{o}C$ (operative temperature $29.3^{o}C$). The thermal acceptability assessment shows that more than 80% of occupants were satisfied at the effective temperature of $32.5^{o}C$, which is over $6.5^{o}C$

upper boundary of the ASHRAE comfort zone. Moreover, naturally ventilated classrooms and air-conditioned offices of the University were simulated by TRNSYS simulation, and the comparative systems between the conventional air-conditioning and the radiant cooling were also investigated. In the simulation, cooling tower was used to regenerate cooling water for the radiant panel. The results show that the radiant cooling system can achieve thermal comfort for most of the time of the year without a risk of condensation of moisture from air on the cooling surfaces. A comparison of the energy consumption estimates show that savings of 80% is possible when using the radiant cooling system instead of conventional air-conditioning.

In this study, the desiccant dehumidification involves modeling the moist air as multiphase flows of fluid mixture between dry air and water vapour through the solid desiccant as porous media. Mixture model in the Euler-Euler approach is used to model a simplified multiphase flows with phases move at different velocities. The porous media model, which is used for the multiphase problems, including flow through packed beds, adds a momentum source term to the standard fluid flow equations. The source term composed of two parts: a viscous loss term (Darcy), and an inertial loss term. In a simple homogeneous porous media case, it can be represented as Eq. 2.18 (ANSYS FLUENT, 2009).

$$S_i = -\left(\frac{\mu}{\alpha}v_i + C\frac{1}{2}\rho|v|v_i\right) \qquad \text{Eq. 2.18}$$

Where S_i is the source term for the momentum equation (kg/m^2.s^2), $|v|$ is the magnitude of the velocity, μ and ρ being dynamic viscosity (N.s/m^2) and density of fluid properties (kg/m^3), respectively, α is the permeability and C is the inertial resistance factor.

As a porous media model, consider the modeling of a packed bed. In turbulent flows, packed beds are modeled using both permeability and inertial loss coefficient. One technique for deriving the appropriate constants involves the use of the Ergun equation, a semi empirical correlation applicable over a wide range of Reynolds numbers and for many types of packing (Ergun, 1952):

$$\frac{|\Delta p|}{L} = \frac{150\mu}{D_p^2}\frac{(1-\varepsilon)^2}{\varepsilon^3}v_\infty + \frac{1.75\rho}{D_p}\frac{(1-\varepsilon)}{\varepsilon^3}v_\infty^2 \qquad \text{Eq. 2.19}$$

In these equations, µ is the viscosity, D_p is the mean particle diameter, L is the bed depth, and ε is the void fraction, defined as the volume of voids divided by the volume of the packed bed region. Comparing Eq. 2.18 with Eq. 2.19, the permeability and inertial loss coefficient in each component direction may be identified as

$$\frac{1}{\alpha} = \frac{150}{D_p^2} \frac{(1-\varepsilon)^2}{\varepsilon^3}$$

Eq. 2.20

$$C = \frac{3.5}{D_p} \frac{(1-\varepsilon)}{\varepsilon^3}$$

Eq. 2.21

Furthermore, the k-ε and Reynolds stress models (RSM) are solved for turbulence closure. A simple algorithm gives a method of calculating pressure and velocities. Under the finite volume method (Versteeg and Malalasekera, 1995), although the first-order upwind scheme discretization can yield better convergence, it generally will lead to less accurate results with only first-order accuracy. Therefore, the quadratic upwind differencing scheme (QUICK) discretization with third-order accuracy is used in calculating momentum, volume fraction, turbulence kinetic energy and its dissipation rate. SIMPLEC arithmetic is used in pressure-velocity coupling in order to accelerate the convergence of the continuity equation. PRESTO! scheme is applied in discretizing pressure gradient taking into account non-staggered grid.

2.5 Experimental Design

Response surface methodology (RSM) is an empirical modeling approach for determining the relationship between various interesting parameters and responses with the various desired criteria including the significance of these independent parameters on the coupled response (Myers and Montgomery, 1995). The RSM is a design experimental tool for building and optimizing an empirical regression model with collection of mathematical and statistical procedures. Consequentially, the RSM is one of the most widely used methods to solve the analysis and optimization problem in the manufacturing environments.

Fuping Qian and Mingyao Zhang (2005) used the RSM to study the natural vortex length in cyclones for determine the relationship among the natural vortex length, geometries and operating conditions. The regression models can be used for optimizing the design at a required performance level. Optimization of process variables for the preparation of expanded finger millet using the RSM with a central composite design (CCD) to fit a second order polynomial by a least square technique was investigated by Ushakumari et al. (2007). The process variables were moisture content, shape factor, and drying time, when predicted responses were expansion ratio, bulk density, sphericity, texture, and overall acceptability. The contour plots of results were superimposed to define the regions that best satisfied with compromised values, and select as the optimum conditions. Moreover, the investigating the influence of designing parameters of the parallel-plain fin (PPF) heat sink with an axial-flow cooling fan on the thermal performance, the experiment design based on the RSM was studied by Chiang (2007). Thermal performance characteristics on the thermal resistance and pressure drop are predicted by various designing parameters, such as height and thickness of fin, width of passage between fins, or distance between the cooling fan and the tip of fins in the experiment.

Furthermore, Jeong and Mumma (2003, 2004, 2007) developed a simplified cooling capacity estimating relation for top insulated and suspended metal ceiling radiant cooling panels by statistically performance data collected from analytical model using the factorial 2^k fractional experiment design method of resolution 5. The proposed regression model estimates the cooling capacity not only for the natural convection condition, but also for the mixed convection condition present in mechanically ventilated spaces. Moreover, the simplified model also clearly showed that the panel cooling capacity is enhanced by the mechanical ventilation system installed within the range of 10-39% in both steel and aluminum panels.

In topic of simulation and optimization of designed parameters for a desiccant column in radiant cooling system, the RSM with the 3^k factorial design is employed to optimize the designing parameters of desiccant column in order to obtain the low pressure drop and the high adsorption rate. The studied of designing parameters are a diameter of the column (D), an outer diameter of the radial flow bed (D_{ro}), and an inner diameter of the radial flow bed (D_{ri}). The desired responses are the

pressure drop and the adsorption rate, which assumed to be affected by three independent variables. In the 3^3 factorial designs, the quantitative form of relationship between desired responses and independent input variables can be represented as following.

$$. \ Y = f(D_v, D_{ro}, D_{ri})$$

Eq. 2.22

Where Y is the desired responses and f is the response function.

Furthermore, in topic of parametric studies for solid desiccant dehumidification in a tropical humid climate, the RSM with CCD is employed to study the effects of operating parameter. The studied of designing parameters were the temperature (T), humidity ratio (W) and mass flow rate (M) of air-stream through desiccant column. In the regression models, the quantitative form of relationship between desired responses and independent input variables can be represented as following.

$$Y = f(T, W, M)$$

Eq. 2.23

The approximation of Y is proposed using the various fitted regression models, i.e. liner with interaction model, quadratic model and squared with interaction model. The model proposed for the response Y can be represented as following (Montgomery, 2005).

$$Y = \beta_0 + \sum_{i=1}^{k}\beta_i X_i + \sum_{i=1}^{k}\beta_{ii}X_i^2 + \sum_{i<j}^{k}\beta_{ij}X_i X_j + E$$

Eq. 2.23

Where β_0 is constant, β_i, β_{ii}, β_{ij} represent the coefficients of linear, quadratic and cross product terms, respectively and E is the random error. X_i, X_j reveal the coded variables corresponding to the studied designing parameters.

Chapter 3

Methodology

This dissertation aims to design and develop the solid desiccant dehumidification with the use of the radiant cooling system for tropical climate to achieve thermal comfort. The three steps of this research works consist of system design, simulation assessment, and experiment verification. The following sections describe a methodology used in this study.

3.1 Design of Dehumidification, Radiant Cooling and Control System

3.1.1 Design of Dehumidification System

The experimental dehumidifiers consist of two columns. The first column is an adsorbed bed and the other is a desorbed bed or prepared bed. The second column is used when the desiccant media in the first column is saturated in equilibrium with surround air. The vertical and radial flow beds with spherical particles of silica-gel are also investigated in this study, as seen in Fig. 3.1.

Fig. 3.1 Experimental room (PSU low energy house)

3.1.2 Design of Radiant Cooling System

The radiant cooling system is designed using cool water supplied from cooling tower passing through the cooling panels which made of copper tube bond with aluminium sheet, which are installed at the ceiling and opaque wall in the experimental room.

3.1.3 Design of Control System

The dehumidification system uses the solid desiccant dehumidifiers to remove water vapour from the ventilation air before passing into the experimental room. In the radiant cooling system, cool water is supplied to cooling panels (wall and ceiling radiant cooling panels) and continuously circulated to the cooling tower with a closed system. Cooling tower produces cool water and stored in the storage tank. The circulated pump is operated by solenoid valve with signal from temperature sensor. The cool water is supplied to the panels in the experimental room, and circulated between cooling tower and panel, as illustrated in Fig. 3.2.

Fig. 3.2 Radiant cooling operation and control system

3.2 Simulation

The simulation tools under investigation consist of ANSYS version 13.0 and TRNSYS version 16.0 software. The ANSYS software is used to design the dehumidifiers. The influence of flow-bed geometries and the designed parameters of the desiccant column have been proposed. Moreover, TRNSYS software is used to

assess the thermal comfort of the radiant cooling system. Simulation details are given in Chapter 4. The diagram of research methodology is given in Fig. 3.3.

```
┌─────────┐      ┌──────────────────────────────────────┐
│  Start  │─────▶│ Input:                               │
└─────────┘      │   - Geometry & Meshing               │
                 │   - Solver & Viscous model Settings  │
                 │   - Fluid & Materials Properties     │
                 │   - Boundary & Initial Conditions    │
                 │   - Solution Methods                 │
                 └──────────────────────────────────────┘
                            │
                            ▼
                 ┌──────────────────────────────────────┐
                 │ Calculate :                          │
                 │   - Conservation equation            │
                 │   - Algebraic equation               │
                 │   - User-Defined Function (UDF)      │
                 └──────────────────────────────────────┘
                            │
                            ▼
                 ┌──────────────────────────────────────┐
                 │ Output:                              │
                 │   - Properties of air (T, %RH, h, ΔW, ΔP) │
                 │   - Fluid Profile (Contours & Vectors) │
                 └──────────────────────────────────────┘
                            │
           YES              ▼            NO
┌─────────┐ ◀──────────   ◇ Optimization ◇   ──────────▶
│   End   │
└─────────┘
```

(a) ANSYS software

```
┌─────────┐      ┌──────────────────────────────────────┐
│  Start  │─────▶│ Input:                               │
└─────────┘      │   - Meteorological data              │
                 │   - Configuration of construction    │
                 │   - Internal heat grains             │
                 │   - Equipment system                 │
                 └──────────────────────────────────────┘
                            │
                            ▼
                 ┌──────────────────────────────────────┐
                 │ Calculate :                          │
                 │   - Thermodynamics properties of fluid │
                 │   - Energy consumption & Economics   │
                 │   - User-Defined component Proforma  │
                 └──────────────────────────────────────┘
                            │
                            ▼
                 ┌──────────────────────────────────────┐
                 │ Output:                              │
                 │   - Properties of air (T, %RH, W, h) │
                 │   - Thermal comfort (PMV, PPD)       │
                 │   - Energy consumption               │
                 └──────────────────────────────────────┘
                            │
           YES              ▼            NO
┌─────────┐ ◀──────────   ◇ Comfort ◇   ──────────▶
│   End   │
└─────────┘
```

(b) TRNSYS software

Fig. 3.3 Research methodology for simulations

3.3 Experiment

The experiment systems is set up at the 2nd floor of the low energy house in Prince of Songkla University (PSU), Hatyai Campus, Songkhla Province located in the Southern part of Thailand (120° SE, $7^{o}0'30''$ N, $100^{o}30'25''$ E). The total floor area of the experiment room is 19.25 m^2 and height 2.8 m. The location of the experimental room is shown in Fig. 3.4.

Fig. 3.4 Location of the experiment room

In this study, the experiments are investigated including desiccant dehumidifiers testing, desiccant dehumidification for air-conditioning system and desiccant dehumidification for radiant cooling system. The first experiment is to investigate the influence of parametric studies for the solid desiccant dehumidification. Second, the solid desiccant dehumidification system for tropical climate to reduce the latent load of air-conditioning system, and improve the thermal comfort is investigated. Furthermore, the application of the desiccant dehumidifier for the radiant cooling system is also examined. The desiccant columns and the cooling panels are shown Fig. 3.5 and Fig. 3.6, respectively.

Fig. 3.5 Dehumidifiers and desiccant media
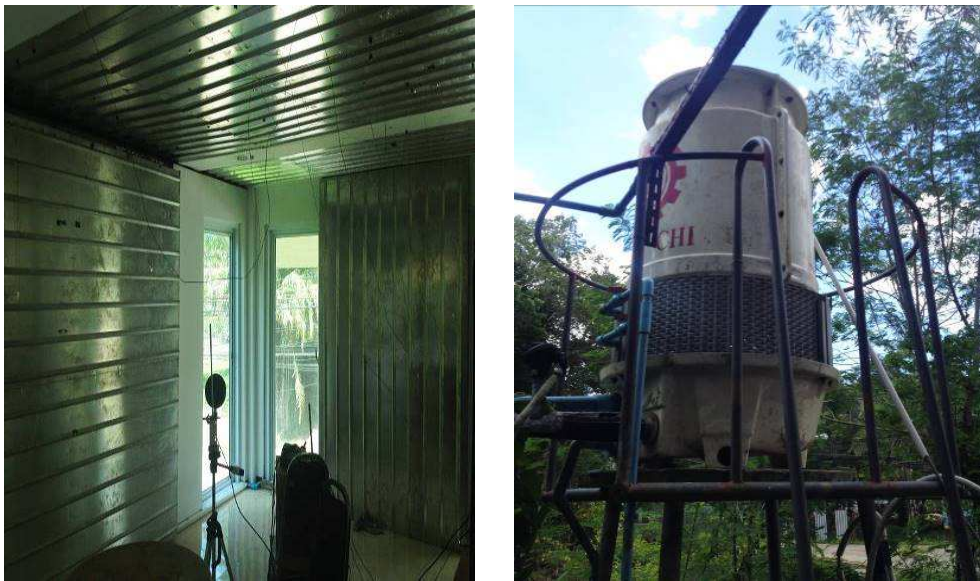
Fig. 3.6 Radiant cooling panel and cooling tower

3.4 Data Collection

For the dehumidification system, the temperature and relative humidity of the ventilation air are measured by temperature and humidity transmitter, and the mass flow rate is measured by velocity transmitter. The pressure drop in dehumidifier is measured by differential pressure transmitter. In the experimental room, the temperature and humidity transmitters, thermocouple type K, and globe thermometer

are installed to measure temperatures of interior and exterior air, relative humidity of interior and exterior air, surface temperatures of radiant cooling panels, and mean radiant temperature of interior air, respectively. Moreover, the water temperature and air mass flow rate of cooling tower are measured by thermocouple type K and anemometer. The measurement data were recorded every five minutes using data logger. In addition, the thermal comfort as PMV and PPD are calculated using the equations proposed by Fanger (1970). Table 3.1 shows the record data and the instruments used in this study. The details of instrument are described in Table 3.2.

Table 3.1 Record parameters and instruments

Item	Parameter	Instrument
	Dehumidification system	
1	Inlet and outlet air temperature	Temperature transmitter
2	Inlet and outlet air relative humidity	Relative humidity transmitter
3	Mass flow rate of ventilation air	Velocity transmitter
4	Pressure drop across dehumidifier	Differential pressure transmitter
	Radiant cooling system	
5	Interior and exterior air temperature	Temperature transmitter
6	Interior and exterior air relative humidity	Relative humidity transmitter
7	Surface temperature of cooling panels	Thermocouple type K
8	Mean radiant temperature	Globe thermometer
	Cooling tower	
9	Inlet and outlet water temperature	Thermocouple type K
10	Mass flow rate of cooling air	Anemometer

Table 3.2 Detail of instruments

Item	Instrument lists	Details
1	Temperature and humidity transmitter (duct mount)	Temperature and humidity transmitters – Model: THS64-A61-4200-N, duct-mounting type. The sensor for humidity and temperature are thin-film capacitor and RTD Pt100Ω, respectively. Output signals of these transmitters are 0-10V three wires. The linear accuracy are $\pm0.2^{\circ}$C for temperature range: 0-120°C, and $\pm2\%$RH for relatives humidity range: 0-100%RH.
2	Velocity transmitter (duct mount)	Velocity transmitter – Model: FTS04-1061-N, duct-mounting type. Output signals of these transmitters are 0-10V three wires. The linear accuracy are $\pm3\%$ of F.S. +0.2 m/s for velocity of measuring range 0-30 m/s.

Table 3.2 Detail of instruments (Continued)

Item	Instrument lists	Details
3	Differential pressure transmitter	Differential pressure transmitter – Model: 699, full scale adjustable. The sensor and diaphragm are Ceramic Al_2O_3 (96%) and Silicone with Polycarbonate PC housing. Output signals of these transmitters are 0-10V three wires. The linear accuracy are ±1% of F.S. for differential pressure of measuring range 0-500 Pa.
4	Temperature and humidity transmitter (wall mount)	Temperature and humidity transmitters – Model: testo 6651 transmitters (testo 6601 probes), wall-mounting type. The capacitive humidity sensor is in principle a plate capacitor consisting of two electrically conductive plates opposite each other. A humidity-sensitive polymer serves as the dielectric. Output signals of these transmitters are 0-10V three wires. The linear accuracy is ±0.2^{o}C for temperature range: -20-70°C and ±1.7% RH for relative humidity range: 0-90%RH, or ±1.9%RH for range: 90-100%RH.
5	Thermocouple type K	Measurement accuracy for Thermocouple type K in the range $-100 < T < 1,370^o$C is ±0.05%.
6	Globe thermometer	Globe thermometer – Model: QUESTEMP-15 is used for measurement of globe temperature to determine the mean radiant temperature. The sensor is RTD Pt100Ω. Output signals of these transmitters are 0-10V three wires. The linear accuracy of this instrument is ±0.5^{o}C for temperature range: 0-100°C.
7	Multifunction instrument for HVAC	Multifunction instrument for HVAC – Model: testo 450 is used for measurement of air mass flow rate in the cooling tower. This instrument can measure four parameters such as velocity, humidity, dew point or temperature. The linear accuracy are ±0.4^{o}C for temperature range: 0-50°C, ±2%RH for relatives humidity range: 2-98%RH, and ±3% of F.S. +0.2 m/s for velocity of measuring range 0-30 m/s.

Chapter 4

Design and Simulations

Design of solid desiccant dehumidifier and radiant cooling system are presented in this chapter. The simulation through the use of the commercial software programs, namely ANSYS version 13.0 and TRNSYS version 16.0 are also investigated. The designed parameters for optimization and the effects of different flow-bed geometries and flow-directions of air-stream through desiccant media within the desiccant column are considerate. In the radiant cooling system, the simulations are used to predict the thermal comfort assessment and air phenomena profile in the experimental room.

4.1 Desiccant column design

For this desiccant column design, the conditions at 29°C and 75%RH are considered as an exterior air (Khedari et al, 2002), and the acceptable comfort at 25°C and 50%RH is considered as an interior air (ANSI/ASHRAE Standard 55, 1992). Moreover, outdoor air supply rates recommended is 15 cfm per person for occupancy based (ANSI/ASHRAE Standard 62, 1999), and standard for air-conditioning and ventilation systems of engineering institute of Thailand under H.M. the King's Patronage (2005) is 2 m^3/h per m^2 (area based). Amount of fresh air about 50 kg/h is used to supply as ventilation air in this design. The adsorption equilibrium and breakthrough time of solid desiccant dehumidifier are calculated by Langmuir equation and Klinkenberg model. The details of calculated procedure are given in Appendix B. The column designs used in this study are presented in Table 4.1.

Table 4.1 Desiccant column design

Item	Parameter	Value
1	Exterior air temperature and relative humidity	29°C, 75%RH
2	Exterior air humidity ratio (C_o)	19 g_w/kh_{da}
3	Interior air temperature and relative humidity	25°C, 50%RH
4	Exterior air humidity ratio (C_f)	10 g_w/kh_{da}
5	Ventilation air	50 kg/h
6	Silica-gel requirement	10 kg
7	Breakthrough time (C_f/C_o = 0.82)	3.77 hour
8	Equilibrium time (C_f/C_o = 0.99)	5.86 hour

4.2 Effect of Flow-Bed Geometries on Desiccant Column

        The aim of this section is to investigate the effects of different flow-bed geometries and flow-directions of air-stream through desiccant media upon pressure drop (ΔP) and adsorption rate (ΔW). The influence of flow-bed geometries and flow-directions of air-stream within the desiccant column are considerate, i.e. vertical bed, segment bed, radial bed, conical bed and the flow from inner to outer of desiccant (α_1-direction), the flow from outer to inner of desiccant (α_2-direction), with approximately 3 mm diameter, porosity of 0.4, and bulk density of 670 kg/m^3 of silica-gel as the working desiccant.

        For dehumidifier design, requirement of silica-gel in the bed is 10 kg with column volume of 0.045 m^3 and various mass flow rates between 10 and 85 kg/h. The bed geometries under investigation are vertical bed, segment bed, radial bed and conical bed (S1, S2, S3 and S4), as shown in Fig. 4.1. In this study are examined in 2 cases for flow-directions through desiccant media namely, flow from inner to outer and flow from outer to inner, as given in Fig. 4.2.
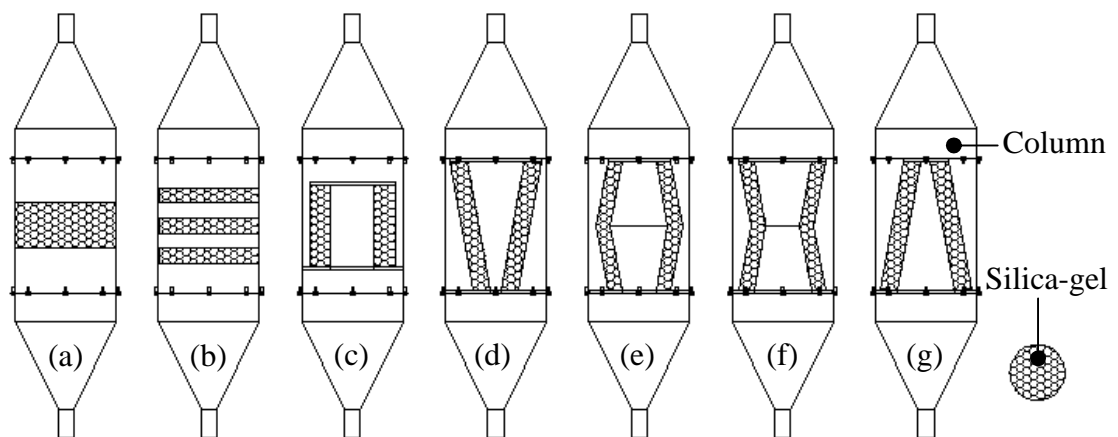
Fig. 4.1 Schematic of the bed geometries: (a) vertical bed (b) segment bed (c) radial bed (d) conical bed S1 (e) conical bed S2 (f) conical bed S3 (g) conical bed S4

4.2.1 The Influence of Flow-bed Geometries

        The comparative numerical simulations for the pressure drop and the adsorption rate of these bed geometries in α_1-direction are depicted in Fig. 4.3. In

consideration of the pressure drop, increasing mass flow rates rises the pressure drop, which are classified according to three ranges as high pressure drop (6.59-565.23 Pa), medium pressure drop (6.52-123.03 Pa) and low pressure drop (1.10-58.97 Pa) for the conical bed S1, the vertical and segment bed, and the radial and conical bed S2, S3, S4. In consideration of the adsorption rate, increasing mass flow rates rapidly increases the adsorption rate especially with the low mass flow rates (less than 30 kg/h); after that, it is almost constant value because of its maximum designed adsorption rate (0.46 kg$_w$/h). However, the adsorption rate is less than 0.38 kg$_w$/h for the conical bed S1.

(a) α$_1$-direction   (b) α$_2$-direction
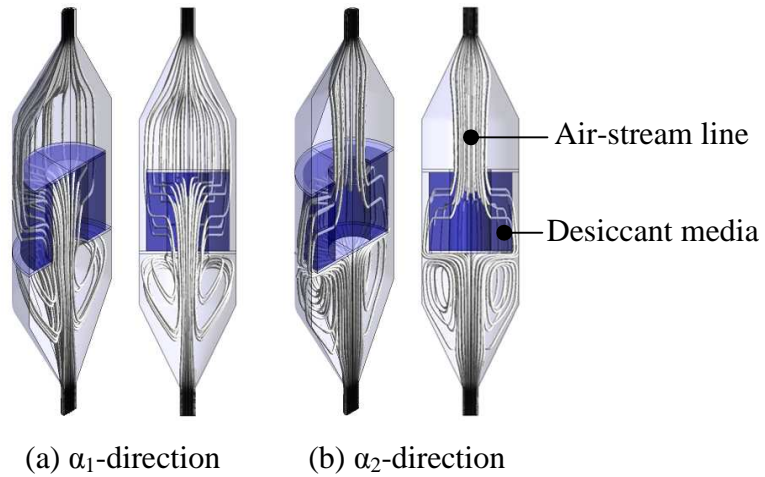
Fig. 4.2 The cross-section of the radial bed with the different flow-directions of air-stream through desiccant media
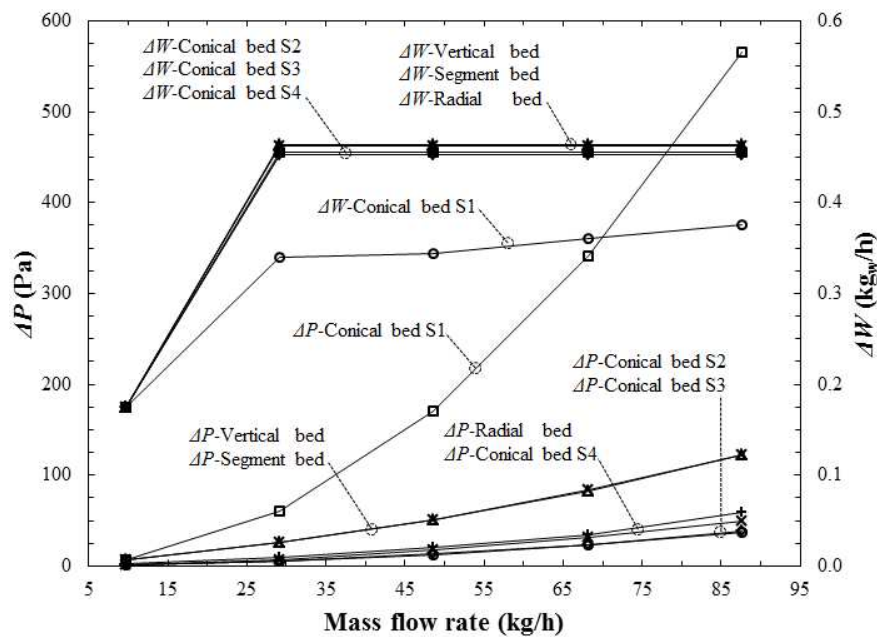
Fig. 4.3 The effect of flow-bed geometries with α$_1$-direction

The pressure and humidity ratio distributions within the column with mass flow rate of 48.65 kg/h predicted through simulation are given in Fig. 4.4. The conical bed S1 has high static pressure (175 Pa) in bottom column or inlet zone (red zone) and zero Pa (gage) in outlet zone to ambient (blue zone). Moreover, the vertical bed, the radial bed and the conical bed S2 have less pressure drop than 50.75, 20.61 and 12.99 Pa, respectively. For moisture air with inlet humidity ratio of 0.0180 kg_w/kg (red zone) passes through desiccant media, outlet humidity ratio of vertical, radial, conical bed S1 and S4 decrease to 0.0087, 0.0086, 0.0111 and 0.0088 kg_w/kg, respectively.
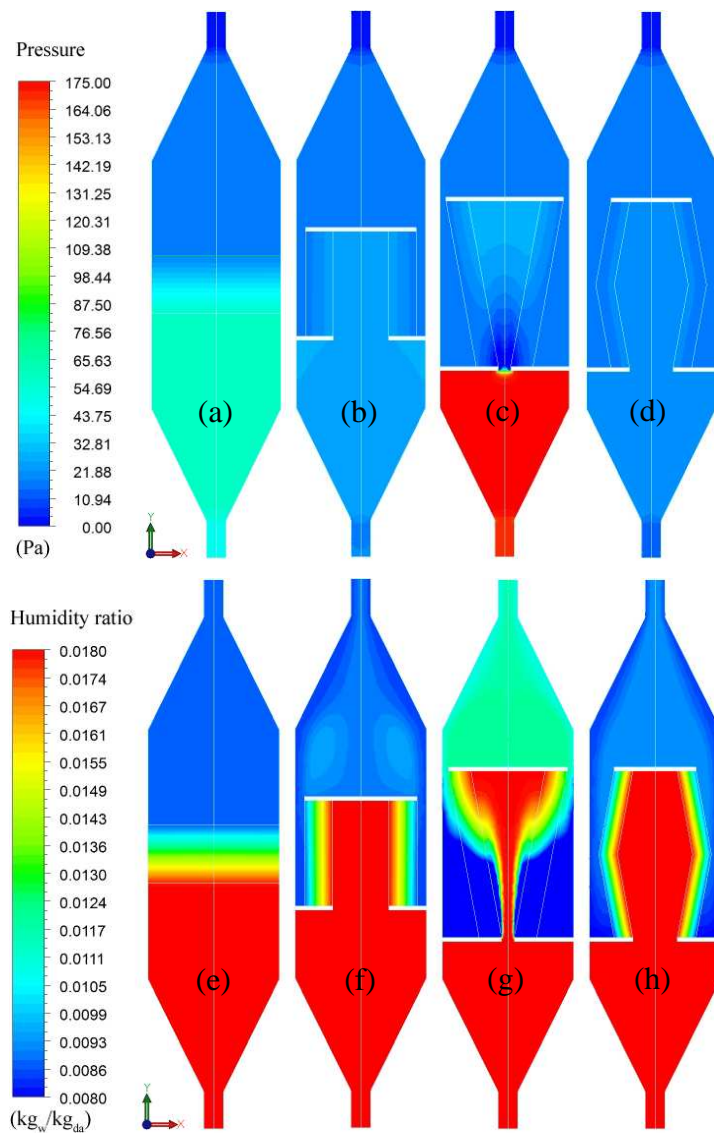
Fig. 4.4 The contour plots of static pressure and humidity ratio with mass flow rate of 48.65 kg/h for (a) vertical bed (b) radial bed (c) conical bed S1 (d) conical bed S2 and (e) vertical bed (f) radial bed (g) conical bed S1 (h) conical bed S2

In α_2-direction, the phenomenon within the desiccant columns and capacity are similar to the air-stream through desiccant media in α_1-direction except the conical bed S1 and S4. The conical bed S1 with α_2-direction has less pressure drop than the conical bed S1 with in α_1-direction, and increasing the adsorption rate. Moreover, the conical bed S4 with α_2-direction is more pressure drop than the conical bed S4 with α_1-direction, and decreasing the adsorption rate. The capacity of desiccant column with mass flow rate of 48.65 kg/h for α_1-direction and α_2-direction are described in Fig. 4.5.
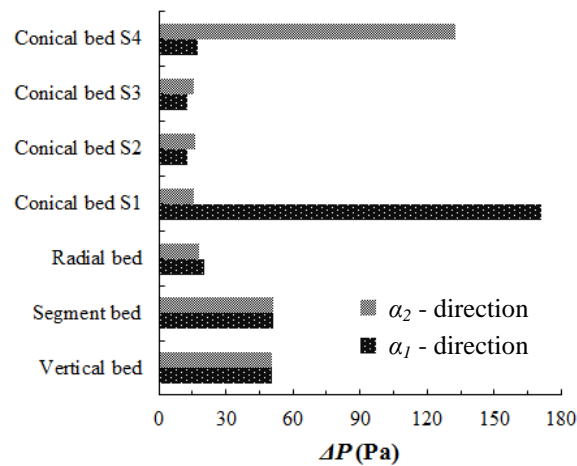
(a) Pressure drop
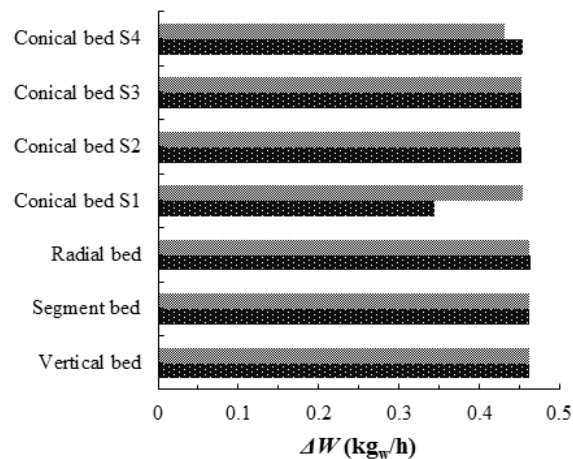
(b) Adsorption rate

Fig. 4.5 The capacity of desiccant column with mass flow rate of 48.65 kg/h

The velocity fields inside central plane of the radial bed with mass flow rate of 48.65 kg/h predicted through simulation are given in Fig. 4.6, which display the air-stream patterns are expressed with a collection of vector arrows. The

magnitude of velocity is represented with collections of colours which the meanings of these colours are explained with the vertical colour bars in the figure. In α_1-direction and α_2-direction, the incoming process of air-stream was forced from bottom column with inlet velocity 5 m/s through dehumidifier by the flow from inner to outer and outer to inner of desiccant media, respectively. The maximum magnitude of velocity is occurred in the centre and middle layer of the column. The reverse swirl of α_1-direction is found the near inlet and outlet region of radial bed, while it is appeared especially the near inlet region of bottom layer for α_2-direction.
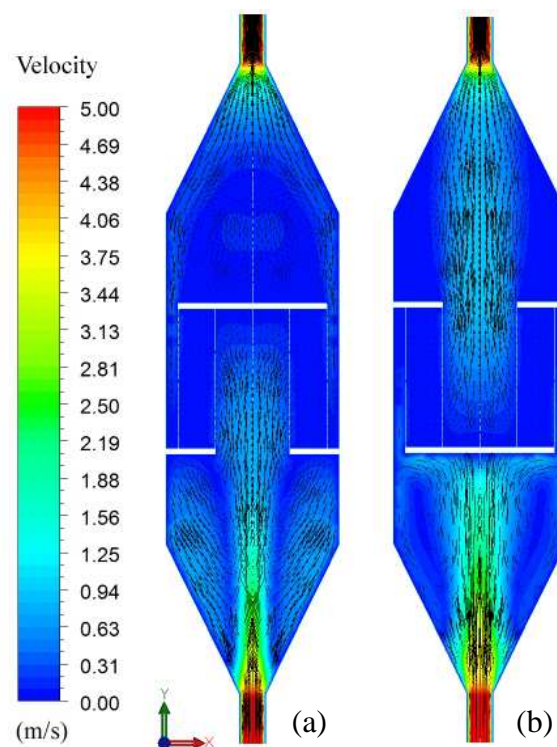
Fig. 4.6 Velocity vectors and velocity magnitude for the radial bed with different flow direction (48.65 kg/h): (a) α_1-direction (b) α_2-direction

4.2.2 ANOVA analysis

In this study for the influence of flow-bed geometries, the adsorption rate is converted to convergent designed value with high mass flow rate, whereas increasing mass flow rates rises the pressure drop. The test for significance of the regression model and the test for significance on individual model coefficients need to be performed for reliability of the prediction model obtained. Through the backward elimination process, the final fitted regression models of the pressure drop in terms of

the mass flow rate are presented in Table 4.2. The effect examinations of model coefficients, a small probability value (P-value) suggests that the influence of the factor is significant. The probability values for those terms are lower than 0.1. Therefore, the influential degree of the factor is higher than the 90% confidence level.

Table 4.2 Regression models for the pressure drop

Type	Regression models	Reliability
Vertical bed		
	ΔP (Pa) = 11.039340 + 0.014861× Flowrate^2 (kg/h)	R^2=0.991, R^2 adjusted=0.988 R^2 prediction=0.960
Radial bed		
α_1-direction	ΔP (Pa) = 2.180799 + 0.007346× Flowrate^2 (kg/h)	R^2=0.998, R^2 adjusted=0.987 R^2 prediction=0.994
α_2-direction	ΔP (Pa) = 3.132560 + 0.005659× Flowrate^2 (kg/h)	R^2=0.991, R^2 adjusted=0.988 R^2 prediction=0.953
Conical bed S2		
α_1-direction	ΔP (Pa) = 1.080438 + 0.004851× Flowrate^2 (kg/h)	R^2=0.999, R^2 adjusted=0.999 R^2 prediction=0.997
α_2-direction	ΔP (Pa) = 0.533183 + 0.006273× Flowrate^2 (kg/h)	R^2=0.997, R^2 adjusted=0.996 R^2 prediction=0.990

4.3 Optimization of Designed Parameters for a Desiccant Column

This section concentrates on the numerical simulations of desiccant column with various dimensions of designed parameters for optimization in order to minimize the value of pressure drop (ΔP) and maximize the value of adsorption rate (ΔW). The comparing beds under investigation were vertical and radial flow with approximately 3 mm-diameter of silica-gel as the working desiccant in the column.

The ranges of the geometrical designed parameters are 0.2, 0.3, 0.4 m for diameter of vertical flow bed (D); 0.75, 1.00, 1.25 for ratio of outer diameter of radial flow bed (D_{ro}) to diameter of vertical flow bed and 0.375, 0.500, 0.625 for ratio of inner diameter of radial flow bed (D_{ri}) to outer diameter of radial flow bed, as shown in Fig. 4.7. Twenty-seven simulation test units of radial flow bed with different values of diameter ratio are used. For all units, amount of desiccant in the bed being 10 kg of silica-gel, column volume of 0.045 m^3 and ventilation air of 26 kg/h are used in the simulations.
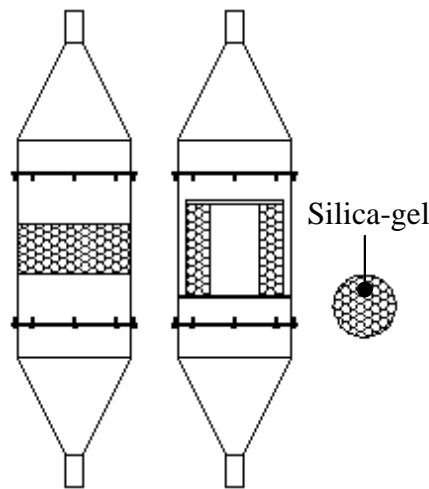
(a) Vertical and radial flow bed
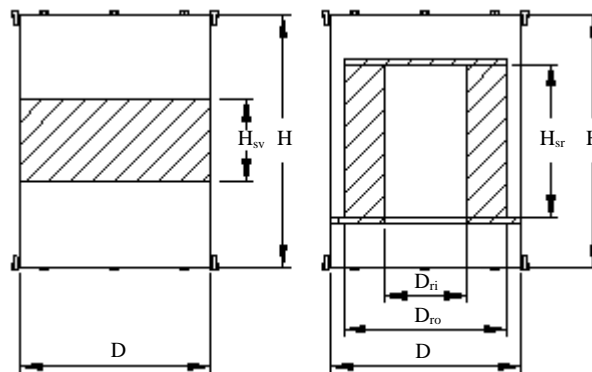
(b) Dimensions of desiccant column
Fig. 4.7 Schematic display of desiccant column and designed parameters

In this simulation study, spherical particles of silica-gel are used as the working desiccant in the column. The physical properties of silica-gel are 3 mm diameter, porosity of 0.4, and bulk density of 670 kg/m^3. The desiccant beds under investigation are the vertical flow and radial flow, as shown in Fig. 4.7a. The dimensions of designed parameters are shown in Fig. 4.7b where H_{sv}, H_{sr}, D_{ri}, and D_{ro} represent height of silica-gel for vertical bed, height of silica-gel for radial bed, inlet diameter of silica-gel for radial bed, and outlet diameter of silica-gel for radial bed, respectively, whereas H and V are height and diameter of the column.

The 3^3 factorial design, the three-level factorial design was employed to optimize the designing parameters of desiccant column in order to obtain the low pressure drop and the high adsorption rate. The studied of designing parameters are the diameter of the vertical flow bed, and the inner diameter and the outer diameter of

the radial flow bed. The desired responses are the pressure drop and the adsorption rate which assumed to be affected by three independent variables as mentioned earlier. The three levels of the geometrical designed parameters are chosen to obtain the low pressure drop and the high adsorption rate. These level settings are presented in Table 4.3 which denote the low, intermediate, and high levels by -1, 0, and +1, respectively. The simplest design in the 3^3 factorial design, which has three factors, each at three levels. Therefore, the CFD simulations are 27 treatment combinations.

Table 4.3 The simulation range and levels of designing parameter

Parameters	Ranges and levels		
	-1	0	+1
Diameter of vertical flow bed, D (m)	0.2	0.3	0.4
Outer diameter of radial flow bed, D_{ro} (m)	$0.75 \times D$	$1.00 \times D$	$1.25 \times D$
Inner diameter of radial flow bed, D_{ri} (m)	$0.375 \times D_{ro}$	$0.500 \times D_{ro}$	$0.625 \times D_{ro}$

4.3.1 Comparison between Vertical Flow Bed and Radial Flow bed

The pressure drop and the adsorption rate comparisons between vertical flow bed and radial flow bed are depicted in Fig. 4.8.
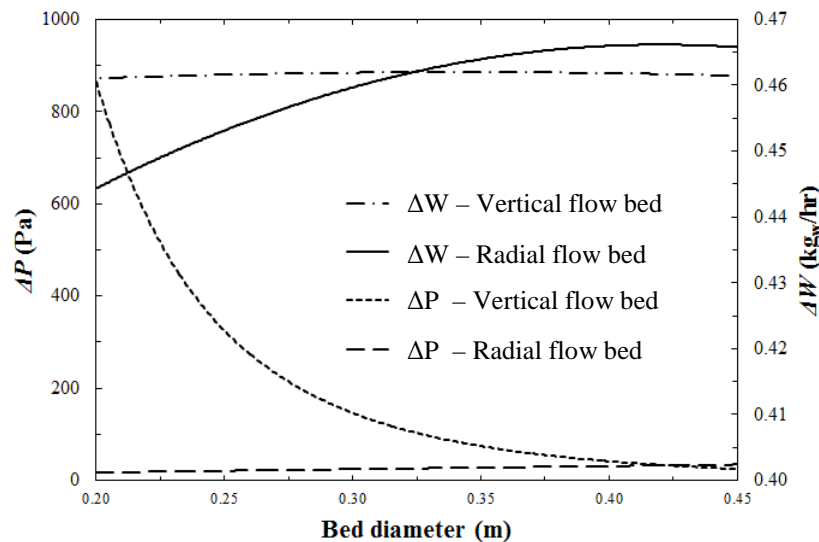
Fig. 4.8 Pressure drop and adsorption rate for various bed diameter of the column

In case of bed diameter between 0.20 to 0.45 m, increasing vertical flow bed diameter decreases the pressure drop within the column and varies the adsorption rate around 0.4615 kg_w/h, and increasing radial flow bed diameter rises the pressure drop and the adsorption rate simultaneously.

However, the pressure drop of vertical flow bed is too high comparing with the radial flow bed under the same column diameter, but the adsorption rate of the radial flow bed is usually higher than the other one for the column diameter more than 0.32 m. The predicted pressure and humidity ratio profiles through simulation within the column for bed diameter 0.35 m are given in Fig. 4.9.
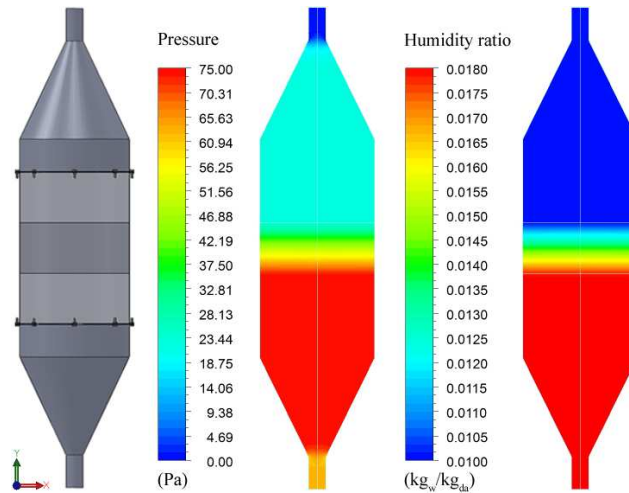
(a) The vertical flow bed
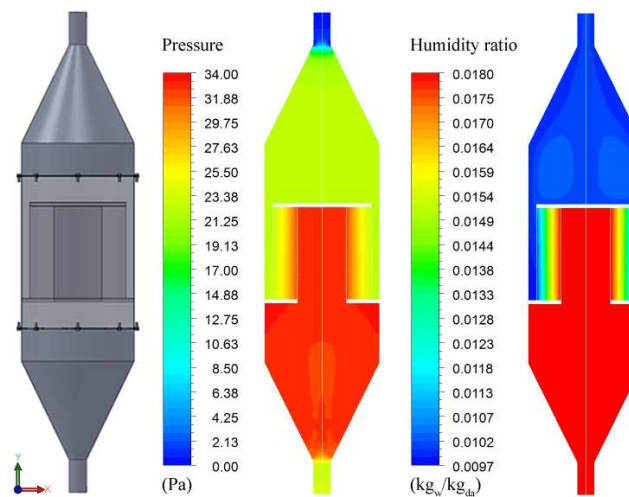
(b) The radial flow bed

Fig. 4.9 Contours of pressure and humidity ratio for bed diameter 0.35 m

4.3.2 Optimization of Designing Parameters

The purpose of optimization for the desiccant column in this study is to find the optimal values of designing parameters, the inner diameter and the outer diameter of radial flow bed, in order to minimize the value of the pressure drop and

maximize the value of the adsorption rate. The graphical optimization technique is adopted. For diameter of the vertical flow bed being 0.20, 0.30 and 0.40 m, the contour plots are superimposed and the regions that best satisfied, which the pressure drop less than 30 Pa and the adsorption rate more than 0.4615 kg$_w$/h. The overlapped area between the inner diameter and the outer diameter of radial flow bed shown in Fig. 4.10 can be recommended as optimum zone. The practical optimum zone of the inner diameter and the outer diameter are 0.15 and 0.30 m, respectively; as a result, the feasible and optimum condition values are 23.34 Pa and 0.4634 kg$_w$/h.

(a) Radial flow bed with D$_v$ = 0.2 m

(b) Radial flow bed with D$_v$ = 0.3 m

(c) The radial flow bed with D$_v$ = 0.4 m
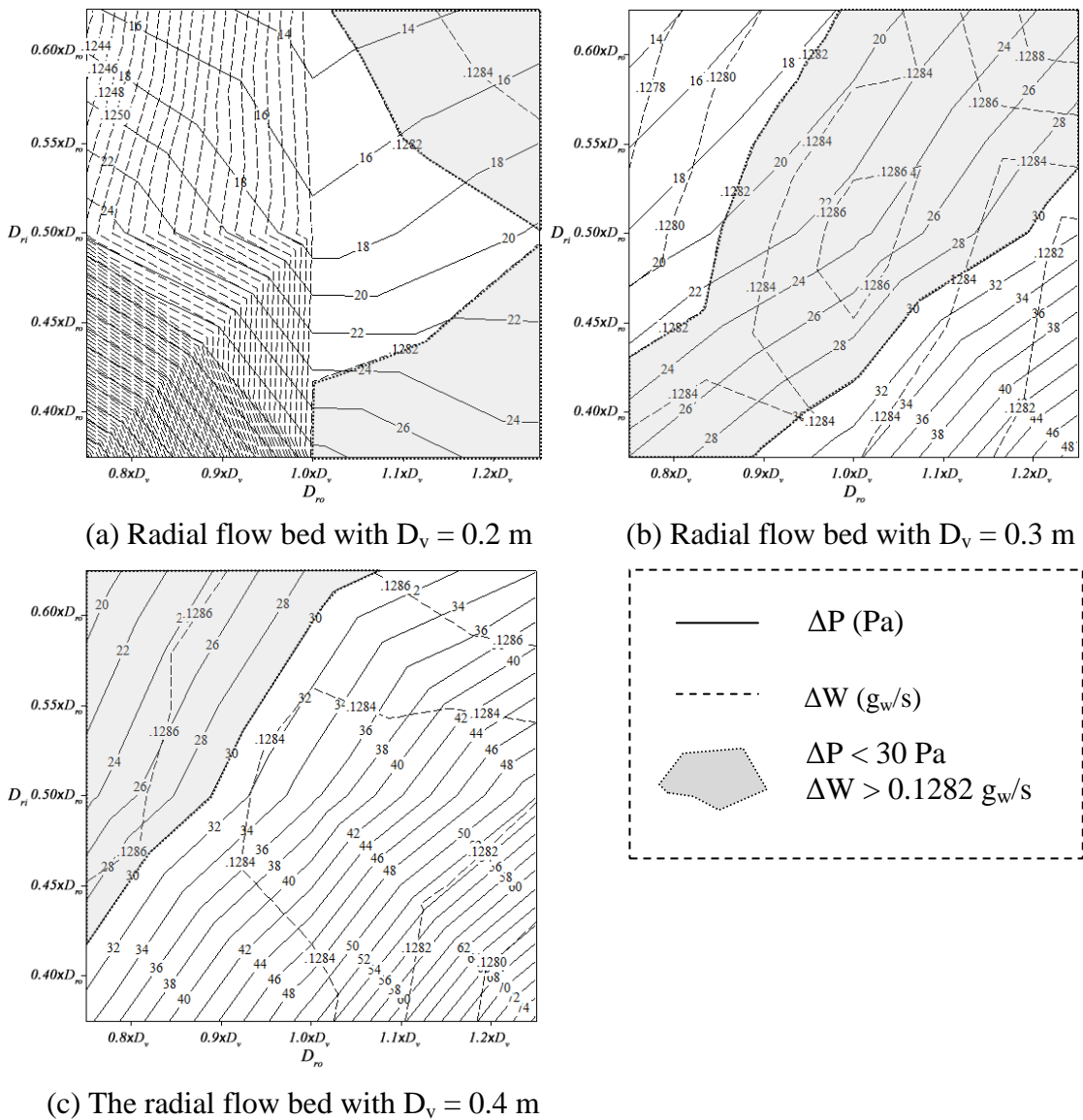
Fig. 4.10 Superimposed contour plots showing the shaded overlapping area for which

ΔP < 30 Pa, ΔW > 0.1282 g$_w$/s

4.3.3 ANOVA Analysis

For reliability of the prediction model obtained in this study, the test for significance of the regression model and the test for significance on individual model coefficients need to be performed. Through the backward elimination process, the final fitted regression models of the pressure drop and the adsorption rate of radial flow bed for 0.20, 0.30 and 0.40 m in terms of the inner diameter and the outer diameter are presented in Table 4.4. The effect examinations of model coefficients are tabulated in Table 4.5. A small probability value (P-value) suggests that the influence of the factor is significant. The probability values for those terms are lower than 0.05. Therefore, the influential degree of the factor is higher than the 95% confidence level.

Table 4.4 Regression models of the radial flow bed for D_v 0.20, 0.30, and 0.40 m

D_v (m)	Regression models	
0.2	ΔP (Pa)	$= 270.298645 - 305.044619 \times D_{ro} - 270.825267 \times D_{ri} + 93.989565 \times D_{ro} \times D_{ro} + 191.054880 \times D_{ro} \times D_{ri}$
	ΔW (g_w/s)	$= -0.013303 + 0.161669 \times D_{ro} + 0.205078 \times D_{ri} - 0.054507 \times D_{ro} \times D_{ro} - 0.076377 \times D_{ro} \times D_{ri} - 0.115395 \times D_{ri} \times D_{ri}$
0.3	ΔP (Pa)	$= 45.483137 + 54.227742 \times D_{ro} \times D_{ro} - 239.036379 \times D_{ro} \times D_{ri} + 169.067363 \times D_{ro} \times D_{ri} \times D_{ri}$
	ΔW (g_w/s)	$= 0.131645 - 0.014442 \times D_{ri} - 0.003185 \times D_{ro} \times D_{ro} + 0.014360 \times D_{ro} \times D_{ri}$
0.4	ΔP (Pa)	$= -51.972707 + 175.119314 \times D_{ro} - 234.084622 \times D_{ro} \times D_{ri} + 126.977604 \times D_{ri} \times D_{ri}$
	ΔW (g_w/s)	$= 0.129107 - 0.001625 \times D_{ro} + 0.001915 \times D_{ro} \times D_{ri}$

Table 4.5 ANOVA table for the regression models using radial flow bed with $D_v = 0.3$ m (after backward elimination)

Pressure drop, ΔP

Term	Coefficient	Standard error	T-ratio	P-value
Constant	45.483137	7.312315	6.220074	0.001570
$D_{ro} \times D_{ro}$	54.227742	7.513510	7.217365	0.000796
$D_{ro} \times D_{ri}$	-239.036379	61.678333	-3.875532	0.011695
$D_{ro} \times D_{ri} \times D_{ri}$	169.067363	61.629797	2.743273	0.040634

Standard error	= 1.534078	R^2	= 0.987413	
Coefficient of variation	= 5.793317	R^2 adjusted	= 0.979862	
PRESS	= 47.619197	R^2 for prediction	= 0.949064	

Table 4.5 ANOVA table for the regression models using radial flow bed with $D_v = 0.3$ m (after backward elimination) (Continued)

Adsorption rate, ΔW

Term	Coefficient	Standard error	T-ratio	P-value
Constant	0.131645	0.000997	132.082556	0.000000
D_{ri}	-0.014442	0.003551	-4.067257	0.009660
$D_{ro} \times D_{ro}$	-0.003185	0.000883	-3.606138	0.015443
$D_{ro} \times D_{ri}$	0.014360	0.003471	4.137794	0.009016

Standard error	= 0.000230	R^2	= 0.810534
Coefficient of variation	= 0.179285	R^2 adjusted	= 0.696854
PRESS	= 0.000001	R^2 for prediction	= 0.400748

4.4 Solid Desiccant Dehumidification for Air-conditioning System

The aim of this section is to study and design the solid desiccant dehumidification system suitable for tropical climate to reduce the latent load of air-conditioning system, and improve the thermal comfort. Different dehumidifiers such as desiccant column and desiccant wheel are investigated, as shown in Fig. 4.11. The ANSYS and TRASYS softwares are used to predict the results of dehumidifiers and the desiccant cooling systems, respectively.
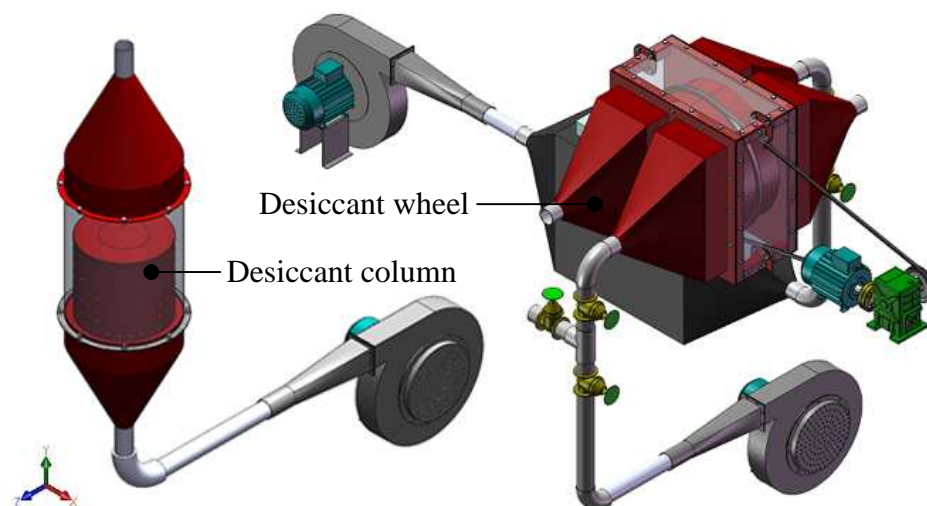
Fig. 4.11 The types of solid desiccant dehumidifiers

The bed geometry of the stationary dehumidifier on desiccant column is radial, i.e. a hollow cylindrical bed, with an inner and outer diameter of 0.15 m and 0.30 m, respectively. A length of the packed bed was 0.465 m. For rotary beds, the

desiccant wheel with a diameter of 0.5 m and a length of 0.2 m is divided into two equal parts for dehumidification and regeneration process. The air to be dried flows through one side of the wheel, while at the same time, the heated air stream dries the desiccant on the other side of wheel. The spherical particles of silica-gel are used as the working desiccant in the dehumidifiers. Amount of desiccant in the bed is close to 15 kg of silica-gel. The physical properties of silica-gel are: average diameter: 3 mm, porosity: 0.4, and bulk density: 670 kg/m^3. Moreover, the air flow rate of 60 kg/h is used in the simulations.

4.4.1 Comparison between desiccant column and desiccant wheel

The pressure drop of desiccant column is higher compared to the desiccant wheel under the same conditions, but the adsorption rate of the desiccant column is also higher than the desiccant wheel. The predicted static pressure and humidity ratio distributions through simulation for the desiccant column and the desiccant wheel are given in Fig. 4.12 and Fig. 4.13, respectively.
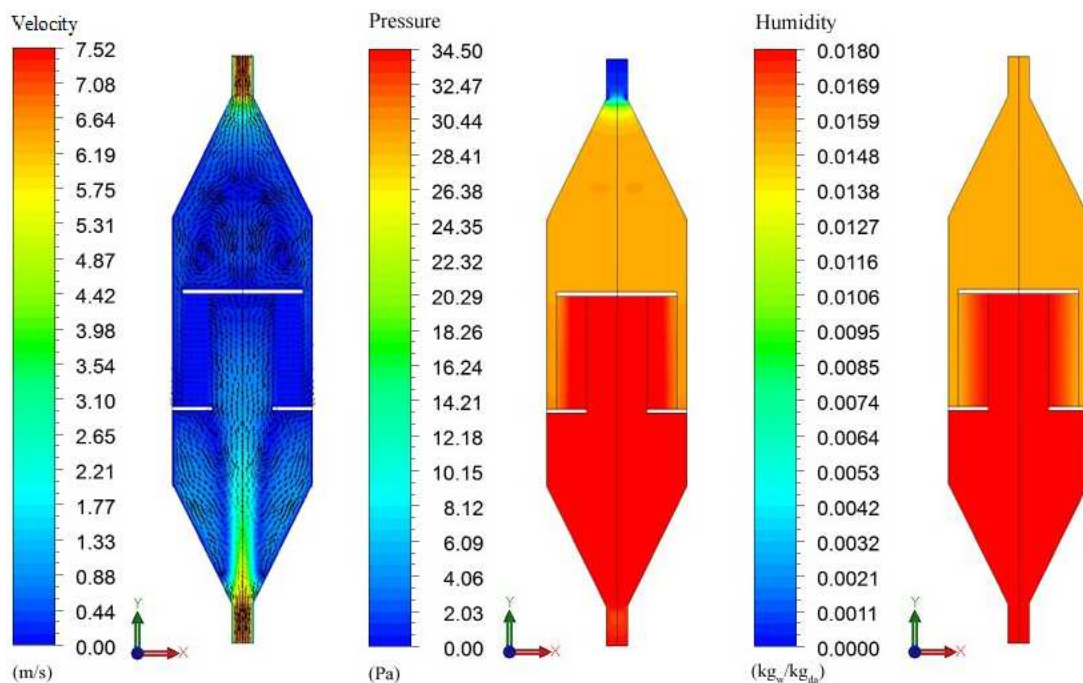
Fig. 4.12 The contour plots inside central plane (z=0) of the desiccant column
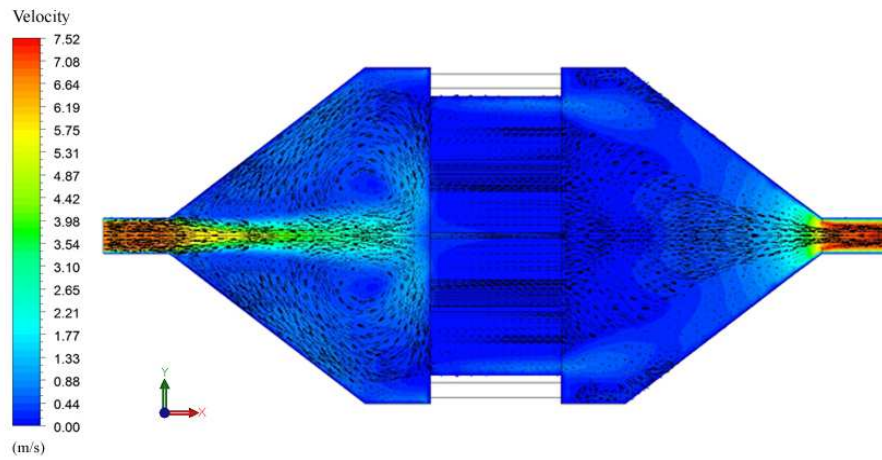
(a) Contour plots of velocity
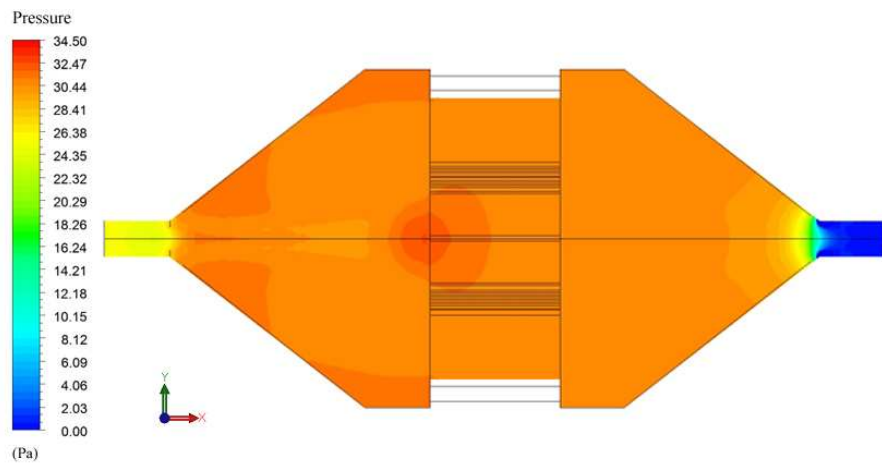
(b) Contour plots of static pressure
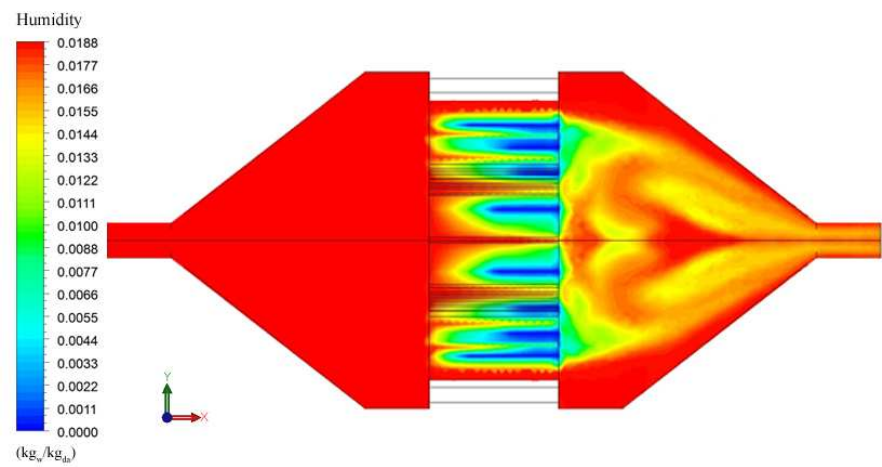
(c) Contour plots of humidity ratio
Fig. 4.13 The contour plots inside central plane (z=0) of the desiccant wheel

(Adsorption part)

The desiccant column has high static pressure (34.49 Pa) in bottom column or inlet zone (red zone) and zero Pa (gage) in outlet zone to ambient (blue zone). The desiccant wheel has a pressure drop less than 25.77 Pa. For inlet moist air with humidity ratio of 0.0180 kg_w/kg (red zone) passes through desiccant media, the humidity ratio at the outlet of the desiccant column decreased to 0.0154 kg_w/kg (orange zone). In the case of the desiccant wheel, humidity ratio at the outlet decreases to 0.0168 kg_w/kg (yellow zone). The velocity fields inside central plane of the desiccant column and the desiccant wheel predicted through simulation are also shown. The results display the air-stream patterns with a collection of vector arrows. The magnitude of velocity is represented by the colours. The maximum magnitude of velocity occurs in the centre and middle layer of the dehumidifiers. A reverse swirl is found near the inlet and outlet regions of the desiccant media.

4.4.2 Desiccant cooling system

TRASYS version 16.0 software is used to predict the results of the desiccant cooling systems. The dehumidifiers are used to remove water vapor from the ventilation air before passing into the experimental room with split type air conditioner. The simulation results of the standard air-conditioning system and the desiccant cooling system are compared with the experimental tests under tropical humid climate incorporating the applicable criteria, as illustrated in Chapter 5.

4.5 Solid Desiccant Dehumidification for Radiant Cooling System

The aim of this section is to investigate and design a solid desiccant dehumidification and radiant cooling system, which are suitable for tropical climate to achieve thermal comfort. The influence of an interior ventilation fan to thermal comfort assessment is also examined. The total area of the ceiling and wall radiant cooling panels are 16.83 m^2 and 16.32 m^2 with 26.28 litre/min of supplied water by the cooling tower for radiant cooling system. The solid desiccant dehumidifiers are the hollow cylindrical packed bed dehumidifier with containing 10 kg of silica-gel. The physical properties of silica-gel are: average diameter: 3 mm, porosity: 0.4, and bulk density: 670 kg/m^3. The flow rate of supply air is approximately 90 kg/h.

The simulation tools under investigation consist of TRNSYS software and ANSYS software. First of all, the TRNSYS software is used to assess the thermal comfort of the radiant cooling system. Moreover, the phenomena of the air flow rate and the temperature profile can explain by ANSYS software. In the TRNSYS software, the details of the experiment room are used to construct the model for simulation. Two system configurations are used for experiment. The first system is the experimental room without the cooling panels. The second system couples the radiant cooling system installation to the building. The considered parameters are the environmental conditions in the experimental room (temperature, relative humidity, and air velocity) for thermal comfort assessment. The weather data used in this simulation can be distinguished into four patterns namely hot day (March), early rain (July), late rain (September), and cool day (December).

The flow diagram of TRNSYS and TRNSYS subroutine used to model each component is shown in Fig. 4.14. In the ANSYS software, two system configurations are investigated. The first system is only the cooling panels with the dehumidifier. The second system couples a ventilation fan installation to the radiant cooling system. The schematic of system is shown in Fig. 4.15. In this assessing thermal comfort level, the occupants are assumed to have a clothing insulation value of 1 clo. This corresponds to an office worker dressed in slacks, shirt, shoes, and socks. The occupants are also assumed to be doing sedentary work, with a metabolic rate of 1.2 met. Moreover, the local air velocity is about 0.1 m/s.
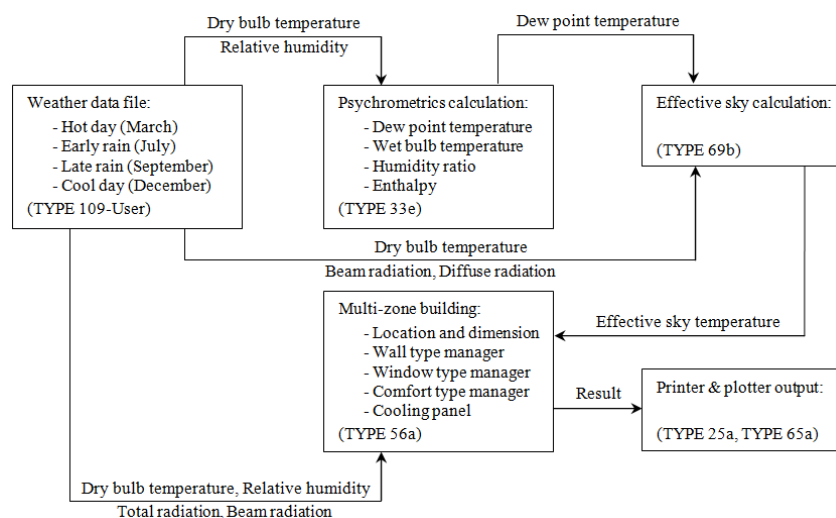
Fig. 4.14 TRNSYS information flow diagram for the simulation
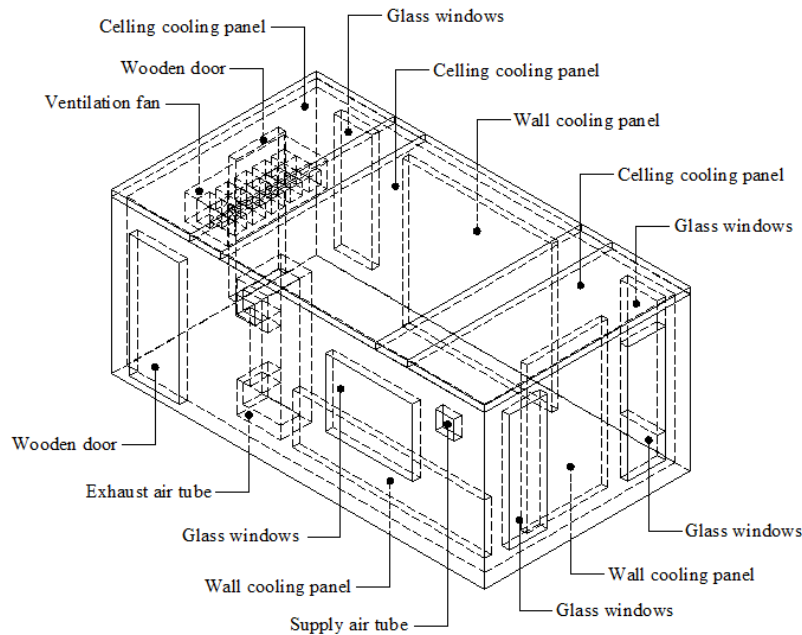
Fig. 4.15 The experimental room in ANSYS software

4.5.1 Thermal comfort assessment of the radiant cooling system

The climate of Thailand can be distinguished into four patterns corresponding to a period of the year. Therefore, the weather data used in the simulation consist of four patterns that March for hot day, July for early rain, September for late rain, and December for cool day. The predicted mean vote, a particularly defined of the thermal comfort in the thermal environment, is investigated for the radiant cooling system. The TRNSYS simulation results of the radiant cooling system are compared with the case of standard experimental room without the cooling panels in Fig. 4.16-4.19.

In the hot day period in March, temperature and relative humidity of exterior air are in the range of 21.23-35.22^{o}C (28.74^{o}C average) and 51.50-95.00% (72.95% average) while average temperature and relative humidity of interior air are 28.15^{o}C and 81.97% as shown in Fig. 4.16 (a). The variations of the different quantities in case of the uses of radiant cooling system are shown in Fig. 4.16 (b). Temperature and relative humidity of interior air are in the range of 24.08-28.04^{o}C (25.84^{o}C average) and 81.89-100.00% (93.21% average), respectively. Moreover, values of PMV can be improving from 1.74 to 1.28 with cooling panels that shows in

Fig. 4.16 (c). During the early rain period in July, temperature and relative humidity of exterior air are in the range of 21.95-33.86^{o}C (28.33^{o}C average) and 48.00-98.00% (76.24% average) while average temperature and relative humidity of interior air are 26.65^{o}C and 88.81% in case of without cooling panels as shown in Fig. 4.17 (a). Temperature and relative humidity of interior air are in the range of 24.06-27.11^{o}C (25.49^{o}C average) and 86.46-100.00% (95.08% average) in case of radiant cooling system as given in Fig. 4.17 (b). Furthermore, values of PMV can be improving from 1.43 to 1.20 with cooling panels as seen in Fig. 4.17 (c).

Variations of the different quantities within experimental room without cooling panels are shown in Fig. 4.18 (a) during the late rain period in September. Temperature and relative humidity of exterior air are in the range of 22.45-34.39^{o}C (27.45^{o}C average) and 54.00-100.00% (81.00% average), respectively, while, average temperature and relative humidity of interior air are 26.13^{o}C and 90.87%. Fig. 4.18 (b) illustrated temperature and relative humidity of interior air in case of the uses of radiant cooling system which were in the range of 23.99-27.70^{o}C (25.34^{o}C average) and 83.52-100.00% (95.78% average). In addition, values of PMV can be improving from 1.32 to 1.17 with the use of cooling panels as shown in Fig. 4.18 (c). In the cool day period in December, in case of without cooling panels are shown in Fig. 4.19 (a). Temperature and relative humidity of exterior air are in the range of 17.03-33.67^{o}C (25.64^{o}C average) and 45.00-93.00% (69.45% average), and average temperature and relative humidity of interior air are 26.40^{o}C and 88.19%. Temperature and relative humidity of interior air are in the range of 23.24-27.85^{o}C (25.39^{o}C average) and 82.78-100.00% (94.97% average) for the uses of radiant cooling system in Fig. 4.19 (b). Moreover, values of PMV can be improving from 1.36 to 1.18 with cooling panels as given in Fig. 4.19 (c).

The use of cooling panels with cool water supplied from cooling tower in the tropical climate can improve thermal comfort through TRNSYS simulation. The predicted mean vote is in the range of 0.69-1.74 (1.21 average). In December, the PMV values are low because of low exterior air temperature, while, these values are high in the hot day period. The radiant cooling system can satisfy only sensible heating, so that the relative humidity is high value in the range of 81.89-100% (94.76% average).
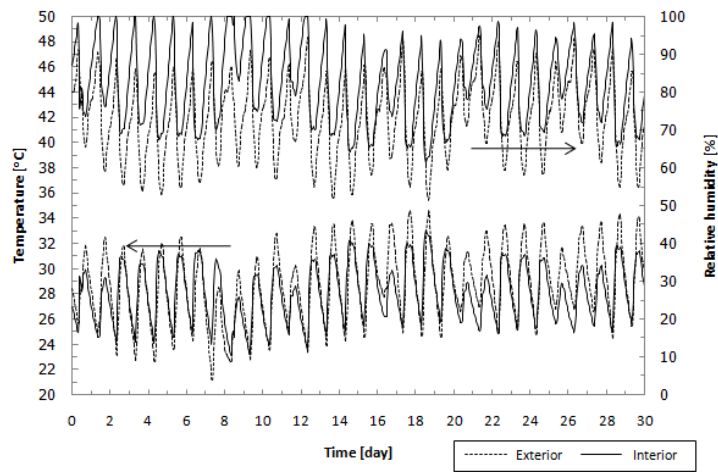
(a) Temperature and relative humidity without cooling panel on March 2015
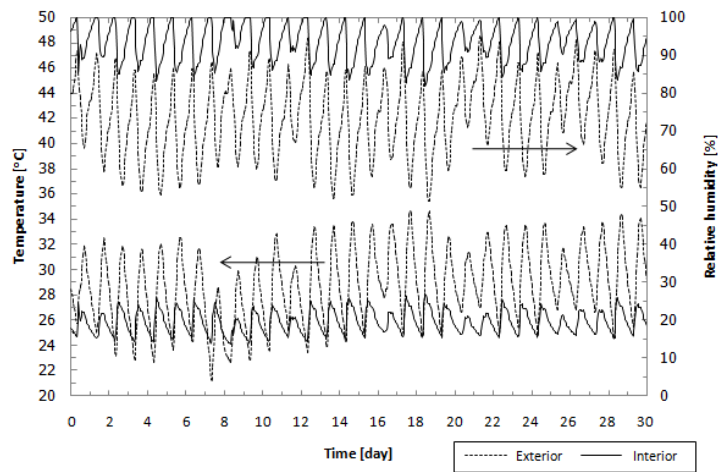
(b) Temperature and relative humidity with cooling panel on March 2015
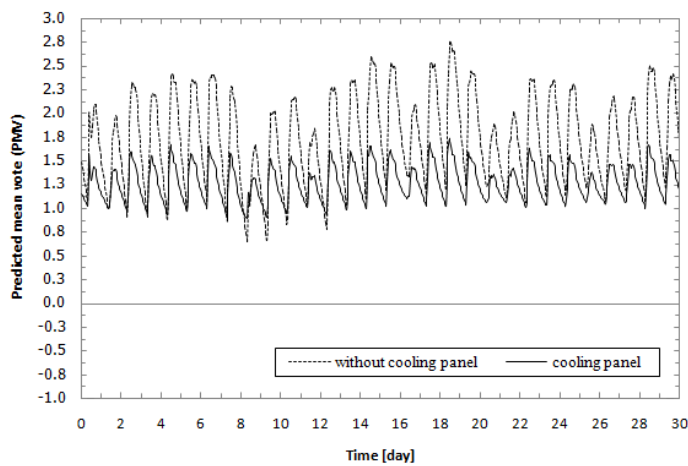
(c) Predicted mean vote on March 2015

Fig. 4.16 The air temperature, relative humidity, and PMV from TRNSYS simulation

for March 2015
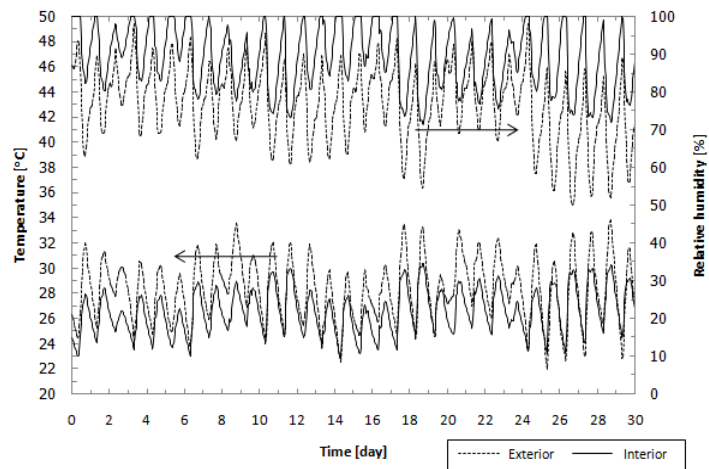
(a) Temperature and relative humidity without cooling panel on July 2015
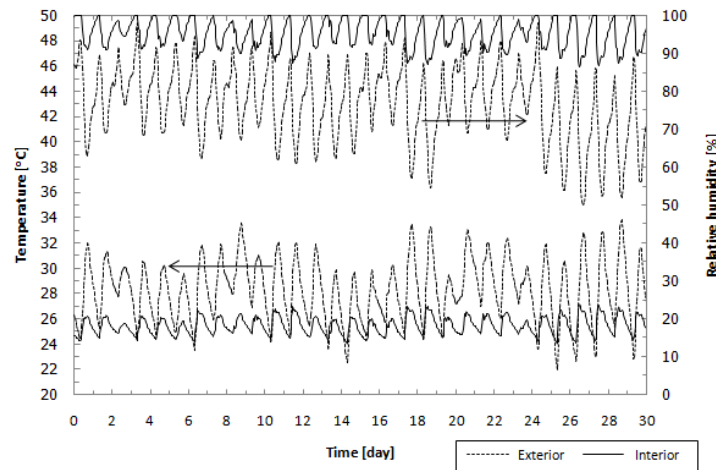
(b) Temperature and relative humidity with cooling panel on July 2015
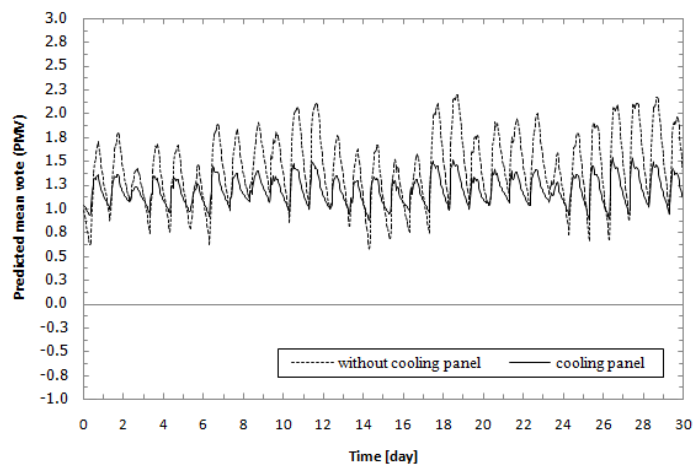
(c) Predicted mean vote on July 2015

Fig. 4.17 The air temperature, relative humidity, and PMV from TRNSYS simulation

for July 2015
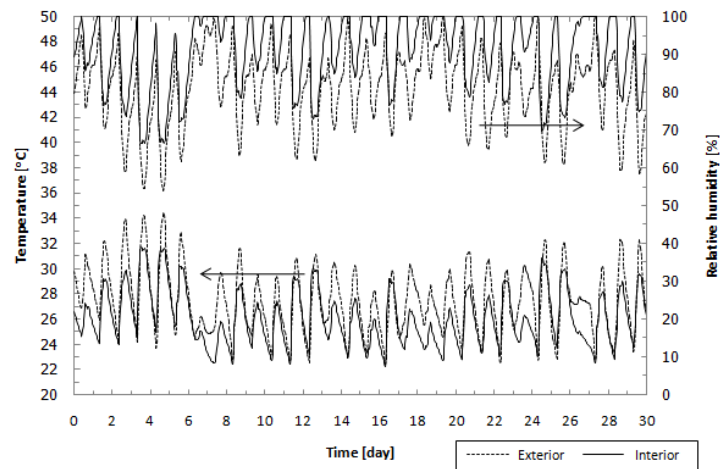
(a) Temperature and relative humidity without cooling panel on September 2015
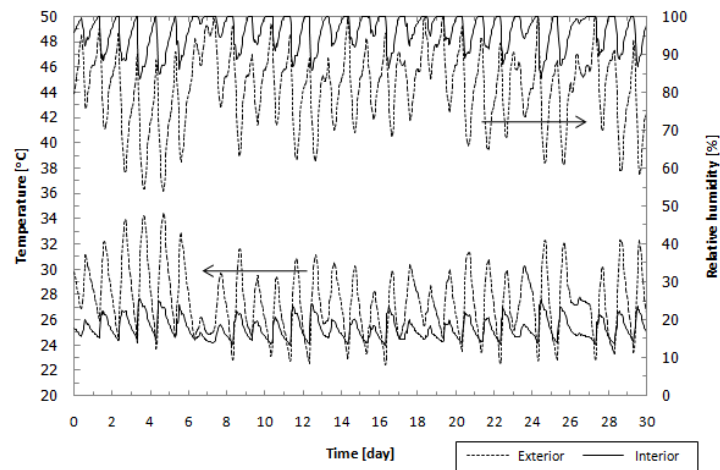
(b) Temperature and relative humidity with cooling panel on September 2015
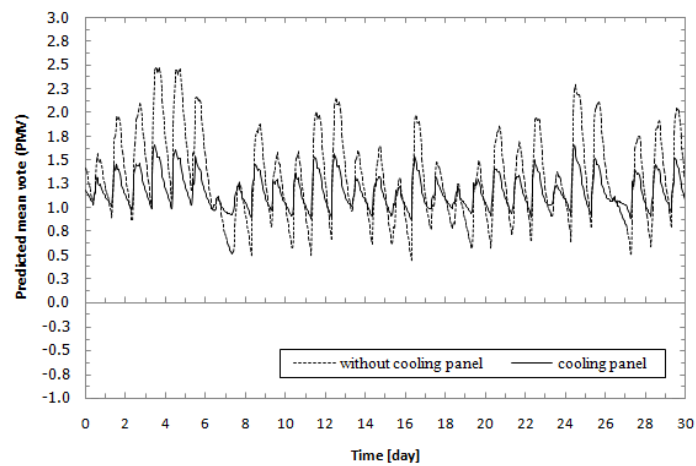
(c) Predicted mean vote on September 2015

Fig. 4.18 The air temperature, relative humidity, and PMV from TRNSYS simulation

for September 2015
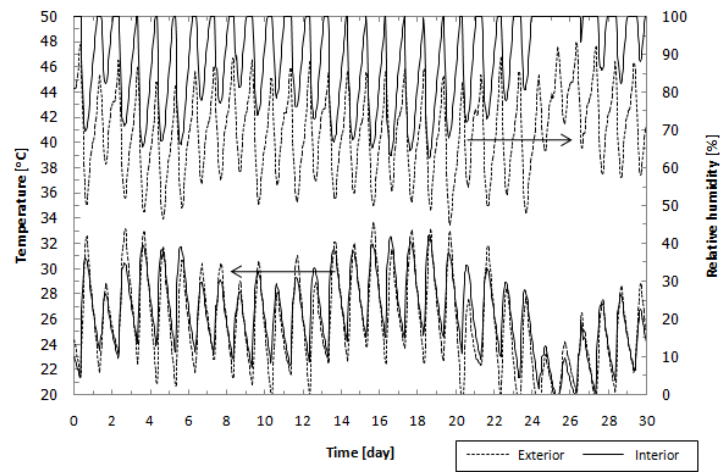
(a) Temperature and relative humidity without cooling panel on December 2015
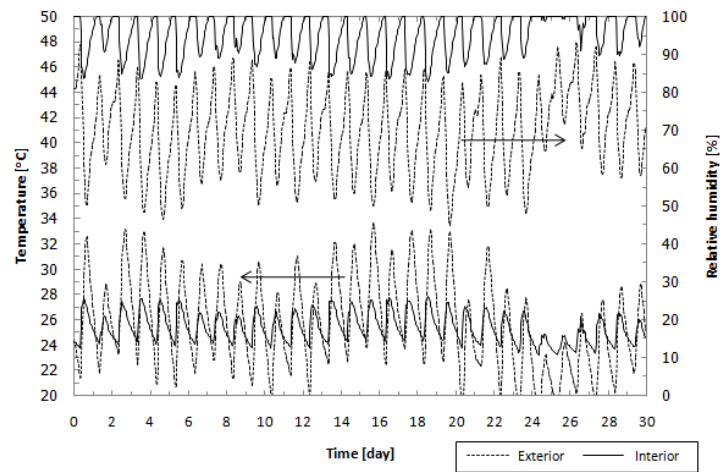
(b) Temperature and relative humidity with cooling panel on December 2015
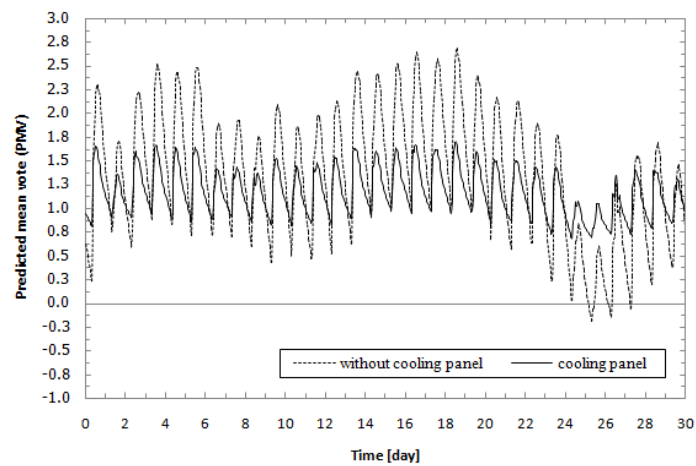
(c) Predicted mean vote on December 2015

Fig. 4.19 The air temperature, relative humidity, and PMV from TRNSYS simulation

for December 2015

4.5.2 Phenomena of air conditions with radiant cooling system

In the ANSYS software, the phenomena of the interior air conditions of the experimental room were investigated, such as the temperature profile, the relative humidity profile, the air flow rate distribution, or the predicted mean vote. The previous experimental data are used as input for the simulation. The temperature and relative humidity of the exterior air, the temperature surface of the cooling panels, or the temperature and relative humidity of ventilation supply air are used for the boundary and initial conditions. The use of cooling panels with dehumidifier is investigated for comparison with experimental results. Moreover, the second system couples a ventilation fan installation to the radiant cooling system is also studied.

The air temperature and the relative humidity distribution inside central plane (front view, top view, and side view) of the experimental room for the radiant cooling system and dehumidification are shown in Fig. 4.20 and Fig. 4.21, respectively. In the hot day period (March 2016, 8:00 am), the average temperature and relative humidity of the interior air are 27.17^{o}C and 36.94%. Moreover, the average moisture content of the interior air is 8.66 g_{w}/kg_{da}.

In the case of the radiant cooling system with dehumidifier and ventilation fan in the experimental room, the air temperature and the relative humidity distribution inside central plane (front view, top view, and side view) are shown in Fig. 4.22 and Fig. 4.23, respectively. In the hot day period (March 2016, 8:00 am), the average temperature and relative humidity of the interior air are 26.06^{o}C and 38.61%; and the average moisture content is 8.44 g_{w}/kg_{da}.

The PMV distribution inside central plane (front view) of the experimental room for the comparison between the radiant cooling system with dehumidification and ventilation fan installation in the experimental room are shown in Fig. 4.24 and Fig. 4.25, respectively. The thermal comfort usually occurred in the closer to the cooling panels and the higher magnitude of the local velocity (blue zone). The average value of PMV for the interior air is -0.02 in case of the radiant cooling with dehumidifier. On the other hand, it is -0.93, when installing the ventilation fan in the experiment room. The average air velocity increases to 0.49 m/s.
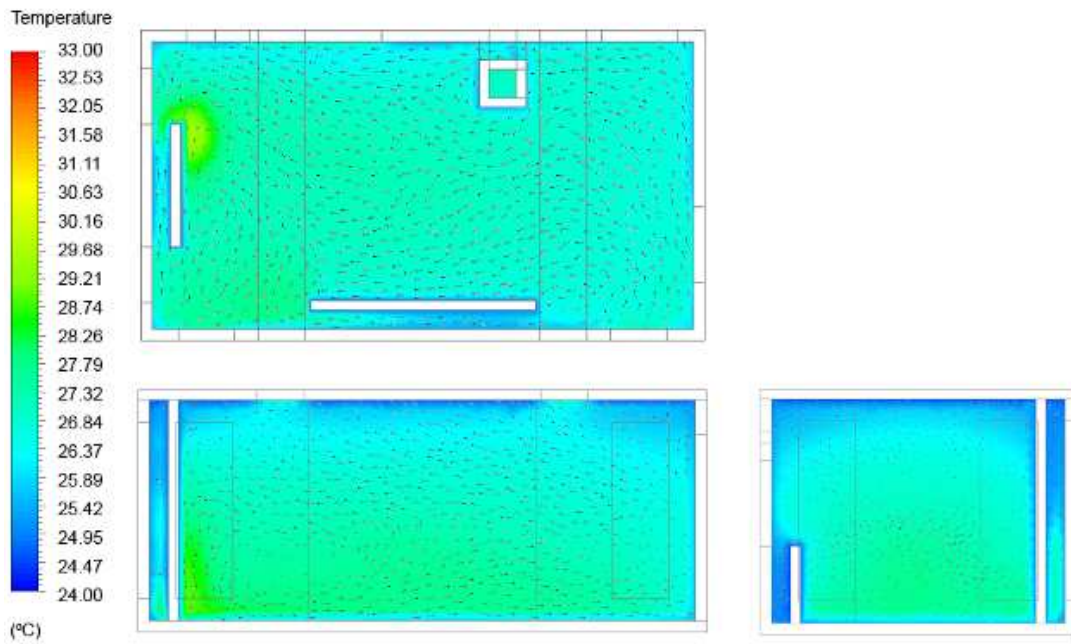
Fig. 4.20 Contour plots inside central plane of air temperature for the radiant cooling system with dehumidification at 8:00 am.
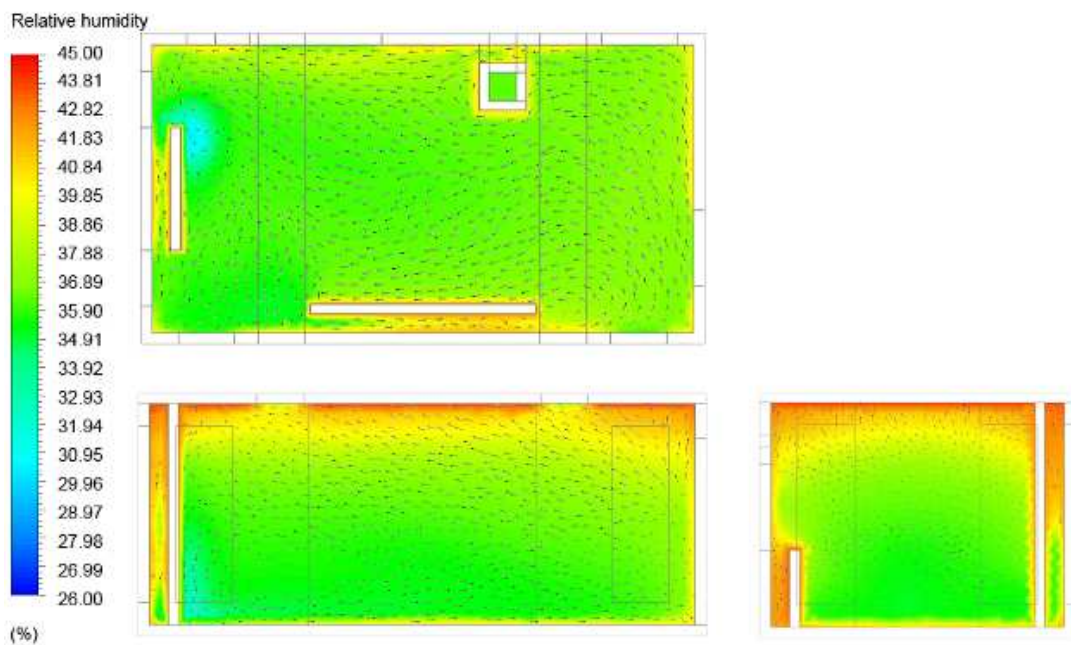
Fig. 4.21 Contour plots inside central plane of relative humidity for the radiant cooling system with dehumidification at 8:00 am.
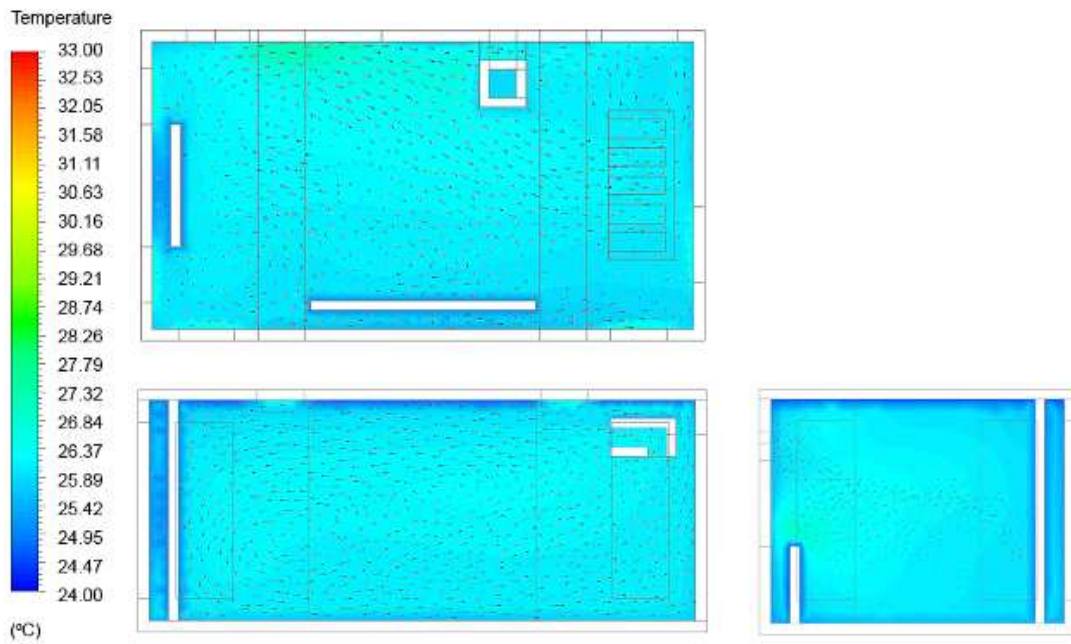
Fig. 4.22 Contour plots inside central plane of air temperature for radiant cooling system and dehumidification with ventilation fan at 8:00 am.
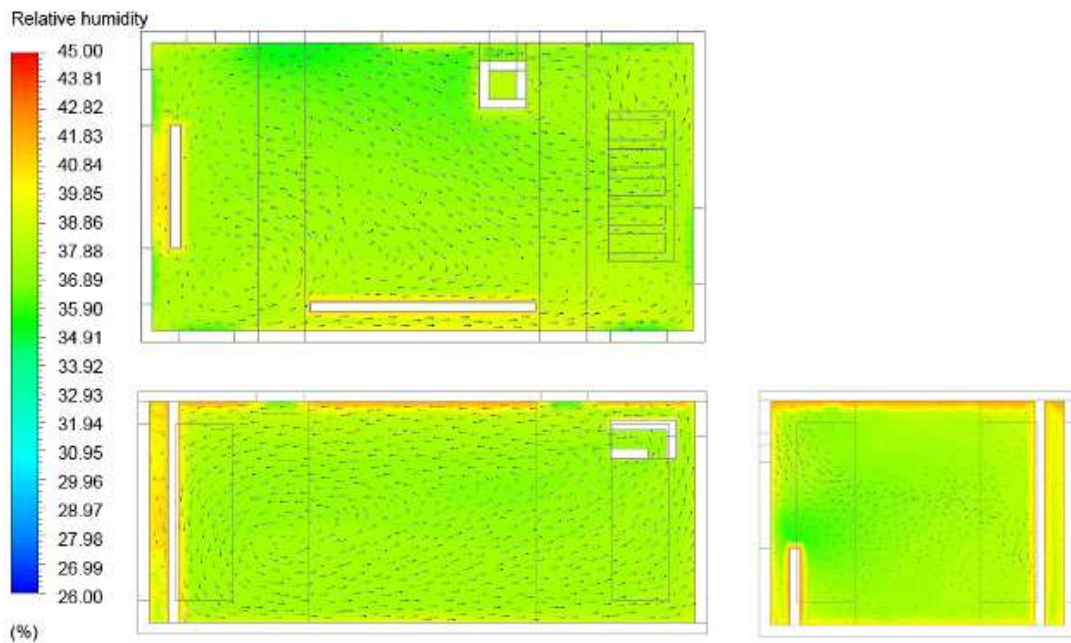
Fig. 4.23 Contour plots inside central plane of relative humidity for radiant cooling system and dehumidification with ventilation fan at 8:00 am
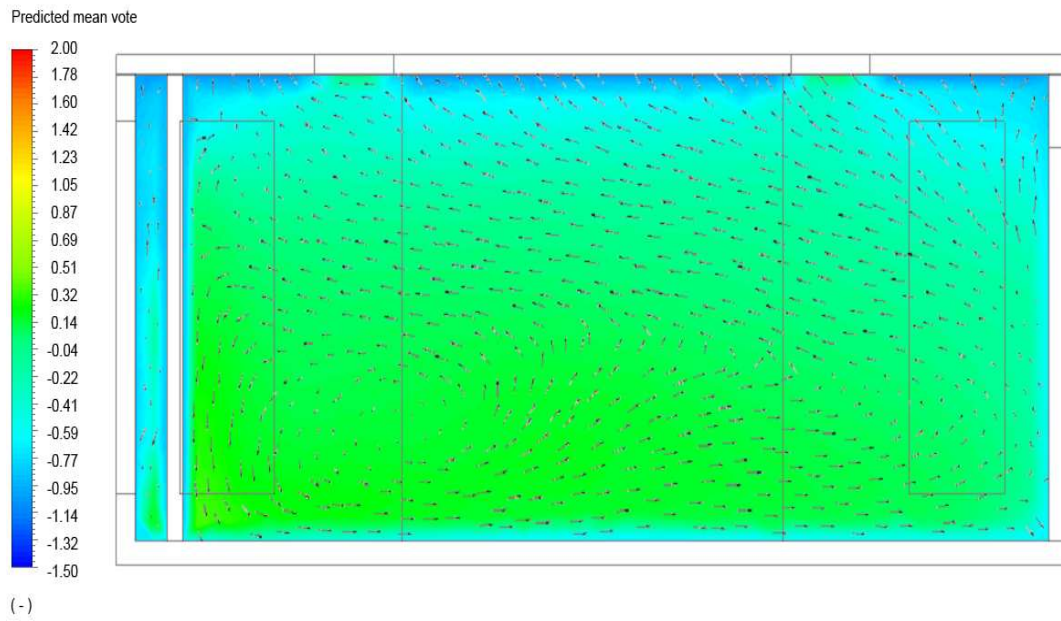
Fig. 4.24 Contour plots inside central plane (side view) of PMV for radiant cooling system and dehumidification without ventilation fan at 8:00 am.
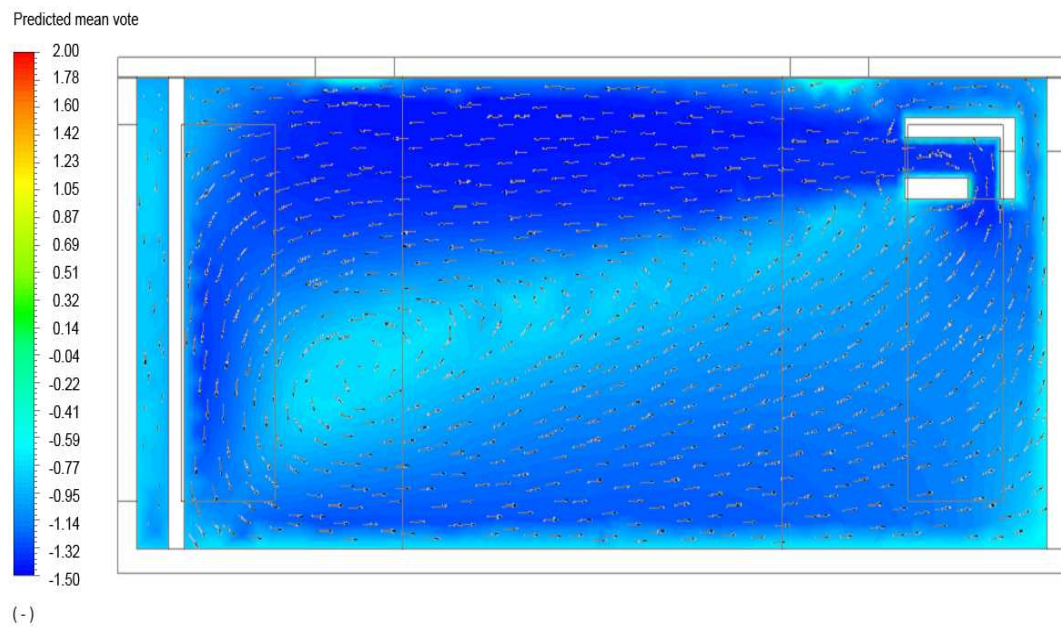
Fig. 4.25 Contour plots inside central plane (side view) of PMV for radiant cooling system and dehumidification with ventilation fan at 8:00 am.

Chapter 5

Experimental Results

The prevent details, Chapter 3 describes the methodology used in this study, and the simulations are used to predict the thermal comfort assessment and air phenomena profile in the experimental room, as illustrated in Chapter 4. The experimental results are described in this section including the simulation results comparing with the experimental tests under tropical humid climate incorporating the applicable criteria.

5.1 Desiccant Dehumidifiers Testing

This section is to investigate the influence of parametric studies for the solid desiccant dehumidification using the desiccant column in tropical climate of Thailand. The effects of temperature, humidity ratio and mass flow rate of air-stream through desiccant column upon pressure drop (ΔP) and adsorption rate (R_{adsorp}) are examined. The desiccant dehumidifiers testing is illustrated in Fig. 5.1.
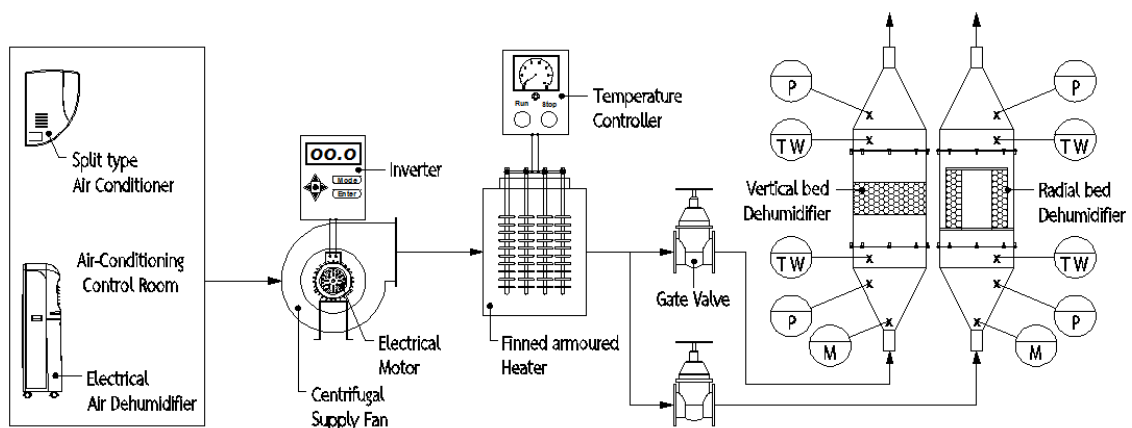
Fig. 5.1 Schematic diagram of desiccant dehumidification testing

The dehumidification system uses the solid desiccant dehumidifiers with spherical particles of silica-gel for working adsorbed media to remove water vapor from supplied air before using. The experimental dehumidification systems consist of two desiccant columns, vertical flow bed and radial flow bed or hollow

cylindrical packed bed, with an inner and outer diameter of 0.15 m and 0.30 m, respectively. A length of the packed bed is 0.465 m containing 10 kg of silica-gel in each column. The physical properties of silica-gel are: average diameter: 3 mm, porosity: 0.4 (the open volume fraction of the medium) and bulk density: 670 kg/m^3. The solid desiccant dehumidifier under investigation is shown in Fig. 5.2. The first column is the vertical flow bed and the second column is radial flow bed. In the last column, the cross-section of the radial bed shows the flow-direction of air-stream through the desiccant media.
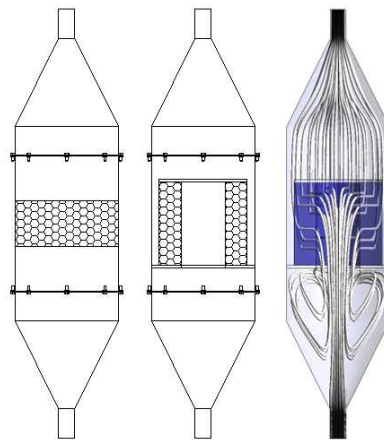
Fig. 5.2 The solid desiccant packed bed dehumidifiers

The RSM is employed to study the effects of operating parameter. The studied of designing parameters are the temperature (T), humidity ratio (W) and mass flow rate (M) of air-stream through desiccant column. The desired responses are the pressure drop (ΔP) and the adsorption rate (R_{adsorp}) which be affected by three independent variables as mentioned earlier. The RSM, with 5-level and 3-factor CCD with 4-centerpoints is used to investigation. In the case of three variables, the axial parameter (α) is 1.682 for assure that the designs being rotatable. The experiment is designed for 5 levels of varying independent variables which were codes as -1.682, -1, 0, +1, and +1.682. Therefore, the experimental setups are 18 treatment combinations. The code independent variables used in this study are presented in Table 5.1.

The air temperature and humidity ratio are controlled by the air-conditioning control room, which consists of a split type air conditioner and an electrical air dehumidifier. The finned armoured heater is used to increases the temperature when the designing temperature is higher than surrounding temperature.

The temperatures are kept around 25, 28, 33, 37, and 40°C, when the humidity ratios are 10, 12, 15, 18, and 20 g_w/kg_{da}. Moreover, the flow rates of supply air are controlled around 60, 72, 90, 108, 120 kg/h by a centrifugal supply fan driven by an inverter and gate valves. All treatments in the experimental setup are continuously operated for 60 minutes, with recorded every five minutes using data logger.

Table 5.1 The experimental range and levels of designing parameter

Parameters	Ranges and levels				
	-1.682	-1	0	+1	+1.682
Temperature, T (°C)	25	28	33	37	40
Humidity ratio, W (g_w/kg_{da})	10	12	15	18	20
Mass flow rate, M (kg/h)	60	72	90	108	120

Experimental results reveal that the pressure drop of vertical bad flow dehumidifier is higher compared to the radial flow bad dehumidifier, whereas the adsorption rate of the radial bad dehumidifier is higher than the vertical bad flow under the same conditions. For example, in the case of the inlet air temperature of 33°C, the inlet humidity ratio of 15 g_w/kg_{da}, and an air flow rate of 90 kg/h, the measured air temperature and humidity ratio at inlet and outlet positions of the dehumidifiers are given in Fig. 5.3. The pressure drop and the adsorption rate of the comparing bed dehumidifiers are given in Fig. 5.4.
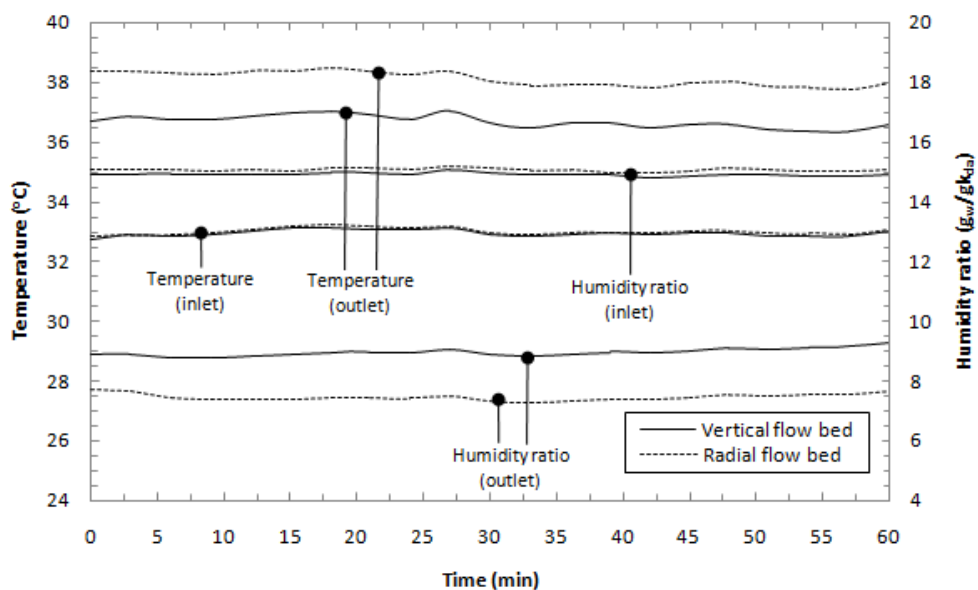
Fig. 5.3 The measured air temperature and humidity ratio at inlet and outlet positions of the dehumidifiers
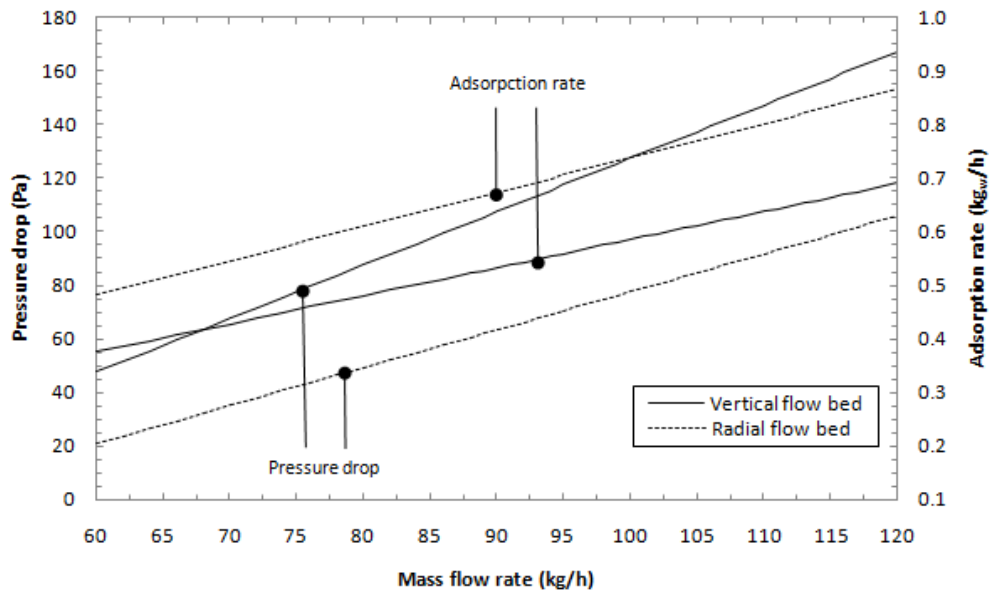
Fig. 5.4 The relationship between the pressure drop, the adsorption rate and the mass flow rate

For the vertical bed flow dehumidifier testing, the average inlet air conditions at the temperature of 32.95°C and the relative humidity of 47.28% or the humidity ratio of 14.92 g_w/kg_{da} indicate that the average outlet air temperature and the relative humidity are 36.70°C and 23.33% or the humidity ratio of 8.97 g_w/kg_{da}. Moreover, the pressure drop and the adsorption rate are 110.55 Pa and 0.54 kg_w/h, respectively. For the radial bed flow dehumidifier testing, the average inlet air conditions at the temperature of 33.02°C and the relative humidity of 47.58% or the humidity ratio of 15.07 g_w/kg_{da} indicate that the average outlet air temperature and the relative humidity are 38.13°C and 17.99% or the humidity ratio of 7.46 g_w/kg_{da}. Moreover, the pressure drop and the adsorption rate are 64.42 Pa and 0.68 kg_w/h.

The RSM with central composite design using to find the performance evaluation of the solid desiccant dehumidifier and the influence of parametric studies are tabulated in Table 5.2. In this study, the average operating parameters of the air temperature, the humidity ratio and the mass flow rate are range of 24.91-40.12°C, 9.96-20.10 g_w/kg_{da}, and 59.80-120.35 kg/h, respectively. In the vertical bed flow dehumidifier, the humidity ratio is decrease to 3.97-7.95 g_w/kg_{da} (5.81 g_w/kg_{da} averages value). However, the outlet air temperature is increase about 1.11 times from the heat of adsorption of the latent heat of condensation of water vapor in the silica-gel particles. Moreover, the pressure drop and the adsorption rate are 55.79-161.08 Pa

(107.14 Pa averages value) and 0.34-0.77 kg$_w$/h (0.52 kg$_w$/h averages value), respectively. In the radial bed flow dehumidifier, the humidity ratio is decrease to 4.72-10.09 g$_w$/kg$_{da}$ (7.34 g$_w$/kg$_{da}$ averages value). However, the outlet air temperature is increase about 1.15 times. Moreover, the pressure drop and the adsorption rate are 27.31-104.29 Pa (63.23 Pa averages value) and 0.43-0.98 kg$_w$/h (0.66 kg$_w$/h averages value), respectively.

Table 5.2 The response surface methodology with central composite design

Run no.	Parametric studies			Vertical flow bed		Radial flow bed	
	T	W	M	ΔP	R$_{adsorp}$	ΔP	R$_{adsorp}$
	^{o}C	g$_w$/kg$_{da}$	kg/h	Pa	kg$_w$/h	Pa	kg$_w$/h
1	28	12	72	62.90	0.3444	33.20	0.4372
2	37	12	72	68.74	0.3366	36.72	0.4273
3	28	18	72	61.44	0.5171	32.43	0.6556
4	37	18	72	67.29	0.5050	35.94	0.6407
5	28	12	108	138.41	0.5164	85.93	0.6560
6	37	12	108	149.28	0.4459	92.69	0.5082
7	28	18	108	135.72	0.7730	84.26	0.9816
8	37	18	108	146.60	0.6706	91.92	0.8483
9	25	15	90	102.25	0.5654	58.97	0.7190
10	40	15	90	116.56	0.4206	68.53	0.5294
11	33	10	90	112.46	0.3580	65.55	0.4541
12	33	20	90	108.35	0.7163	63.12	0.9127
13	33	15	60	55.79	0.3595	27.31	0.4552
14	33	15	120	161.08	0.7050	104.29	0.8923
15	33	15	90	110.55	0.5357	64.42	0.6820
16	33	15	90	110.73	0.5313	64.43	0.6806
17	33	15	90	109.99	0.5434	64.19	0.6815
18	33	15	90	110.38	0.5373	64.29	0.6808

For the checking of the goodness of fit of the predicted equations obtained in this study, the test of significance of the regression model, the test for significance on individual model coefficients and test for lack-of-fit need to be performed. The analysis of ANOVA is usually applied to summarize the above tests performed. Table 5.3 and Table 5.4 present the statistical significance of the regression models for the pressure drop and the adsorption rate of the vertical bad flow dehumidifier and the radial bad flow dehumidifier, respectively. The backward elimination process to adjust the predicted equations of the pressure drop and the adsorption rate eliminate the insignificant terms.

Table 5.3 ANOVA table for the regression models using vertical flow bed dehumidifier (after backward elimination)

Pressure drop, ΔP

Term	Coefficient	Standard error	T-ratio	P-value
Constant	-71.810	6.533214	-10.991474	0.000000
M	1.633	0.125025	13.061825	0.000000
T×M	0.011	0.003136	3.462663	0.003480

Standard error	= 4.739918	R^2	= 0.981243	
Coefficient of variation	= 4.424058	R^2 adjusted	= 0.978742	
PRESS	= 516.167012	R^2 for prediction	= 0.971271	

Adsorption rate, R_{adsorp}

Term	Coefficient	Standard error	T-ratio	P-value
Constant	-1.174	0.362146	-3.242275	0.006423
T	0.051	0.022325	2.289053	0.039452
W	0.035	0.002277	15.334654	0.000000
M	0.005	0.000379	13.809264	0.000000
T^2	-0.001	0.000344	-2.603168	0.021874

Standard error	= 0.025146	R^2	= 0.972118	
Coefficient of variation	= 4.824663	R^2 adjusted	= 0.963539	
PRESS	= 0.018671	R^2 for prediction	= 0.936667	

Table 5.4 ANOVA table for the regression models using radial flow bed dehumidifier (after backward elimination)

Pressure drop, ΔP

Term	Coefficient	Standard error	T-ratio	P-value
Constant	-63.962	3.455104	-18.512465	0.000000
M	1.182	0.066120	17.876764	0.000000
T×M	0.007	0.001658	4.262266	0.000682

Standard error	= 2.506715	R^2	= 0.989503	
Coefficient of variation	= 3.964277	R^2 adjusted	= 0.988104	
PRESS	= 151.742050	R^2 for prediction	= 0.983101	

Adsorption rate, R_{adsorp}

Term	Coefficient	Standard error	T-ratio	P-value
Constant	-1.547	0.568036	-2.724247	0.017372
T	0.069	0.035018	1.981933	0.069035
W	0.046	0.003571	12.820730	0.000000
M	0.006	0.000595	10.754981	0.000000
T^2	-0.001	0.000539	-2.268007	0.041019

Standard error	= 0.039442	R^2	= 0.958772	
Coefficient of variation	= 5.995045	R^2 adjusted	= 0.946087	
PRESS	= 0.042626	R^2 for prediction	= 0.913101	

In Table 5.3 for using vertical flow bed dehumidifier, the resulting ANOVA table of the reduced the liner with interaction model for the pressure drop and the quadratic model for the adsorption rate reveals this models are still significant in the status of the value of "P-value" is less than 0.05. The other important coefficient R^2 in the resulting ANOVA table is defined as the ratio of explained variation to the total variation and is a measure of the degree of fit. For the pressure drop predicted equation, the value of R^2 calculated in Table 5.3 for this reduced model is over 0.97, while R^2 for the adsorption rate predicted equation is over 0.93, reasonable close to unity, which is acceptable. It demotes that about 95% of variability in the data is explained by this model. It also confirms this model provides an excellent explanation of the relationship between the independence factors and the response. The same procedure is applied to deal with using radial flow bed dehumidifier, the resulting ANOVA table of the reduced the liner with interaction model for the pressure drop and the quadratic model for the adsorption rate are show in Table 5.4. The value of "P-value" is also less than 0.05 (i.e. α=0.05, or 95% confidence). Therefore, this model is considered be statistically significant.

Through the backward elimination process, the final regression models of response equation are presented as follows:

Pressure drop for the vertical flow bed

$$\Delta P = -71.810 + 1.633 \times M + 0.011 \times T \times M \qquad \text{Eq. 5.1}$$

Adsorption rate for the vertical flow bed

$$R_{adsorp} = -1.174 + 0.051 \times T + 0.035 \times W$$

$$+ 0.005 \times M - 0.001 \times T^2 \qquad \text{Eq. 5.2}$$

Pressure drop for the radial flow bed

$$\Delta P = -63.962 + 1.182 \times M + 0.007 \times T \times M \qquad \text{Eq. 5.3}$$

Adsorption rate for the radial flow bed

$$R_{adsorp} = -1.547 + 0.069 \times T + 0.046 \times W$$

$$+ 0.006 \times M - 0.001 \times T^2 \qquad \text{Eq. 5.4}$$

Where ΔP is the pressure drop (Pa); R_{adsorp} is the adsorption rate (kg_w/h); W is humidity ratio (kg_w/kg_{da}); T is temperature (^{o}C), and M is mass flow rate (kg/h).

The effects of operating parameters on the performances using the dehumidifiers were investigated. According to the results in ANOVA, a sensitivity analysis for percent contribution for each significant operating parameter, the most significant factors in the pressure drop across the dehumidifier is the mass flow rate. The temperature is the less influent factor, while the humidity ratio is not significant. For the adsorption rate, the two significant factors are the temperature and the humidity ratio, respectively, whereas the mass flow rate is a lower influent factor. In addition, the three dimensional surface demonstrate the effect of operating parameters on the performances using the vertical and radial flow bed dehumidifier are shown in Fig. 5.5 and Fig. 5.6, respectively.

Fig. 5.5 (a) presents that the influences of the mass flow rate and the humidity ratio on the pressure drop and the adsorption rate of vertical bad flow dehumidifier, while keeping the temperature at 33^oC. The pressure drop and the adsorption rate increase when the mass flow rate changes from 60 to 120 kg/h. Moreover, only the adsorption rate also increases when the humidity ratio rises from 10 to 20 g_w/kg_{da}. In Fig. 5.5 (b) the humidity ratio at 15 g_w/kg_{da}, the pressure drop increase when the temperature changes from 25 to 40^oC, whereas the adsorption rate decrease in this range. Moreover, in Fig. 5.5 (c), the pressure drop and the adsorption change in a little range value when keeping the mass flow rate at 90 kg/h.

The same procedure is applied to deal with the pressure drop and the adsorption rate of radial bad flow dehumidifier, the resulting of the response surfaces as a function of two different factors is shown in Fig. 5.6. The patterns of the pressure drop and the adsorption rate are in the same trend with the previous dehumidifier. However, the pressure drop of the vertical flow bed is higher and the adsorption rate is lower, when comparing with the radial flow bed. It can use a smaller size of a supply fan with using the hollow cylindrical packed bed, so that the electrical power consumption of a motor decrease in the same dehumidifier capacity.
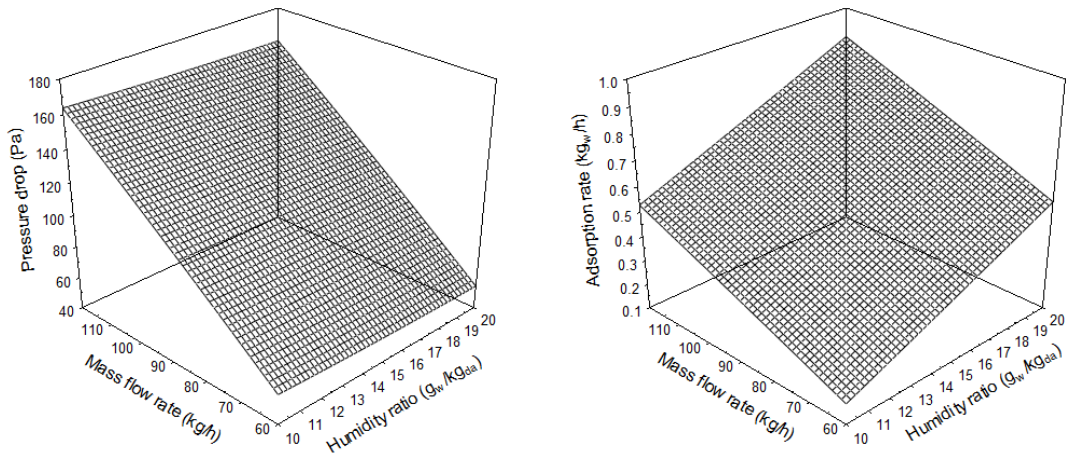
(a) Hold value for temperature at 33°C
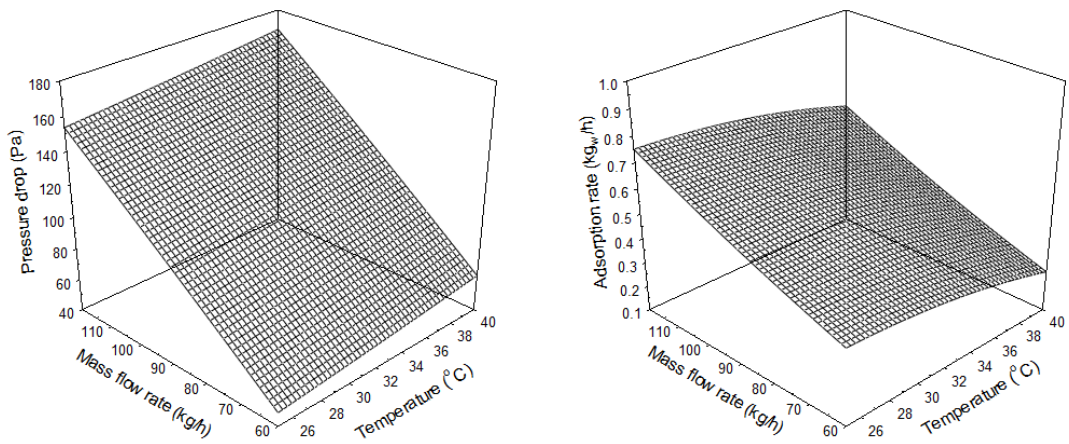
(b) Hold value for humidity ratio at 15 g_w/kg_{da}
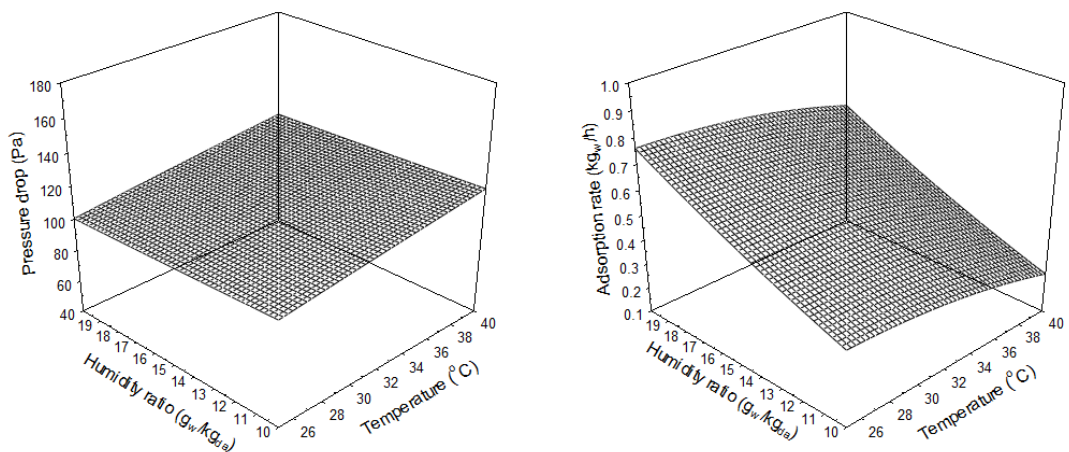
(c) Hold value for Mass flow rate at 90 kg/h

Fig. 5.5 Response surfaces as a function of two different factors for pressure drop and adsorption rate using the vertical flow bed dehumidifier

(a) Hold value for temperature at 33°C
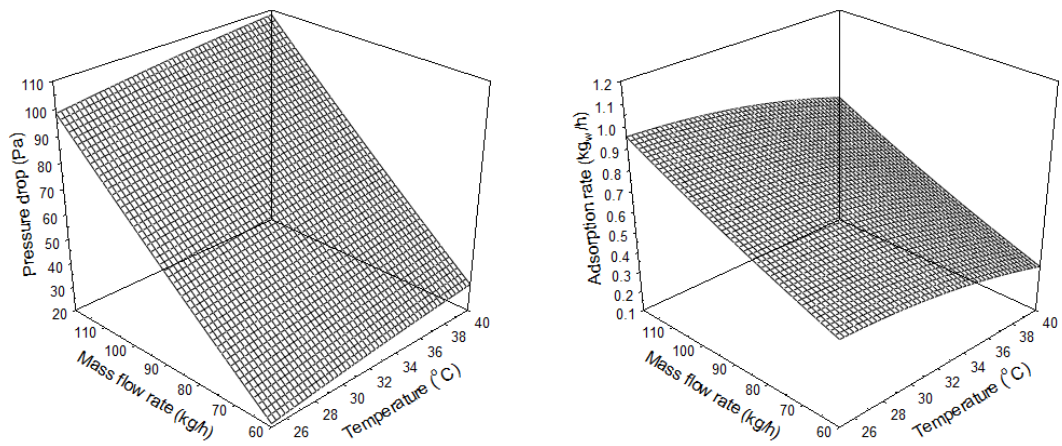
(b) Hold value for humidity ratio at 15 g$_w$/kg$_{da}$
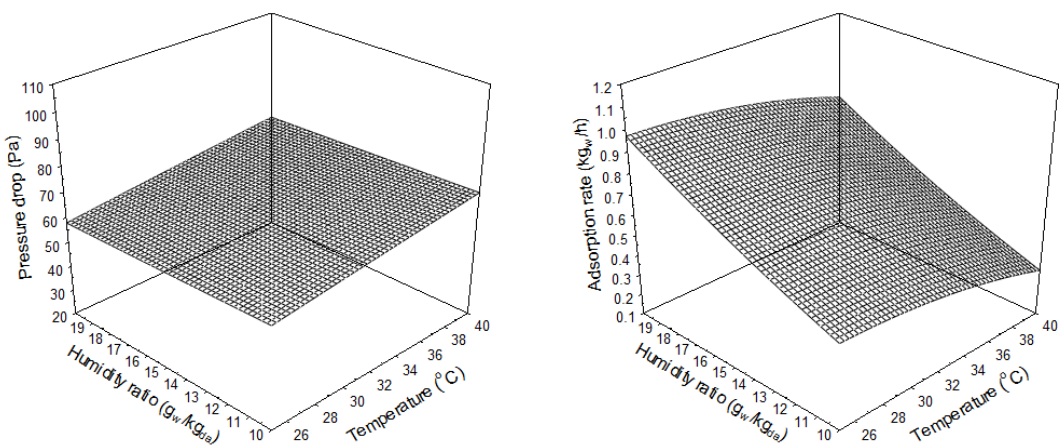
(c) Hold value for Mass flow rate at 90 kg/h

Fig. 5.6 Response surfaces as a function of two different factors for pressure drop and adsorption rate using the radial flow bed dehumidifier

5.2 Desiccant Dehumidification for Air-conditioning System

This section is to concentrate on the solid desiccant dehumidification system for tropical climate to reduce the latent load of air-conditioning system, and improve the thermal comfort. The experimental systems under investigation consist of the solid desiccant dehumidification and air-conditioning system. The first system is used to remove water vapor from the ventilation air before passing into the air-conditioning system. The second system consists of split type air conditioner (9,000 Btu/h) to maintain the desired indoor conditions. In this section, the desiccant dehumidifier is a radial bed dehumidifier. The bed geometry of the stationary dehumidifier on desiccant column is radial, i.e. a hollow cylindrical bed, with an inner and outer diameter of 0.15 m and 0.30 m, respectively. A length of the packed bed is 0.465 m. The silica-gel media are used as the working desiccant in the dehumidifiers. Amount of desiccant in the bed is close to 15 kg. The flow rate of supply air is approximately 60 kg/h.

The results of the desiccant cooling system are compared with the standard air-conditioning system in Fig. 5.7. The variations of the different quantities within the experimental room with the standard air-conditioning system are shown in Fig. 5.7 (a). The measured temperature (T_{oa}-Exp) and relative humidity (Rh_{oa}-Exp) of the outdoor air are in the ranges of 26.7-31.6^{o}C and 62.8-95.0%, respectively, whereas, the measured average temperature (T_{oa}-Exp) and relative humidity (Rh_{oa}-Exp) of the indoor air are around 25.3^{o}C and 60.4%. The variations of the same quantities within the experimental room with the desiccant cooling system are shown in Fig. 5.7 (b). When the temperature and the relative humidity of the outdoor air are in the ranges of 25.5-32.7^{o}C and 55.5-95.6%, respectively, the average temperature and relative humidity of the indoor air are found to be around 25.3^{o}C and 52.3%. Results indicate that the humidity ratio of conditioning space and cooling load of split type air conditioner are decreased by 0.002 kg_w/kg_{da} (14%) and 0.71 kW_{th} (19.26%) respectively. Consequently, the predicted mean vote was improved from 0.3-0.6 (0.5 averages value) to 0.1-0.4 (0.3 averages value) or the predicted percentage dissatisfied was reduced from 6.77-12.85% (10.12% averages value) to 5.17-8.81% (7.04% averages value).
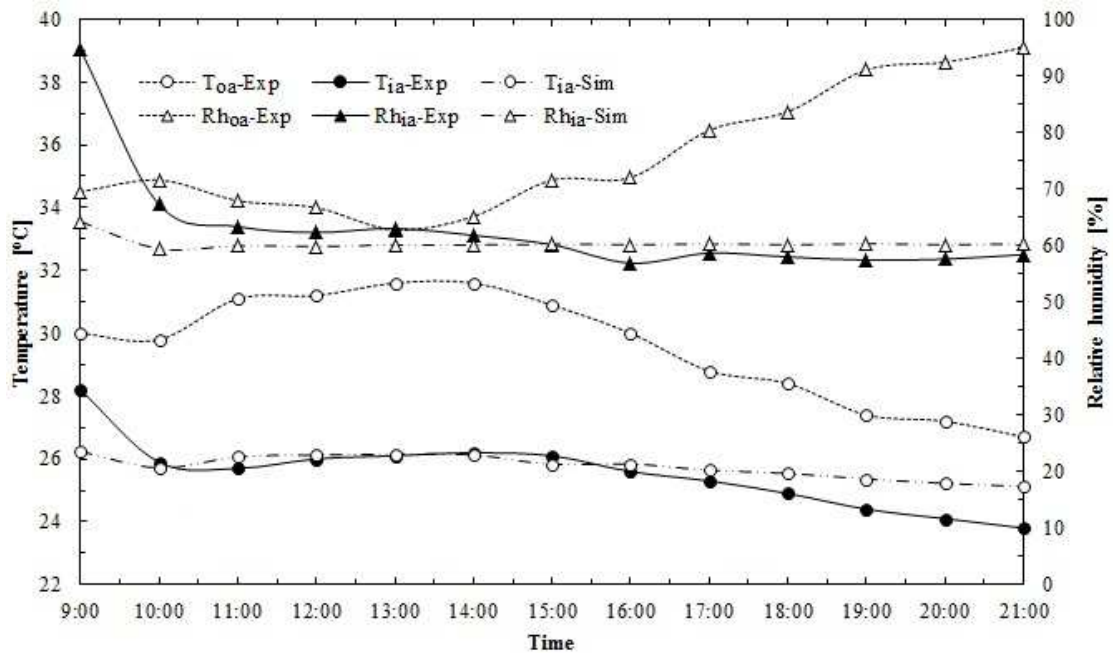
(a) The air-conditioning systems
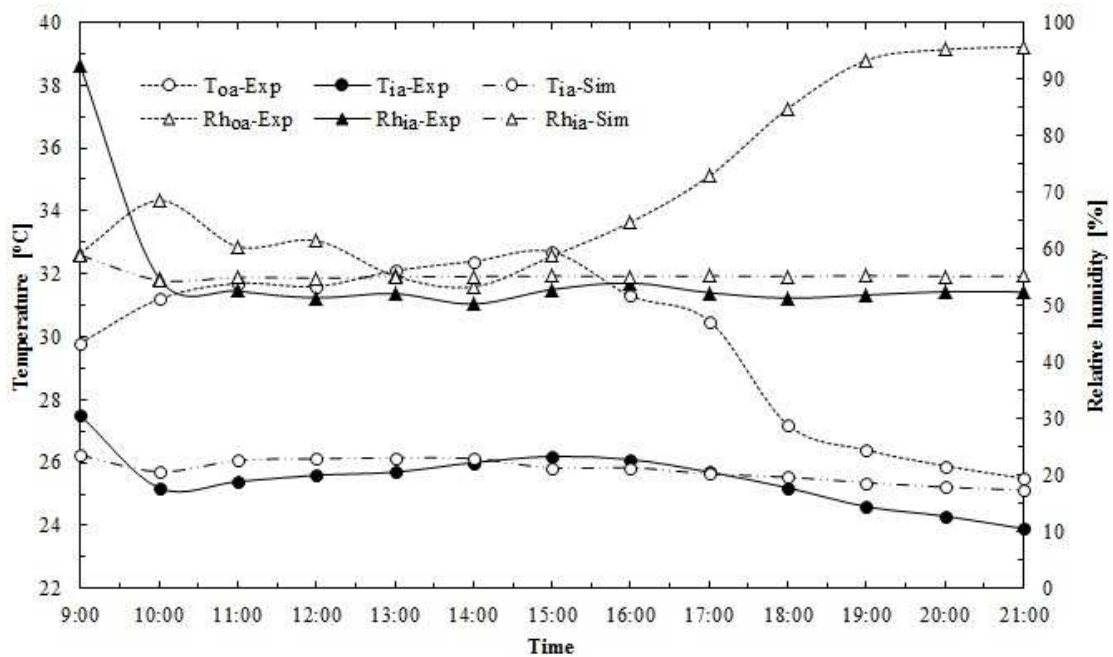
(b) The desiccant cooling systems

Fig. 5.7 The experiment and prediction of interior air conditions

The predicted value, such as the temperature (T_{oa}-Sim), or relative humidity (Rh_{oa}-Sim) within the experimental room is in good agreement with the experiment measurements, except at the beginning of operating the air temperature

and humidity of the experimental room is higher than the value of simulation because of the residual time in the transient effect. The average errors of prediction are less than 2.1% and 5.4% for the temperature and the relative humidity of the interior air, respectively.

5.3 Desiccant Dehumidification for Radiant Cooling System

This section is to investigate on the solid desiccant dehumidification and radiant cooling system, which are suitable for tropical climate to achieve thermal comfort. The total area of the ceiling and wall radiant cooling panels were 16.83 m^2 and 16.32 m^2 with 26.28 litre/min of supplied water by the cooling tower for radiant cooling system. The solid desiccant dehumidifier is the hollow cylindrical packed bed dehumidifier with containing 10 kg of silica-gel. The flow rate of supply air was approximately 90 kg/h.

The experimental results in cases of without and with radiant cooling system were examined. The first case is an experimental room without cooling panel. The second case has the cooling panel installation. Moreover, the moisture content was reduced by the dehumidifier in the second case. For the first case, the temperature and relative humidity of the exterior air are in the range of 26.00-34.46°C (29.40°C average) and 61.44-83.38% (75.29% average), while, the average temperature and relative humidity of the interior air are 30.31°C and 72.77% in the hot day period (March 2016) as given in Fig. 5.8. The average moisture content of the interior air is 19.89 g$_w$/kg$_{da}$. The surface temperature of the cooling panels is around 24.04-29.61°C (26.75°C average) in case of with radiant cooling system. The temperature and relative humidity of the exterior air are in the range of 25.83-34.79°C (29.62°C average) and 60.71-83.43% (73.64% average), while, the average temperature and relative humidity of the interior air are 28.43°C and 80.90% in the hot day period (March 2016) as illustrated in Fig. 5.9. The mean radiant temperatures of the radiant cooling system are in the interval of 25.18-30.55°C (27.61°C average). Moreover, the average moisture content of the interior air is 19.81 g$_w$/kg$_{da}$.
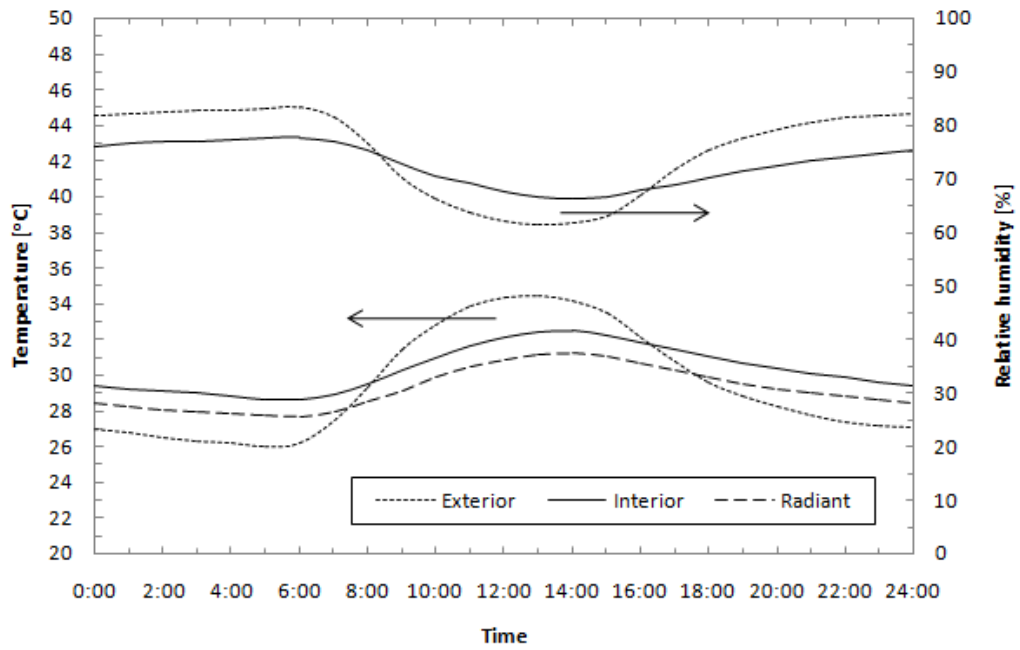
Fig. 5.8 Air temperature, relative humidity, and radiant temperature without cooling panel
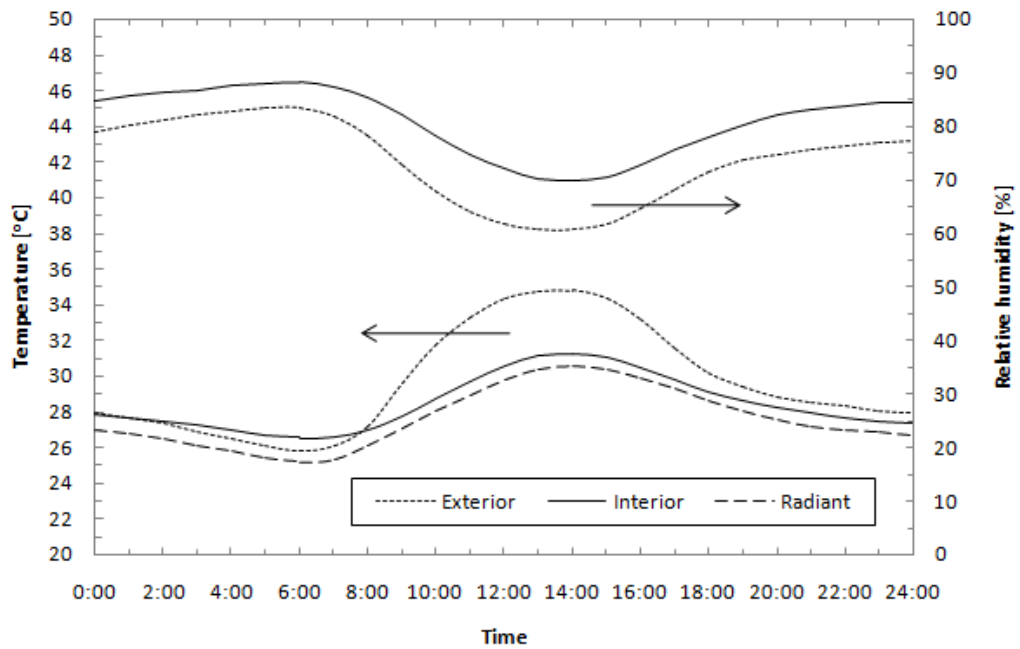
Fig. 5.9 Air temperature, relative humidity, and radiant temperature with cooling panel

In the case of the cooling panels and dehumidifier installation in the experimental room, the surface temperature of the cooling panels is around 24.58-29.18°C (26.60°C average value). The temperature and relative humidity of the exterior air are in the range of 26.19-34.14°C (29.35°C average value) and 62.68-82.52% (75.50% average value), respectively; while, the average temperature and relative humidity of the interior air are 28.72°C and 41.70% in the hot day period (March 2016) as seen in Fig.5.10. The mean radiant temperatures of the radiant cooling system with dehumidifier are in the interval of 25.76-30.71°C (27.75°C average value). Moreover, the average moisture content of the interior air is reduced to 10.28 g_w/kg_{da}.
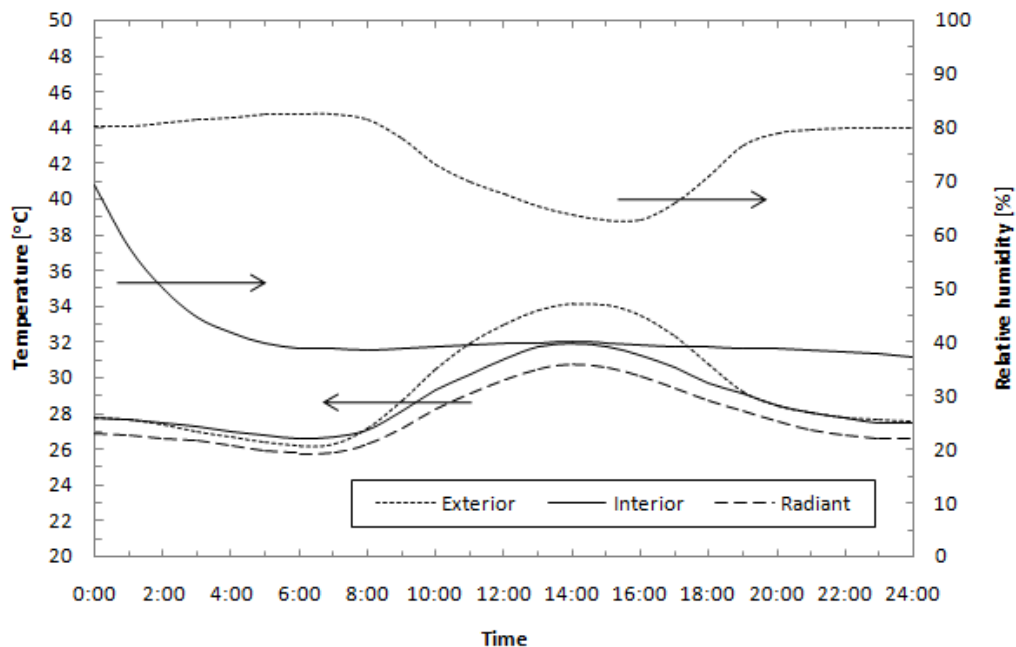
Fig. 5.10 Air temperature, relative humidity, and radiant temperature with cooling panel and dehumidifier

In addition, thermal comfort can improve by operating at the lower air temperature and humidity ratio, or higher the local velocity from the experiment and simulation results. The predicted mean vote from measured values and ANSYS simulation data for E1 (experiment without cooling panel), E2 (experiment with the cooling panel), E3 (experiment with cooling panel and dehumidifier), S1 (simulation

without cooling panel), and S2 (simulation for the cooling panel, dehumidifier, and ventilation fan) are shown in Fig. 5.11.
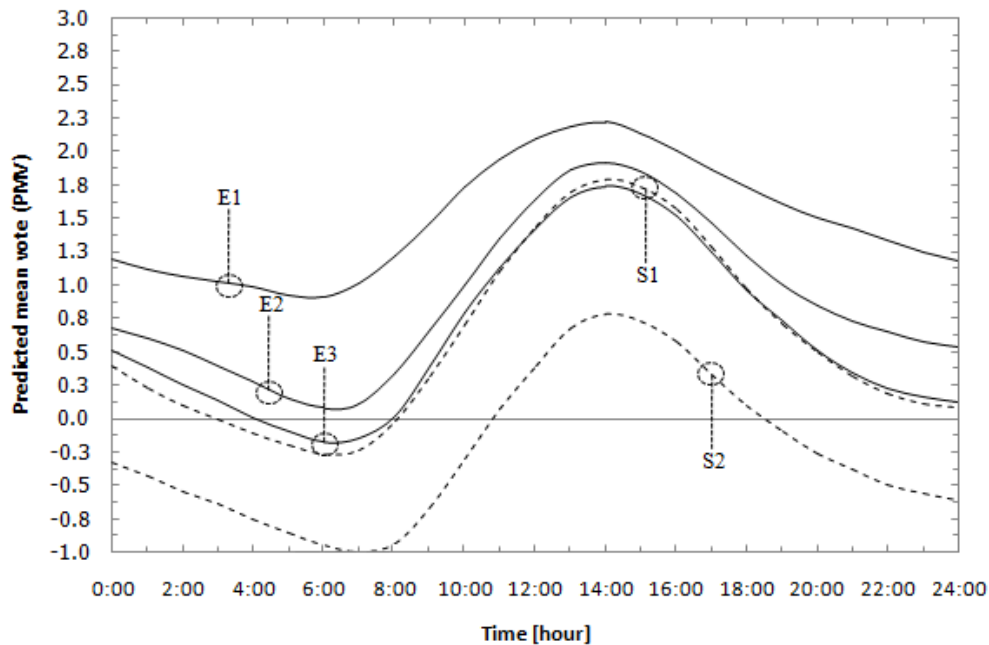
Fig. 5.11 The predicted mean vote from measured values and ANSYS simulation

In case of experiment without cooling panel (E1), the interior air temperature and the relative humidity are high values due to influent of the hot and humid climate. It consists of the hot or warm condition for the human thermal sensation, that the predicted mean vote is in the range of 0.91-2.22 (1.48 average) and the predicted percentage dissatisfied is 22.49-85.62% (50.08% average). In the case E2, the thermal comfort can improve by the uses of cooling panel. The predicted mean vote is in the range of 0.08-1.92 (0.89 average) and the predicted percentage dissatisfied is reduced to 5.13-73.02% (21.60% average). In the third experiment (E3), the solid desiccant dehumidifier was installed with the radiant cooling system. The predicted mean vote is in the range of -0.17-1.74 (0.62 average) and the predicted percentage dissatisfied is reduced to 5.60- 63.88% (13.13% average).

The patterns of temperature, the relative humidity and the predicted mean volte from ANSYS simulation in case of S1 are in the same agreement with the experimental results. Although the thermal comfort can improve by the radiant

cooling and dehumidification system, the values of predicted mean vote are remaining high in the afternoon (12:00-17:00). The value of predicted mean vote is more than 1.25 (PPD 37.73%). In second case of the ANSYS simulation (S2), the ventilation fan installed in the radiant cooling system was investigated. The values of predicted mean vote improve to -0.99-0.78 (-0.24 average) and the value of predicted percentage dissatisfied is in the range of 17.82-25.70% (6.24% averages).

Chapter 6
Conclusion and Recommendation

6.1 Conclusion

The objective of this research is to design and develop a solid desiccant dehumidification and radiant cooling system, which are suitable for tropical climate to achieve thermal comfort. The experiment systems is set up at the 2nd floor of the low energy house in Prince of Songkla University (PSU), Hatyai Campus, Songkhla Province located in the Southern part of Thailand. Dehumidification system uses solid desiccant dehumidifiers with silica-gel bed in column to remove water vapour from the ventilation air before passing into the experimental room. Radiant cooling system is designed using cool water supplied from cooling tower passing through the radiant cooling panel which made from copper tube bond with aluminium sheet.

Design of solid desiccant dehumidifier and radiant cooling panel using the simulation by commercial software programs, namely ANSYS version 13.0 and TRNSYS version 16.0 are also investigated. The designed parameters for optimization and the effects of different flow-bed geometries and flow-directions of air-stream through desiccant media within the desiccant column are considerate. In the radiant cooling system, the simulations are used to predict the thermal comfort assessment and air phenomena profile in the air-conditioning room.

The bed geometries under investigation are vertical bed, segment bed, radial bed and conical bed. In hollow cylindrical bed, the symmetry beds are the feasible and practical dehumidifier such as the radial bed and the conical bed. Under the conditions with amount of desiccant in the bed being close to 10 kg of silica-gel, column volume of 0.045 m^3 and air ventilation of 26 kg/h, the practical optimum zone of the inner diameter and the outer diameter are 0.15 and 0.30 m, respectively; as a result, the feasible and optimum condition values are 23.34 Pa and 0.4634 kg_w/h. In the experimental result, the pressure drop of the vertical flow bed is too high compared the radial flow bed with the same conditions, whereas the adsorption rate is a lower value. For the conditions of the air temperature, the humidity ratio and the mass flow rate range: 25-40°C, 10-20 g_w/kg_{da}, and 60-120 kg/h, the performance of

the vertical and radial bed flow dehumidifier are 107.14 Pa with 0.52 kg_w/h, and 63.23 Pa with 0.66 kg_w/h, respectively. In addition, the comparing the dehumidifiers between desiccant column with radial bed and desiccant wheel have been proposed. The adsorption rate of the desiccant wheel is usually lower than the desiccant column, but its value is almost constant and stable varies a time. Moreover, the pressure drop of the desiccant column is higher in a little value.

In the thermal comfort assessment, the results of desiccant dehumidification for air-conditioning system, the temperature and the relative humidity of the outdoor air in the ranges of 25.5-32.7^{o}C and 55.5-95.6%, the use of desiccant cooling system reduced the humidity ratio of conditioned space and the cooling load of the air conditioner by 14% and 19.26% respectively. Consequently, the thermal comfort was improved from 0.5 PMV (10.12% PPD) to 0.3 PMV (7.04% PPD). For the results of desiccant dehumidification for radiant cooling system, the TRNSYS simulation study indicate that the PMV values can be improving from 1.46 to 1.21 throughout the year with the uses of cooling panel in comparison with the case of without cooling panel. The experimental studies with the desiccant humidifier coupled to the radiant cooling system confirmed the accuracy of simulations. The values of predicted mean vote for the cases of without cooling panel, with cooling panel, and cooling panel with dehumidifier are 1.48, 0.89 and 0.62, respectively. In the case of the ventilation fan installation in the radiant cooling system, the value of predicted mean vote improves to -0.24 and the predicted percentage dissatisfied is 6.24%.

Finally, from this research work under hot and high humidity, the radiant cooling system with using cool water supplied from cooling tower can achieve the thermal sensation level. Moreover, the desiccant dehumidification has an extreme effect. Only in the afternoon, there are the warm conditions. However, the thermal comfort assessment can improve with the dehumidifier and the inside ventilation fan in this interval time. Furthermore, the radiant cooling system with dehumidifier, it cannot only decrease the energy consumption in air-conditioning system, but also develop occupant's thermal comfort.

6.2 Recommendation

This study concentrates only the solid desiccant dehumidifiers with a structured packing impregnated with silica-gels to remove water vapour from the ventilation air before passing into the radiant cooling system. The using solid desiccant coated bed can increase the surface area of dehumidifier; therefore it is the ways to improve the performance of dehumidification with increasing the adsorption rate, and decreasing the pressure drop across dehumidifiers for the future work.

References

Ahmed, M.H., Kattab, N.M. and Fouad, M., 2005 "Evaluation and Optimization of Solar Desiccant Wheel Performance," Renewable Energy, Vol. 30, pp. 305-325.

ANSI/ASHRAE Standard 55.1992. Thermal Environmental Conditions for Human Occupancy. Atlanta: ASHRAE, Inc.

ANSI/ASHRAE Standard 62.1999. Ventilation for Acceptable Indoor Air Quality. Atlanta: ASHRAE, Inc.

ANSYS FLUENT. 2009. Technical specifications Public notice. Canonsburg: ANSYS, Inc.

Ar-U-Wat Tantiwichien, 2006. Design and Investigation of Using Radiant Cooling Panel for Passive Cooling in Building. Master thesis, Prince of Songkla University, Hat Yai, Songkhla, Thailand.

ASHRAE Handbook. 2005. Fundamentals (SI). Atlanta: ASHRAE, Inc.

ASHRAE Handbook. 2008. HVAC Systems and Equipment (SI). Atlanta: ASHRAE, Inc.

Awad, M.M., Ramzy K, A., Hamed, A.M. and Bekheit, M.M., 2008, "Theoretical and Experimental Investigation on the Radial Flow Desiccant Dehumidification bed," Applied Thermal Engineering, Vol. 28, pp. 75-85.

Daou, K., Wang, R.Z. and Xia, Z.Z., 2006 "Desiccant cooling air conditioning: a review," Renewable and Sustainable Energy Reviews, Vol. 10, pp. 55-77.

Dhar, P.L. and Singh, S.K., 2001 "Studies on Solid Desiccant Based Hybrid Air-Conditioning Systems," Applied Thermal Engineering, Vol. 21, pp. 119-134.

Energy Policy and Planning Office (EPPO). 2015. Energy Statistics of Thailand. Ministry of Energy. Bangkok: Amarin Printing and Publishing Public Co., Ltd.

Engineering Institute of Thailand under H.M. the King's Patronage. 2005. Standard for Air-conditioning and Ventilation Systems. Bangkok: Engineering Institute of Thailand.

Ergun, S., 1952, "Fluid Flow through Packed Columns," Chem. Eng. Prog., Vol.48(2), pp. 89-94.

Fanger, P.O., 1970. Thermal Comfort Analysis and Applications in Environmental Engineering. New York: Mcgraw-Hill.

Feustel, H.E. and Stetiu, C., 1995 "Hydronic Radiant Cooling-Preliminary Assessment," Energy and Building, Vol. 22, pp. 193-205.

Fuping Qian and Mingyao Zhang, 2005 "Study of the Natural Vortex Length of a Cyclone with Response Surface Methodology," Computers and Chemical Engineering, Vol. 29, pp. 2155-2162.

Gandhidasan, P., Al-Farayedhi, A.A. and Al-Mubarak, A.A., 2001, "Dehydration of Natural Gas Using Solid Desiccants," Energy, Vol. 26, pp. 855-868.

Ge, T.S., Dai, Y.J., Wang, R.Z. and Peng, Z.Z., 2010 "Experimental Comparison and Analysis on Silica gel and Polymer Coated Fin-Tube Heat Exchangers," Energy, Vol. 35, pp. 2893-2900.

Hamed, A.M., 2002, "Theoretical and Experimental Study on the Transient Adsorption Characteristics of a Vertical Packed Porous Bed," Renewable Energy, Vol. 27, pp.525-541.

Hamed, A.M., Abd El Rahman, W.R. and El-Eman, S.H., 2010 "Experimental study of the transient adsorption/desorption characteristics of silica gel particles in fluidized bed," Energy, Vol. 35, pp. 2468-2483.

Hao, X., Zhang, G., Chen, Y., Zou, S. and Moschandreas, D.J., 2007 "A Combined System of Chilled Ceiling, Displacement Ventilation and Desiccant Dehumidification," Building and Environment, Vol. 42, pp. 3298-3308.

Hassan S. Al-Sharqawi and Noam Lior, 2008, "Effect of Flow-Duct Geometry on Solid Desiccant Dehumidification," Ind. Eng. Chem. Res., Vol. 47, pp 1569-1585.

Jeong, J.W. and Mumma, S.A., 2003 "Ceiling radiant cooling panel capacity enhanced by mixed convection in mechanically ventilated spaces," Applied Thermal Engineering, Vol. 23, pp. 2293-2306.

Jeong, J.W. and Mumma, S.A., 2004 "Simplified Cooling Capacity Estimation Model for Top Insulated Metal Ceiling Radiant Cooling Panels," Applied Thermal Engineering, Vol. 24, pp. 2055-2072.

Jeong, J.W. and Mumma, S.A., 2007 "Practical Cooling Capacity Estimation Model for a Suspended Metal Ceiling Radiant Cooling Panel," Building and Environment, Vol. 42, pp. 3176-3185.

Kabeel, A.E., 2009, "Adsorption-Desorption Operations of Multilayer Desiccant Packed Bed for Dehumidification Applications," Renewable Energy, Vol. 34, pp. 255-265.

Keller II, G.E., Anderson, R.A. and Yon, C.M. 1987. Handbook of Separation Process Technology. New York: Wiley-Interscience.

Khedari, J., Sangprajak, A. and Hirunlabh, J., 2002 "Thailand Climatic Zones," *Renewable Energy*, Vol. 25, pp. 267-280.

Khedari, J., Yamtraipat, N., Pratintong, N., and Hirunlab, J., 2000. "Thailand ventilation comfort chart," Energy and Buildings, Vol. 32, pp. 245-249.

Klinkenberg, A. 1954. Ind. Eng. Chem., 46, 2285.

Ko-Ta Chiang, 2007 "Modeling and optimization of designing parameters for a parallel-plain fin heat sink with confined impinging jet using the response surface methodology," Applied Thermal Engineering, Vol. 27, pp. 2473-2482.

Langmuir, I. 1918. J. Amer. Chem. Soc., 40, 1361.

Masoud Rahimi and Mohsen Mohseni, 2008, "CFD Modeling of the Effect of Absorbent size on Absorption Performance of a Packed Bed Column," Korean J. Chem. Eng., Vol. 25(3), pp 395-401.

Mazzei, P., Minichiello, F. and Palma, D., 2005 "HVAC dehumidification systems for thermal comfort: a critical review," Applied Thermal Engineering, Vol. 25, pp. 677-707.

Memon, R.A., Chirarattananon, S. and Vangtook, P., 2008 "Thermal comfort assessment and application of radiant cooling: A case study," Building and Environment, Vol. 43, pp. 1185-1196.

Montgomery, D.C. 2005. Design and Analysis of Experiments, 6th edition. USA: John Wiley.

Mumma, S.A., 2001 "Ceiling Panel Cooling Systems," ASHRAE Journal, November, pp. 28-32.

Myers, R.H. and Montgomery, D.H. 1995. Response Surface Methodology. USA: John Wiley and Sons.

Nia, F.E., Paassen, D.V. and Saidi, M.H., 2006 "Modeling and Simulation of Desiccant Wheel for Air Conditioning," Energy and Building, Vol. 38, pp. 1230-1239.

Nicol, F., 2004. "Adaptive thermal comfort standards in the hot-humid tropics," Energy and Buildings, Vol. 36, pp. 628-637.

Niu, J.L., Zhang, L.Z. and Zuo, H.G., 2002 "Energy Saving Potential of Chilled-Ceiling Combined with Desiccant Cooling in Hot and Humid Climates," Building and Environment, Vol. 34, pp. 487-495.

Prapapong Vangtook and Surapong Chirarattananon, 2006 "An Experimental Investigation of Application of Radiant Cooling in Hot Humid Climate," Energy and Buildings, Vol. 38, pp. 273-285.

Punlek, C., Pairintra, R., Chindaraksa, S. and Maneewan, S., 2009, "Simulation Design and Evaluation of Hybrid PV/T Assisted Desiccant Integrated HA-IR Drying System (HPIRD)," Food and Bioproducts Processing, Vol. 87, pp 77-86.

Stetiu, C. and Feustel, H.E., 1994. Development of a Model to Simulate the Performance of Hydronic/Radiant Cooling Ceilings. California: Lawrence Berkeley Laboratory.

Techajunta, S.,Chirarattananon, S. and Exell, R.H.B., 1999, "Experiments in a Solar Simulator on Solid Desiccant Regeneration and Air Dehumidification for Air conditioning in a Tropical Humid Climate," Renewable Energy, Vol. 17, pp. 549-568.

Thomas, W.J. and Crittenden, B., 1998. *Adsorption Technology and Design*. Elsevier Science & Technology Books.

Tomas Norton and Da-Wen Sun, 2006, "Computational Fluid Dynamics (CFD)-an Effective and Efficient Design and Analysis Tool for the Food Industry: A Review," Trends in Food Science & Technology, Vol. 17, pp 600-620.

Ushakumari, S.R., Rastogi, N.K. and Malleshi, N.G., 2007 "Optimization of process variables for the preparation of expanded finger millet using response surface methodology," Food Engineering, Vol. 82, pp. 35-42.

Versteeg, H.K. and Malalasekera, W. 1995. An introduction to computational fluid dynamics, the finite volume method. England: Longman Limited.

Visit Akvanich, 2009. Applications of Solid Desiccant Dehumidification for Air-conditioning System in Residential Buildings. Master thesis, Prince of Songkla University, Hat Yai, Songkhla, Thailand.

Yamtraipat, N., Khedari, J. and Hirunlabh, J., 2005 "Thermal Comfort Standards for Air Conditioned Buildings in Hot and Humid Thailand Considering Additional Factors of Acclimatization and Education level," Solar Energy, Vol. 78, pp. 504-517.

APPENDIX A

THE SOLID DESICCANT DEHUMIDIFICATION WITH THE USE OF THE

RADIANT COOLING SYSTEM
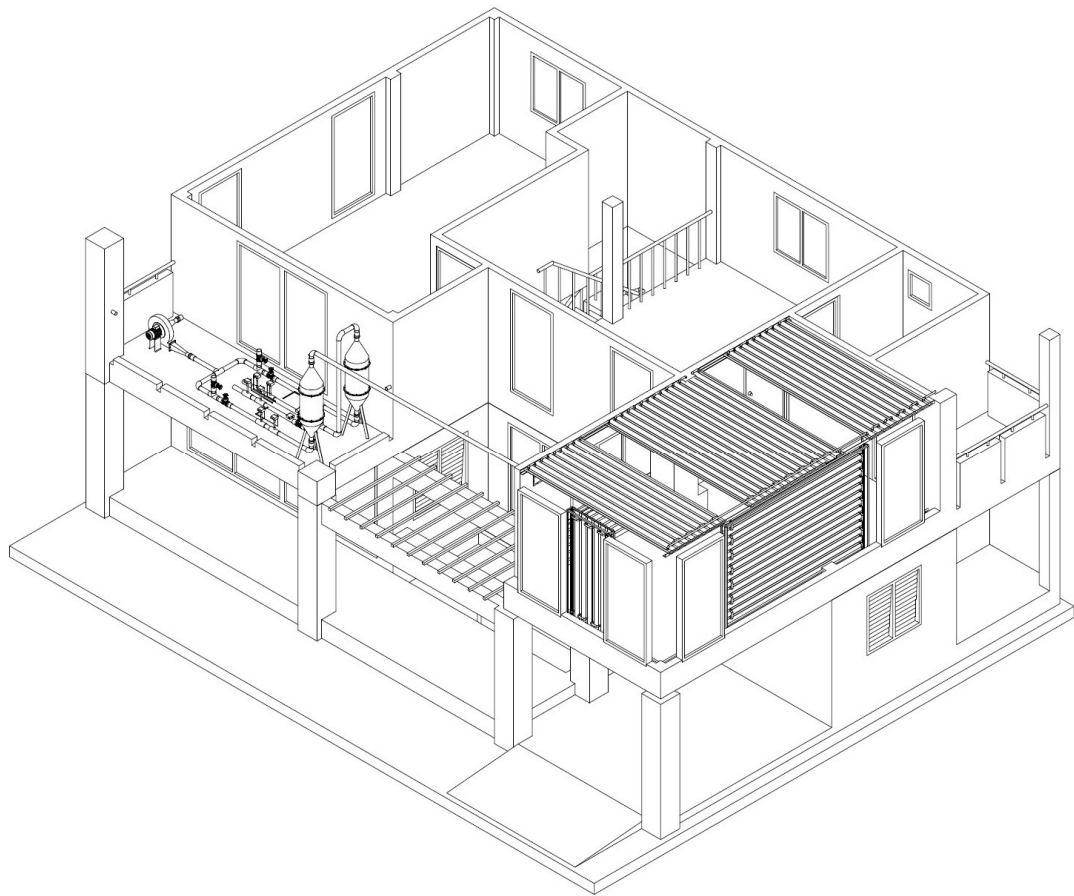
Fig. A.1 The solid desiccant dehumidifiers and the cooling panels
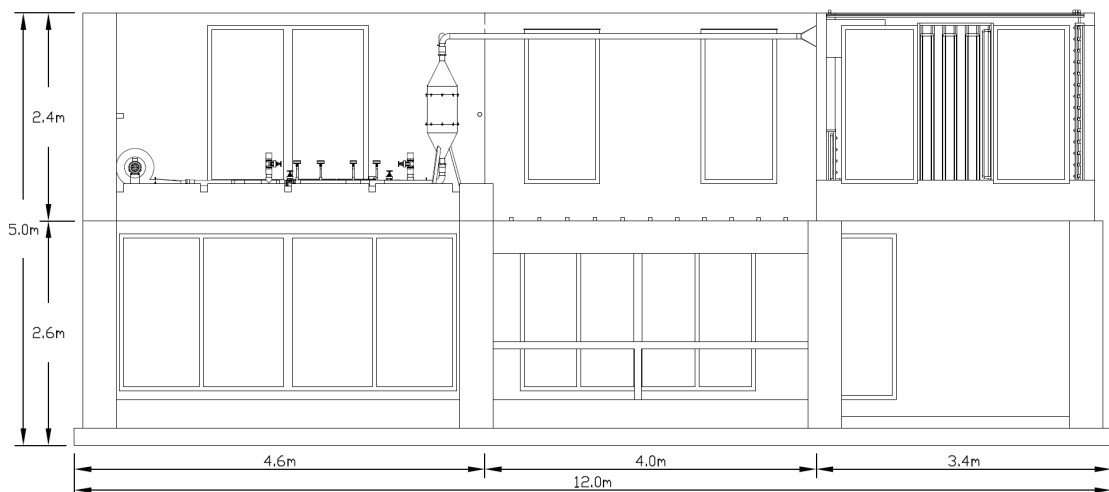
Fig. A.2 Physical dimension in the front view of PSU low energy house
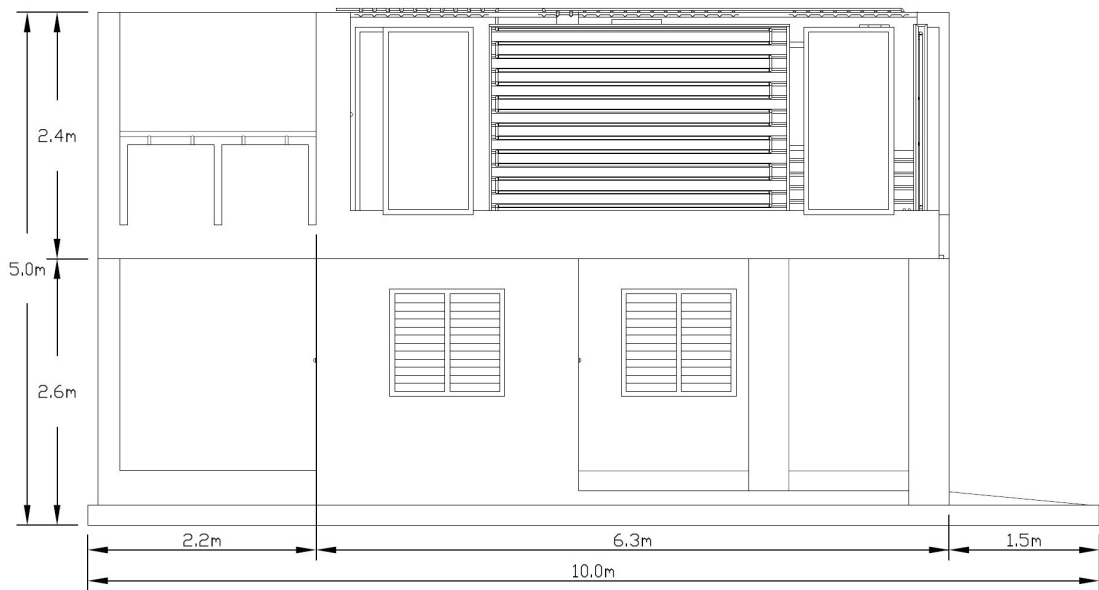
Fig. A.3 Physical dimension in the right side view of PSU low energy house
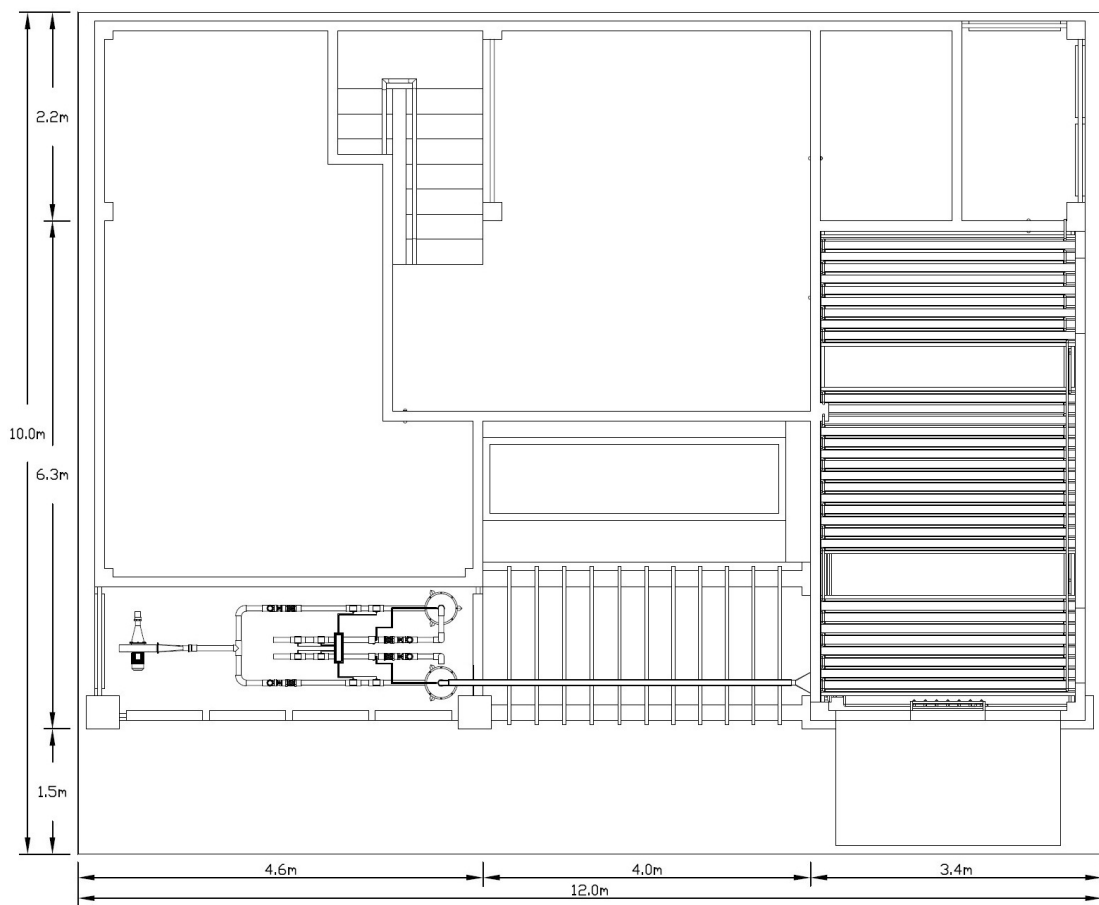
Fig. A.4 Physical dimension in the top view of PSU low energy house
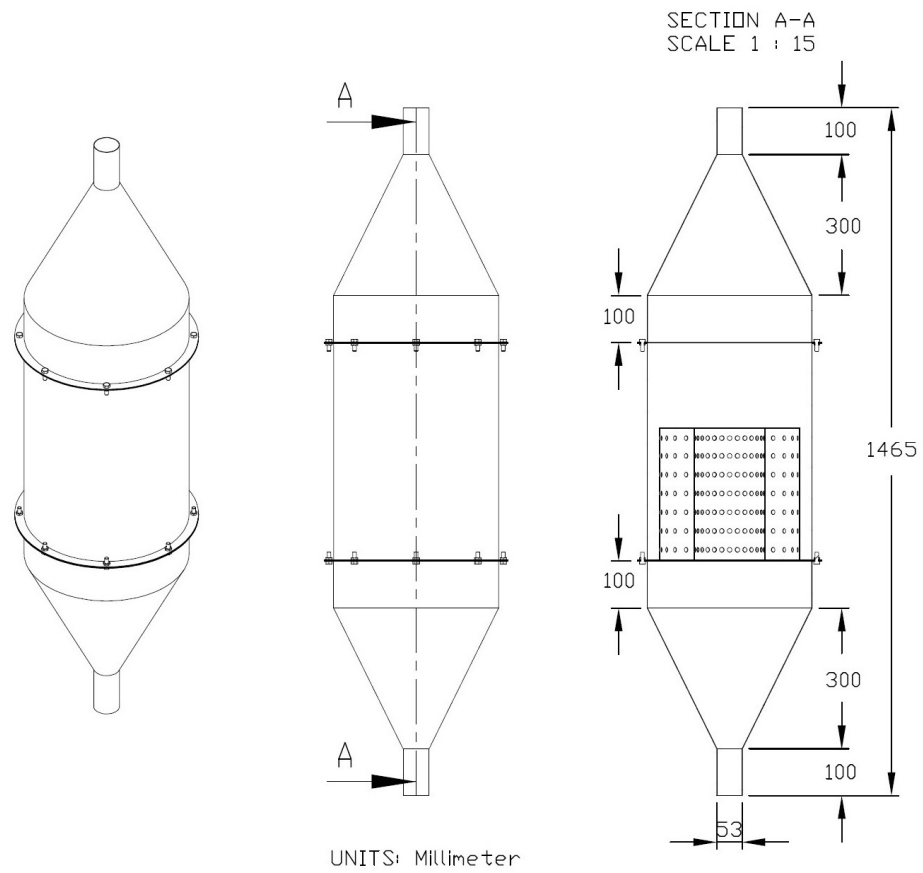
Fig. A.5 Physical dimension of the desiccant column
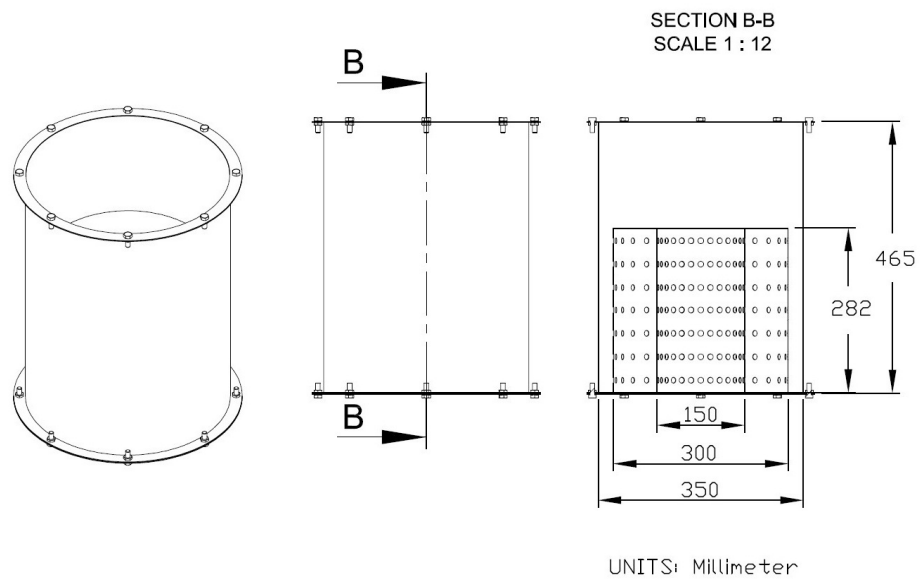
Fig. A.6 Physical dimension of the radial bed

APPENDIX B

THE DETAILS OF CALCULATED PROCEDURE FOR THE DESICCANT

COLUMN DESIGNS

B.1 The adsorption equilibrium of adsorbent-grade silica-gel

From the Langmuir equation (Eq. 2.1), the adsorption properties of silica-gel can be calculated in Table B.1 for a condition at at 1 atm, 25°C.

$$\frac{V}{V_m} = \frac{bC_e}{1 + bC_e}$$

Table B.1 Adsorption properties of silica-gel at 1 atm, 25°C

%RH (%)	W (kg_w/m^3_{da})	V (kg_w/m^3_{ads})	1/W	1/V	$V_{Langmuir}$ (kg_w/m^3_{ads})
5	0.0012	33	864.8786	0.0303	33.11
10	0.0023	66	431.7620	0.0152	64.73
20	0.0046	121	215.2036	0.0083	123.89
30	0.0070	176	143.0175	0.0057	178.18
40	0.0094	231	106.9245	0.0043	228.17
50	0.0117	275	85.2686	0.0036	274.36
60	0.0141	319	70.8314	0.0031	317.16
70	0.0165	352	60.5191	0.0028	356.94
80	0.0189	396	52.7849	0.0025	393.99
90	0.0214	429	46.7694	0.0023	428.60
100	0.0238	462	41.9570	0.0022	461.00

The same procedure is applied to the conditions at 27, 30, 33 and 35°C, the resulting table for the adsorption equilibrium is shown in Fig. B.1
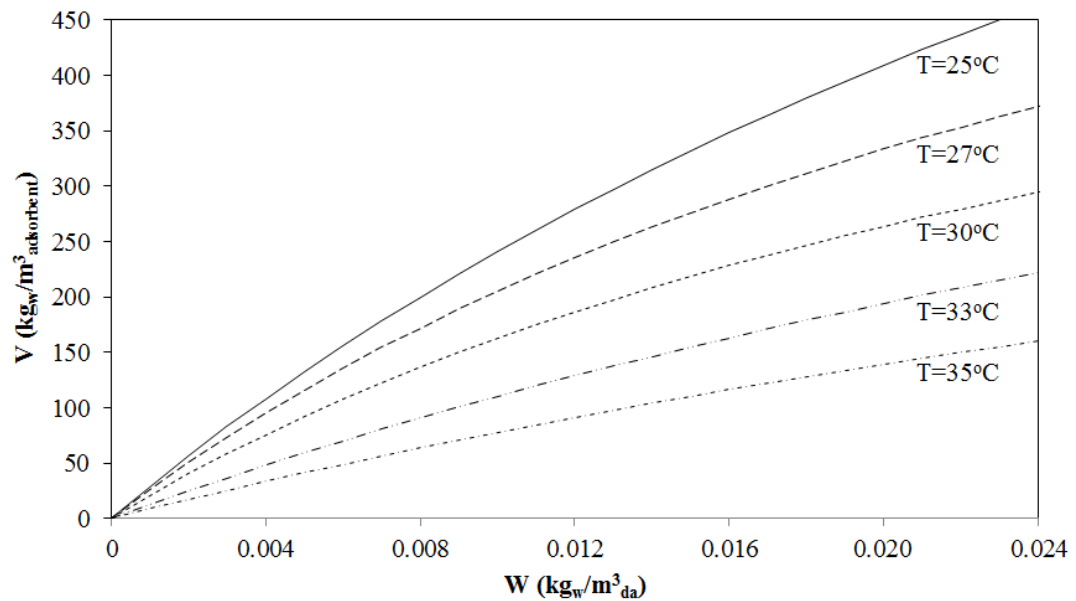
Fig. B.1 The adsorption of water vapor on the silica-gel by Langmuir isotherm

For example, the regression coefficient in the case of 25°C, the Langmuir constant (b) and the quantity V of adsorbate adsorbed in a single monolayer (V_m) are equally 21.7118 m³/kg and 1,351.86 kg/m³, respectively.

B.2 The breakthrough curves of adsorbent-grade silica-gel

From the Klinkenberg equation (Eq. 2.4-2.9), the operation time can be predicted in Table B.2 and illustrated in Fig. B.2.

$$\frac{C_f}{C_o} = \frac{1}{2}\left[1 - erf\left(\sqrt{\xi} - \sqrt{\tau}\right)\right]$$

Table B.2 The concentration of water vapor (outlet/inlet) on the desiccant column

τ	Time (hour)	C_f/C_o	τ	Time (hour)	C_f/C_o
0.5	0.04	0.000000	80	6.47	0.998842
1	0.08	0.000000	90	7.28	0.999932
5	0.40	0.000000	100	8.09	0.999997
10	0.81	0.000000	110	8.90	1.000000
20	1.62	0.000523	120	9.71	1.000000
30	2.43	0.031676	130	10.52	1.000000
40	3.24	0.255126	140	11.33	1.000000
50	4.05	0.654411	150	12.14	1.000000
60	4.85	0.911763	160	12.95	1.000000
70	5.66	0.987106	170	13.75	1.000000

Parameter	Value
Inlet air conditions	29°C, 75%RH
Inlet air humidity ratio (C_o)	19 g_w/kh_{da}
Outlet air conditions	25°C, 50%RH
Outlet air humidity ratio (C_f)	10 g_w/kh_{da}
Ventilation air	50 kg/h
Silica-gel requirement	10 kg
Breakthrough time ($C_f/C_o = 0.52$)	3.77 hour
Equilibrium time ($C_f/C_o = 0.99$)	5.86 hour
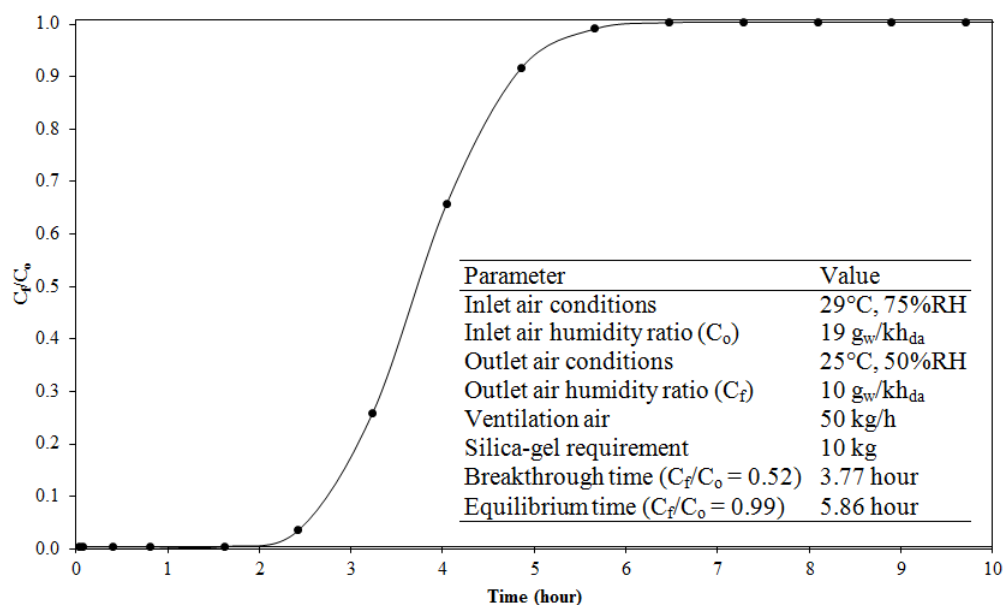
Fig. B.2 The breakthrough curves of the desiccant column

APPENDIX C

THE SIMULATION RESULTS FOR THE EFFECT OF FLOW-BED

GEOMETRIES ON DESICCANT COLUMN

Table C.1 The pressure drop of desiccant column for α_1-direction

ΔP (Pa)	Flow rate (kg/h)				
	9.73	29.19	48.65	68.10	87.56
Vertical	6.52	25.45	50.75	82.89	121.69
Segment	6.61	25.98	51.33	83.80	123.03
Radial	1.97	9.27	20.61	34.82	58.97
Conical bed S1	6.59	60.85	171.13	340.59	565.23
Conical bed S2	1.10	5.23	12.99	23.90	37.95
Conical bed S3	1.11	5.50	12.68	23.15	36.59
Conical bed S4	1.39	7.35	17.59	32.09	49.93

Table C.2 The pressure drop of desiccant column for α_2-direction

ΔP (Pa)	Flow rate (kg/h)				
	9.73	29.19	48.65	68.10	87.56
Vertical	6.52	25.45	50.75	82.89	121.69
Segment	6.61	25.98	51.33	83.80	123.03
Radial	1.88	7.93	18.07	31.19	44.97
Conical bed S1	1.43	6.44	15.46	27.17	41.80
Conical bed S2	1.18	5.89	16.24	27.96	41.07
Conical bed S3	1.38	6.89	15.86	28.97	42.48
Conical bed S4	5.11	47.16	132.63	263.97	438.08

Table C.3 The adsorption rate of desiccant column for α_1-direction

ΔW (kg$_w$/h)	Flow rate (kg/h)				
	9.73	29.19	48.65	68.10	87.56
Vertical	0.175079	0.461826	0.461829	0.461827	0.461828
Segment	0.175079	0.461830	0.461830	0.461830	0.461829
Radial	0.174454	0.463338	0.463270	0.463411	0.463443
Conical bed S1	0.174448	0.339757	0.344379	0.361034	0.376147
Conical bed S2	0.174454	0.452427	0.452430	0.452429	0.452425
Conical bed S3	0.174454	0.452533	0.452595	0.452538	0.452560
Conical bed S4	0.174454	0.454957	0.454931	0.454969	0.454973

Table C.4 The adsorption rate of desiccant column for α_2-direction

ΔW (kg$_w$/h)	Flow rate (kg/h)				
	9.73	29.19	48.65	68.10	87.56
Vertical	0.175079	0.461826	0.461829	0.461827	0.461828
Segment	0.175079	0.461830	0.461830	0.461830	0.461829
Radial	0.174450	0.463036	0.462381	0.462571	0.462746
Conical bed S1	0.173757	0.451839	0.454123	0.454152	0.454371
Conical bed S2	0.174421	0.449947	0.450798	0.451110	0.451075
Conical bed S3	0.174579	0.452857	0.452919	0.452862	0.452884
Conical bed S4	0.174454	0.425914	0.431708	0.432587	0.433532

APPENDIX D

THE SIMULATION RESULTS FOR THE OPTIMIZATION OF DESIGNED

PARAMETERS FOR A DESICCANT COLUMN

Table D.1 The pressure drop of desiccant column for D=200 mm

ΔP, Pa	D_{ri} (mm)		
D_{ro} (mm)	$3/8 \times D_{ro}$	$4/8 \times D_{ro}$	$5/8 \times D_{ro}$
$6/8 \times D$	50.16	25.48	16.21
$8/8 \times D$	28.62	16.65	12.81
$10/8 \times D$	24.68	20.25	14.61

Table D.2 The pressure drop of desiccant column for D=300 mm

ΔP, Pa	D_{ri} (mm)		
D_{ro} (mm)	$3/8 \times D_{ro}$	$4/8 \times D_{ro}$	$5/8 \times D_{ro}$
$6/8 \times D$	26.01	18.10	12.58
$8/8 \times D$	32.06	23.67	18.65
$10/8 \times D$	49.23	31.97	25.25

Table D.3 The pressure drop of desiccant column for D=400 mm

ΔP, Pa	D_{ri} (mm)		
D_{ro} (mm)	$3/8 \times D_{ro}$	$4/8 \times D_{ro}$	$5/8 \times D_{ro}$
$6/8 \times D$	34.71	23.00	18.27
$8/8 \times D$	51.43	35.35	28.29
$10/8 \times D$	76.57	51.79	33.93

Table D.4 The adsorption rate of desiccant column for D=200 mm

ΔW (g_w/s)	D_{ri} (mm)		
D_{ro} (mm)	$3/8 \times D_{ro}$	$4/8 \times D_{ro}$	$5/8 \times D_{ro}$
$6/8 \times D$	0.1143	0.1251	0.1241
$8/8 \times D$	0.1283	0.1280	0.1282
$10/8 \times D$	0.1283	0.1282	0.1286

Table D.5 The adsorption rate of desiccant column for D=300 mm

ΔW (g_w/s)	D_{ri} (mm)		
D_{ro} (mm)	$3/8 \times D_{ro}$	$4/8 \times D_{ro}$	$5/8 \times D_{ro}$
$6/8 \times D$	0.1285	0.1279	0.1277
$8/8 \times D$	0.1284	0.1287	0.1282
$10/8 \times D$	0.1281	0.1281	0.1290

Table D.6 The adsorption rate of desiccant column for D=400 mm

ΔW (g_w/s)	D_{ri} (mm)		
D_{ro} (mm)	$3/8 \times D_{ro}$	$4/8 \times D_{ro}$	$5/8 \times D_{ro}$
$6/8 \times D$	0.1284	0.1287	0.1282
$8/8 \times D$	0.1285	0.1283	0.1285
$10/8 \times D$	0.1278	0.1282	0.1288

APPENDIX E

THE RESULTS FOR THE DESICCANT DEHUMIDIFICATION FOR

AIR-CONDITIONING SYSTEM

Table E.1 The experimental and simulation results for the air-conditioning systems

Time	T_{oa}-Exp	%RH_{oa}-Exp	T_{ia}-Exp	%RH_{ia}-Exp	T_{ia}-Sim	%RH_{ia}-Sim
	^{o}C	%	^{o}C	%	^{o}C	%
9:00	30.0	69.49	28.2	94.65	26.3	63.45
10:00	29.8	71.55	25.9	67.21	25.8	59.31
11:00	31.1	67.90	25.7	63.31	26.1	60.05
12:00	31.2	66.66	26.0	62.27	26.0	60.08
13:00	31.6	62.76	26.1	62.98	26.1	60.10
14:00	31.6	65.10	26.2	61.77	26.2	60.11
15:00	30.9	71.56	26.1	60.10	25.9	60.07
16:00	30.0	71.99	25.6	56.84	26.0	60.05
17:00	28.8	80.38	25.3	58.63	25.8	60.04
18:00	28.4	83.65	24.9	57.94	25.6	60.02
19:00	27.4	91.05	24.4	57.39	25.5	60.05
20:00	27.2	92.40	24.1	57.57	25.4	60.03
21:00	26.7	94.96	23.8	58.38	25.3	60.00

Table E.2 The experimental and simulation results for the desiccant cooling systems

Time	T_{oa}-Exp	%RH_{oa}-Exp	T_{ia}-Exp	%RH_{ia}-Exp	T_{ia}-Sim	%RH_{ia}-Sim
	^{o}C	%	^{o}C	%	^{o}C	%
9:00	29.8	59.27	27.5	92.23	26.1	57.78
10:00	31.2	68.50	25.2	54.73	25.8	54.47
11:00	31.7	60.38	25.4	52.52	26.0	54.50
12:00	31.6	61.43	25.6	51.33	26.2	54.48
13:00	32.1	55.17	25.7	52.05	26.2	54.49
14:00	32.4	53.27	26.0	50.23	26.1	54.50
15:00	32.7	58.72	26.2	52.79	25.9	54.49
16:00	31.3	64.70	26.1	53.94	25.9	54.50
17:00	30.5	72.83	25.7	52.22	25.8	54.48
18:00	27.2	84.78	25.2	51.28	25.6	54.49
19:00	26.4	93.29	24.6	51.84	25.4	54.47
20:00	25.9	95.16	24.3	52.42	25.3	54.46
21:00	25.5	95.62	23.9	52.36	25.2	54.46

APPENDIX F

THE RESULTS FOR THE DESICCANT DEHUMIDIFICATION FOR

RADIANT COOLING SYSTEM

Table F.1 The air temperature, relative humidity, and PMV without cooling panel
from TRNSYS simulation for March 2015

Time (day)	$T_{exterior}$ (^{o}C)	%$Rh_{exterior}$ (%)	$T_{interior}$ (^{o}C)	%$Rh_{interior}$ (%)	PMV
0	28.40	80.00	26.98	87.12	1.50
2	28.30	71.50	26.81	88.02	1.46
4	26.70	69.50	26.96	87.20	1.49
6	27.85	71.50	27.65	83.76	1.63
8	23.65	80.00	25.66	94.19	1.22
10	26.55	76.00	26.20	91.22	1.33
12	26.65	80.50	25.82	93.29	1.26
14	28.30	69.50	27.91	82.50	1.68
16	29.54	75.50	28.59	79.32	1.82
18	28.90	71.50	28.50	79.73	1.80
20	28.69	76.50	28.24	80.92	1.75
22	29.25	78.00	27.16	86.23	1.53
24	28.70	74.50	27.92	82.44	1.69
26	28.90	83.00	26.49	89.66	1.40
28	29.10	74.50	27.44	84.78	1.59
30	29.15	72.50	28.19	81.17	1.74

Table F.2 The air temperature, relative humidity, and PMV with cooling panel from
TRNSYS simulation for March 2015

Time (day)	$T_{exterior}$ (^{o}C)	%$Rh_{exterior}$ (%)	$T_{interior}$ (^{o}C)	%$Rh_{interior}$ (%)	PMV
0	28.40	80.00	25.28	96.31	1.16
2	28.30	71.50	25.26	96.46	1.15
4	26.70	69.50	25.16	97.04	1.13
6	27.85	71.50	25.37	95.83	1.17
8	23.65	80.00	24.66	99.98	1.03
10	26.55	76.00	25.04	97.74	1.11
12	26.65	80.50	24.92	98.42	1.09
14	28.30	69.50	25.46	95.33	1.19
16	29.54	75.50	25.64	94.30	1.23
18	28.90	71.50	25.59	94.58	1.22
20	28.69	76.50	25.50	95.05	1.20
22	29.25	78.00	25.40	95.65	1.18
24	28.70	74.50	25.47	95.23	1.20
26	28.90	83.00	25.23	96.64	1.15
28	29.10	74.50	25.42	95.53	1.19
30	29.15	72.50	25.54	94.86	1.21

Table F.3 The air temperature, relative humidity, and PMV without cooling panel from TRNSYS simulation for July 2015

Time (day)	$T_{exterior}$ (^oC)	%$Rh_{exterior}$ (%)	$T_{interior}$ (^oC)	%$Rh_{interior}$ (%)	PMV
0	26.30	87.00	24.49	100.00	0.99
2	28.94	82.50	26.35	90.40	1.37
4	27.00	82.00	25.32	96.09	1.16
6	26.91	80.50	24.88	98.63	1.07
8	29.20	82.00	26.28	90.76	1.36
10	27.50	82.50	26.12	91.66	1.32
12	27.49	79.00	26.61	89.03	1.42
14	25.80	76.50	25.01	97.87	1.10
16	27.05	84.00	24.75	99.45	1.04
18	28.30	72.50	27.07	86.66	1.51
20	27.21	88.50	25.83	93.23	1.26
22	28.60	82.50	26.72	88.48	1.44
24	27.29	83.00	25.35	95.90	1.17
26	25.27	73.00	25.78	93.53	1.25
28	27.95	71.50	27.12	86.41	1.52
30	26.69	72.50	26.41	90.11	1.38

Table F.4 The air temperature, relative humidity, and PMV with cooling panel from TRNSYS simulation for July 2015

Time (day)	$T_{exterior}$ (^oC)	%$Rh_{exterior}$ (%)	$T_{interior}$ (^oC)	%$Rh_{interior}$ (%)	PMV
0	26.30	87.00	24.71	99.66	1.05
2	28.94	82.50	25.28	96.33	1.16
4	27.00	82.00	24.90	98.51	1.08
6	26.91	80.50	24.82	98.98	1.07
8	29.20	82.00	25.26	96.46	1.15
10	27.50	82.50	25.07	97.53	1.12
12	27.49	79.00	25.16	97.04	1.13
14	25.80	76.50	24.75	99.43	1.05
16	27.05	84.00	24.81	99.08	1.07
18	28.30	72.50	25.37	95.84	1.17
20	27.21	88.50	24.97	98.14	1.10
22	28.60	82.50	25.28	96.36	1.16
24	27.29	83.00	24.90	98.51	1.08
26	25.27	73.00	24.86	98.76	1.07
28	27.95	71.50	25.32	96.11	1.16
30	26.69	72.50	25.06	97.61	1.11

Table F.5 The air temperature, relative humidity, and PMV without cooling panel
from TRNSYS simulation for September 2015

Time (day)	$T_{exterior}$ (^{o}C)	%Rh$_{exterior}$ (%)	$T_{interior}$ (^{o}C)	%Rh$_{interior}$ (%)	PMV
0	29.80	79.50	26.57	89.23	1.42
2	27.60	84.50	26.05	92.04	1.31
4	28.04	72.50	27.98	82.17	1.70
6	27.65	80.00	26.95	87.27	1.49
8	26.81	84.00	24.18	100.00	0.91
10	25.95	86.00	24.53	100.00	0.99
12	24.93	81.00	25.67	94.11	1.23
14	27.00	83.50	25.06	97.59	1.11
16	25.50	83.50	24.00	100.00	0.87
18	28.06	86.00	25.00	97.95	1.10
20	26.30	87.00	24.53	100.00	0.99
22	26.75	77.50	25.42	95.54	1.18
24	28.12	81.00	24.90	98.55	1.08
26	27.52	82.50	26.78	88.17	1.45
28	24.70	87.50	24.89	98.57	1.07
30	25.90	75.50	25.87	93.01	1.27

Table F.6 The air temperature, relative humidity, and PMV with cooling panel
from TRNSYS simulation for September 2015

Time (day)	$T_{exterior}$ (^{o}C)	%Rh$_{exterior}$ (%)	$T_{interior}$ (^{o}C)	%Rh$_{interior}$ (%)	PMV
0	29.80	79.50	25.37	95.83	1.18
2	27.60	84.50	25.08	97.47	1.12
4	28.04	72.50	25.45	95.35	1.19
6	27.65	80.00	25.20	96.76	1.14
8	26.81	84.00	24.72	99.63	1.05
10	25.95	86.00	24.67	99.90	1.04
12	24.93	81.00	24.83	98.92	1.07
14	27.00	83.50	24.83	98.93	1.07
16	25.50	83.50	24.56	100.00	1.01
18	28.06	86.00	24.93	98.34	1.09
20	26.30	87.00	24.74	99.50	1.05
22	26.75	77.50	24.90	98.52	1.08
24	28.12	81.00	24.90	98.51	1.09
26	27.52	82.50	25.21	96.73	1.14
28	24.70	87.50	24.67	99.89	1.03
30	25.90	75.50	24.89	98.57	1.08

Table F.7 The air temperature, relative humidity, and PMV without cooling panel
from TRNSYS simulation for December 2015

Time (day)	$T_{exterior}$ (^oC)	%$Rh_{exterior}$ (%)	$T_{interior}$ (^oC)	%$Rh_{interior}$ (%)	PMV
0	24.36	81.00	22.99	100.00	0.62
2	25.14	77.50	24.74	99.47	1.04
4	26.40	65.00	27.28	85.61	1.55
6	25.20	69.50	26.56	89.31	1.41
8	25.50	73.50	25.50	95.06	1.19
10	24.75	66.50	25.69	94.03	1.23
12	25.61	66.50	25.69	94.02	1.23
14	27.00	68.50	27.09	86.57	1.51
16	27.85	66.50	27.72	83.42	1.64
18	27.65	67.50	27.85	82.81	1.67
20	26.20	59.50	27.13	86.36	1.52
22	26.20	65.50	26.33	90.52	1.36
24	22.05	65.00	23.96	100.00	0.85
26	22.15	82.50	21.01	100.00	0.16
28	23.24	74.50	23.67	100.00	0.78
30	24.00	72.50	23.82	100.00	0.82

Table F.8 The air temperature, relative humidity, and PMV with cooling panel
from TRNSYS simulation for December 2015

Time (day)	$T_{exterior}$ (^oC)	%$Rh_{exterior}$ (%)	$T_{interior}$ (^oC)	%$Rh_{interior}$ (%)	PMV
0	24.36	81.00	24.29	100.00	0.95
2	25.14	77.50	24.63	100.00	1.03
4	26.40	65.00	25.20	96.80	1.14
6	25.20	69.50	24.95	98.23	1.09
8	25.50	73.50	24.80	99.14	1.06
10	24.75	66.50	24.80	99.14	1.06
12	25.61	66.50	24.86	98.77	1.07
14	27.00	68.50	25.24	96.58	1.15
16	27.85	66.50	25.37	95.79	1.18
18	27.65	67.50	25.37	95.79	1.18
20	26.20	59.50	25.11	97.29	1.12
22	26.20	65.50	25.01	97.92	1.10
24	22.05	65.00	24.28	100.00	0.94
26	22.15	82.50	23.82	100.00	0.83
28	23.24	74.50	24.39	100.00	0.97
30	24.00	72.50	24.42	100.00	0.97

Table F.9 The air temperature, relative humidity, and PMV without cooling panel
from the experiment for March 2016

Time (day)	$T_{exterior}$ (^{o}C)	%$Rh_{exterior}$ (%)	$T_{interior}$ (^{o}C)	%$Rh_{interior}$ (%)	PMV
0	27.01	81.92	29.44	76.11	1.20
1	26.73	82.23	29.22	76.68	1.12
2	26.51	82.54	29.08	76.88	1.07
3	26.34	82.78	28.98	76.96	1.03
4	26.17	82.87	28.85	77.17	0.99
5	26.00	83.25	28.67	77.59	0.92
6	26.17	83.38	28.64	77.74	0.91
7	27.43	81.42	28.95	76.83	1.02
8	29.26	76.66	29.52	75.21	1.22
9	31.42	70.22	30.24	72.82	1.46
10	32.83	66.41	31.00	70.64	1.73
11	33.82	63.79	31.62	69.06	1.94
12	34.37	62.07	32.08	67.66	2.09
13	34.46	61.44	32.39	66.62	2.19
14	34.19	61.68	32.48	66.25	2.22
15	33.47	63.17	32.25	66.71	2.14
16	32.13	66.87	31.84	67.77	2.00
17	30.72	71.71	31.41	68.90	1.86
18	29.57	75.27	31.02	70.27	1.73
19	28.82	77.54	30.65	71.50	1.60
20	28.24	79.28	30.34	72.49	1.50
21	27.76	80.48	30.10	73.25	1.42
22	27.38	81.36	29.85	73.99	1.33
23	27.17	81.83	29.63	74.72	1.25
24	27.06	82.08	29.42	75.31	1.18

Table F.10 The air temperature, relative humidity, and PMV with cooling panel
from the experiment for March 2016

Time (day)	$T_{exterior}$ (^oC)	%$Rh_{exterior}$ (%)	$T_{interior}$ (^oC)	%$Rh_{interior}$ (%)	PMV
0	27.97	78.95	27.85	84.84	0.68
1	27.68	80.08	27.65	85.60	0.60
2	27.36	81.20	27.47	86.37	0.51
3	26.89	82.29	27.24	86.76	0.40
4	26.53	82.85	26.99	87.53	0.28
5	26.12	83.29	26.72	87.95	0.15
6	25.83	83.43	26.55	88.27	0.08
7	26.11	81.84	26.62	87.46	0.11
8	27.17	78.29	26.98	85.47	0.35
9	29.64	72.74	27.73	81.99	0.67
10	31.73	67.88	28.69	78.30	1.00
11	33.25	64.17	29.71	74.69	1.35
12	34.32	61.59	30.57	72.04	1.65
13	34.76	60.73	31.10	70.29	1.86
14	34.79	60.71	31.26	69.84	1.92
15	34.31	61.79	31.06	70.62	1.85
16	33.18	64.71	30.48	72.86	1.68
17	31.57	68.27	29.75	75.54	1.46
18	30.21	71.53	29.10	77.97	1.22
19	29.37	73.63	28.58	80.35	1.00
20	28.82	74.82	28.21	82.07	0.85
21	28.50	75.71	27.90	83.12	0.73
22	28.30	76.24	27.69	83.67	0.65
23	28.07	76.94	27.49	84.26	0.58
24	27.97	77.32	27.37	84.55	0.54

Table F.11 The air temperature, relative humidity, and PMV with cooling panel and
dehumidifier from the experiment for March 2016

Time (day)	$T_{exterior}$ (^{o}C)	%Rh$_{exterior}$ (%)	$T_{interior}$ (^{o}C)	%Rh$_{interior}$ (%)	PMV
0	27.73	80.10	27.76	69.34	0.51
1	27.64	80.33	27.65	57.63	0.38
2	27.34	80.72	27.47	49.91	0.25
3	27.01	81.42	27.30	44.60	0.14
4	26.64	81.92	27.00	41.57	0.01
5	26.42	82.32	26.76	39.81	-0.09
6	26.19	82.52	26.56	38.83	-0.17
7	26.29	82.52	26.65	38.69	-0.14
8	27.19	81.42	27.11	38.58	0.02
9	28.74	77.95	28.13	38.80	0.39
10	30.49	73.23	29.28	39.16	0.80
11	31.97	69.80	30.20	39.47	1.13
12	33.00	67.42	31.04	39.69	1.43
13	33.74	65.19	31.70	39.89	1.66
14	34.14	63.55	31.93	39.94	1.74
15	34.07	62.68	31.77	39.86	1.68
16	33.51	62.85	31.29	39.41	1.51
17	32.27	65.87	30.55	39.18	1.25
18	30.74	70.81	29.73	38.97	0.96
19	29.19	76.72	29.09	38.87	0.73
20	28.42	79.02	28.47	38.76	0.51
21	28.03	79.53	28.02	38.42	0.35
22	27.77	79.73	27.70	38.17	0.23
23	27.62	79.83	27.50	37.65	0.16
24	27.53	79.93	27.41	37.25	0.12

Table F.12 The air temperature, relative humidity, and PMV with cooling panel and
dehumidifier from the ANSYS simulation for March 2016

Time (day)	$T_{exterior}$ (^{o}C)	%$Rh_{exterior}$ (%)	$T_{interior}$ (^{o}C)	%$Rh_{interior}$ (%)	PMV
0	27.73	80.10	27.71	67.71	0.40
1	27.64	80.33	27.53	54.95	0.23
2	27.34	80.72	27.36	47.19	0.10
3	27.01	81.42	27.14	42.96	0.00
4	26.64	81.92	26.88	40.14	-0.11
5	26.42	82.32	26.67	38.40	-0.20
6	26.19	82.52	26.52	37.41	-0.26
7	26.29	82.52	26.60	36.80	-0.23
8	27.19	81.42	27.17	36.94	-0.02
9	28.74	77.95	28.12	37.72	0.32
10	30.49	73.23	29.14	38.32	0.70
11	31.97	69.80	30.21	39.10	1.10
12	33.00	67.42	31.12	39.68	1.44
13	33.74	65.19	31.80	40.23	1.70
14	34.14	63.55	32.03	40.34	1.79
15	34.07	62.68	31.92	40.25	1.74
16	33.51	62.85	31.46	39.67	1.57
17	32.27	65.87	30.70	39.07	1.28
18	30.74	70.81	29.89	38.83	0.97
19	29.19	76.72	29.19	38.58	0.71
20	28.42	79.02	28.60	38.40	0.50
21	28.03	79.53	28.13	38.02	0.32
22	27.77	79.73	27.78	37.59	0.19
23	27.62	79.83	27.57	37.30	0.11
24	27.53	79.93	27.48	37.10	0.08

Table F.13 The air temperature, relative humidity, and PMV with the ventilation fan
installed in the radiant cooling system and dehumidifier from the ANSYS
simulation for March 2016

Time (day)	$T_{exterior}$ (^{o}C)	%$Rh_{exterior}$ (%)	$T_{interior}$ (^{o}C)	%$Rh_{interior}$ (%)	PMV
0	27.73	80.10	27.43	41.06	-0.33
1	27.64	80.33	27.24	39.90	-0.43
2	27.34	80.72	27.00	38.91	-0.54
3	27.01	81.42	26.76	38.21	-0.64
4	26.64	81.92	26.50	37.90	-0.75
5	26.42	82.32	26.23	37.73	-0.86
6	26.19	82.52	26.02	37.84	-0.95
7	26.29	82.52	25.91	38.18	-0.99
8	27.19	81.42	26.06	38.61	-0.93
9	28.74	77.95	26.70	39.52	-0.66
10	30.49	73.23	27.55	40.40	-0.30
11	31.97	69.80	28.44	41.27	0.07
12	33.00	67.42	29.21	41.93	0.40
13	33.74	65.19	29.85	42.60	0.68
14	34.14	63.55	30.09	42.69	0.78
15	34.07	62.68	29.99	42.21	0.73
16	33.51	62.85	29.62	41.37	0.57
17	32.27	65.87	29.07	40.71	0.33
18	30.74	70.81	28.53	40.13	0.10
19	29.19	76.72	28.05	39.84	-0.10
20	28.42	79.02	27.67	39.37	-0.26
21	28.03	79.53	27.37	39.16	-0.38
22	27.77	79.73	27.12	38.86	-0.49
23	27.62	79.83	26.96	38.83	-0.56
24	27.53	79.93	26.84	38.66	-0.61

VITAE

Name   Mr.Visit Akvanich

Student ID   5310130006

Educational Attainment

Degree	Name of Institution	Year of Graduation
Bachelor of Engineering (Mechanical Engineering)	Prince of Songkla University	2006
Master of Engineering (Mechanical Engineering)	Prince of Songkla University	2009

Scholarship Awards during Enrolment

1. Faculty of Engineering for financial support of tutorial fee

2. Prince of Songkla University and Energy Policy and Planning Office (EPPO) for providing the research scholarships

List of Publication

1. List of Journal Papers

Taweekun, J., and Akvanich, V., (2013) "The Experiment and Simulation of Solid Desiccant Dehumidification for Air-conditioning System in a Tropical Humid Climate," Engineering, Vol. 5 No. 1A, pp. 146-153.

2. List of Conference Papers

Akvanich, V., and Taweekun, J., (2012) "Computational Fluid Dynamics (CFD) Simulations for the Effect of Flow-Bed Geometries on Desiccant Column," Proceedings of 2012 International Conference on Fluid Dynamics and Thermodynamics Technologies, 17-18 March 2012, Singapore, pp. 19-24.

Taweekun, J., and Akvanich, V., (2012) "Simulation and Optimization of Designed Parameters for a Desiccant Column in Radiant Cooling System," Proceedings of The Asian Conference on Sustainability, Energy & the Environment, 3-6 May 2012, Osaka, Japan, pp. 230-237.